Curriculum Vitae
Name: Phillip Mario Jan Balzano
Contact Information: phillip.balzano@gmail.com
Degree and date to be conferred: Ph.D., 2018

Education

University of Maryland, Baltimore, Baltimore, MD, USA

August 2012 to May 2018

Graduate Program in Molecular Microbiology and Immunology
Advisor: Dr. Eileen Barry, Department of Medicine
Dissertation Title: **The role of MFS family transporters in the lifecycle of Type A *Francisella tularensis* and their viability as vaccine targets**

Drexel University, Philadelphia, PA, USA

August 2010-June 2012

M.S. in Biological Sciences, concentration in Cell/Molecular Biology

Villanova University, Villanova, PA, USA

August 2006-May 2010

B.S. in Biology
Undergraduate Thesis Advisor: Dr. Anil Bamezai, Department of Biology
Thesis Title: **Role of membrane rafts in apoptosis via a glycoslyphosphitidyl-inositol anchored protein, Ly-6A**

Research Experience

University of Maryland, Baltimore

May 2013 - Present
Graduate Research Assistant, Department of Microbiology and Immunology
Dissertation Research: *Laboratory of Dr. Eileen Barry*: The engineering of *fpt* transporters from Type A *Francisella tularensis,* examining their effect on the bacterial life cycle, and the characterization of these strains as live vaccine candidates.

Villanova University

January 2009-May 2010, June 2011-July 2012

Senior Thesis Research: *Laboratory of Dr. Anil Bamezai*: Characterization of the role the GPI-anchored protein Ly-6A/E plays in the extrinsic apoptosis pathway of T cells.

<u>IT'IS Foundation, ETHZ, Zurich, Switzerland</u>

June 2007-August 2007; June 2008-August 2008
Special Projects Manager, Biological Studies

Teaching Experience

<u>Drexel University</u>

September 2010-June 2012: Teaching assistant for Department of Biological Science at Drexel University.

Professional Society Memberships

American Society for Microbiology (National Chapter) *2014-Present*

Publications

Lang, MA., Jenkins,SA., **<u>Balzano, P.</u>**, Owoyele, A., Patel, A., and Bamezai, AK *Investigating the mechanism underlying Ly-6A, a highly expressed protein on activated and transformed lymphocytes, induced growth inhibition and cell death in transformed T-cell lines (TUM2P.879).* The Journal of Immunology, 2014. **192** (1 Supplement): p. 71.3-71.3.

Lang, M. A., Jenkins, S. A., **<u>Balzano, P.</u>**, Owoyele, A., Patel, A. and Bamezai, A. K. (2017), *Engaging Ly-6A/Sca-1 triggers lipid raft-dependent and -independent responses in CD4^{+} T-cell lines*. Immunity, Inflammation and Disease. doi:10.1002/iid3.182

Honors and Awards

Robert C. Byrd Scholar, State of Maryland, August 2006 - May 2010

Sigma Xi research poster symposium: First prize, May 2010

Travel Award: Mid-Atlantic Microbial Pathogenesis Meeting 2015

“Signaling Pathways in Innate Immunity” Training Grant: 5T32AI095190-04 July 2015 - June 2016

Travel Award: American Society for Microbiology - Microbe June 2016

Abstracts

Phillip Balzano, Mark Marohn, Eileen Barry. January 2015. “Attenuation of *Francisella tularensis* following deletion of MFS family transporters.” Poster presented at the Mid-Atlantic Microbial Pathogenesis Meeting, Wintergreen, VA. (Travel award recipient)

Phillip Balzano, Mark Marohn, Eileen Barry. March 2015. “Attenuation of *Francisella tularensis* following deletion of MFS family transporters.” Poster presented at the UMB-UMBC Crosstalk Symposium, UMBC, MD.

Phillip Balzano, Mark Marohn, Eileen Barry. April 2015. “Attenuation of *Francisella tularensis* following deletion of MFS family transporters.” Poster presented at the Graduate Research Conference, UMB, Baltimore, MD.

Phillip Balzano, Mark Marohn, Eileen Barry. September 2015. “Attenuation of *Francisella tularensis* following deletion of MFS family transporters.” Poster presented at the ASM Washington DC Branch meeting, Baltimore, MD.

Balzano PM, Barry EM. February 2016. “Deletion of MFS Family Transporters Alters the Intracellular Lifecycle of *Francisella tularensis.*” Abstracts of the Annual American Society for Microbioly meeting of Biodefense and Emerging Diseases conference, 46B. Arlington, VA. Abstract only.

Phillip Balzano Eileen Barry. June 2016. “Loss of the MFS Transporters *fptG* and *fptB* Delays Host Exit of *Francisella tularensis*.” Poster presented at the Graduate Research Conference, UMB, Baltimore, MD.

Phillip Balzano, Eileen Barry. May 2016. “Loss of the MFS Transporters *fptG* and *fptB* Delays Host Exit of *Francisella tularensis*.” Poster presented at the ASM Washington DC Branch meeting, Baltimore, MD.

Balzano PM, Barry EM. May 2016. “Loss of the MFS Transporters *fptG* and *fptB* Delays Host Exit of *Francisella tularensis*.” Abstracts of the Annual American Society for Microbiology Microbe conference, Sunday628, Boston, MA. (Travel award recipient) Abstract only.

Phillip Balzano, Eileen Barry. March 2017. “Loss Of The MFS Transporters *fptG* And *fptB* Delays Cellular Escape, And Attenuates Francisella tularensis In The C57BL/6J Model.” Talk presented at the Graduate Research Conference, UMB, Baltimore, MD.

Phillip Balzano, Eileen Barry. June 2017. “Loss of the MFS Transporters *fptG* and *fptB* Delays Cellular Escape and Attenuates *Francisella tularensis* in the C57BL/6J Model.” Poster presented at ASM Microbe, New Orleans, LA.

Phillip Balzano, Eileen Barry. June 2017. “Loss of the MFS Transporters *fptG* and *fptB* Delays Cellular Escape and Attenuates *Francisella tularensis* in the C57BL/6J Model.” Poster presented at UMB-UMCP Crosstalk Symposium, Shady Grove, MD.

Abstract

Title of dissertation: The Role of MFS Family Transporters in the Lifecycle of Type A *Francisella tularensis* and Their Viability as Vaccine Targets

Phillip Mario Jan Balzano, Doctor of Philosophy, 2018

Dissertation directed by: Dr. Eileen M. Barry, Professor of Medicine, Center for Vaccine Development, Institute for Global Health, University of Maryland School of Medicine

Francisella tularensis is a Gram negative facultative intracellular coccobacillus that can infect a wide variety of hosts. In humans, *F. tularensis* causes the zoonosis tularemia following insect bites, ingestion, inhalation, and handling infected animals. That a small inoculum delivered by the aerosol route can cause severe disease, coupled with the possibility of its use as an aerosolized bioweapon, have led to the classification of *Francisella tularensis* as a Tier 1 Category A select agent and has renewed interest in vaccine formulation. To this end, this study aimed to engineer and evaluate novel *F. tularensis* strain SchuS4 derivatives containing single deletions of major facilitator superfamily (MFS) transporters *fptG*, *fptE*, *fptF*, and *fptB.* Additionally, these strains developed for vaccine purposes were utilized to study more intimately aspects of the intracellular lifecycle of *F. tularensis*.

Alterations to the intracellular lifecycle of the bacterium were measured using intracellular survival assays in multiple cell types. Two strains, *F. tularensis* SchuS4Δ*fptB* and SchuS4Δ*fptG*, displayed lifecycle alterations. Further analysis with these two strains involved characterization of the early inflammatory immune response from macrophages using ELISAs for cytokine secretion, and measuring alterations to host cell permeability by measuring supernatant lactate dehydrogenase release. In addition to *in vitro* analysis, *F. tularensis* strains SchuS4Δ*fptB* and SchuS4Δ*fptG* were evaluated for attenuation, and later, protective capacity, *in vivo* in the C57BL/6J mouse model.

In vitro studies demonstrated that *F. tularensis* strains SchuS4Δ*fptB* and SchuS4Δ*fptG* were significantly altered in their intracellular lifecycle, exhibiting a novel cytosolic escape delay phenotype that was found to be autophagy-dependent for SchuS4Δ*fptG*. Additionally, *F. tularensis* strain SchuS4Δ*fptB* exhibited a significant replication defect. Moreover, we observed prominent differences in *in vitro* cytokine profiles in human and mouse macrophages for both mutants. Both mutants were attenuated in the C57BL/6J mouse model, and one strain, SchuS4Δ*fptB*, provided partial protection against virulent Type A *F. tularensis* challenge. These results demonstrate a fundamental necessity for these nutrient transporters in the timely progression of *F. tularensis* through its replication cycle, and in pathogenesis. Collectively, these strains validate the strategy of targeting transporters as means of attenuation for *F. tularensis* vaccine strain construction.

The Role of MFS Family Transporters in the Lifecycle of Type A *Francisella tularensis* and Their Viability as Vaccine Targets

by

Phillip Mario Jan Balzano

Dissertation submitted to the Faculty of the Graduate School of the University of Maryland, Baltimore in partial fulfillment of the requirements for the degree of Doctor of Philosophy

2018

Acknowledgements

First and foremost, I must thank my mentor Dr. Eileen Barry for not only training me to the highest level, but trusting me to work on a project that was carried out primarily under biohazard safety level 3 conditions. It is incalculable the amount I have learned in her laboratory, both formally and indirectly.

I'd also like to thank past and present members of the Barry Lab: Dr. Aimée Cunningham, Dr. BreOnna Delaine-Elias, Mrs. Christen Grassel, Dr. Christina Faherty, Dr. Sridevi Ranganathan, Dr. Kurt Hanevik, Ms. Brandi Hobbs, Dr. Carolyn Morris, Mr. Jonathan Moon, and Ms. Tao Wu for providing a relaxed, yet rigorous work environment.

A tremendous thank you to my thesis committee: Dr. Stefanie Vogel, Dr. David Rasko, Dr. Terez Shea-Donohue, and Dr. Robert Ernst for their guidance and advice. I am especially grateful to Dr. Stefanie Vogel for and my inclusion and her mentorship on the training grant she manages.

Finally, I would like to thank my family, especially my wife Heather, for being the support I needed throughout the graduate school process, my brother Max, my sister Anne Marie, and my parents, Jadwiga and Quirino, for the love and encouragement they provided. My father, Dr. Quirino Balzano, has always been the original scientist in my life, inspiring me to pursue a life in science and to never turn away from a challenge. To him especially, I am eternally grateful.

Table of Contents

List of Figures

List of Tables

List of Abbreviations

AIM	Absent in melanoma
Akt	Protein kinase B
AMP	Adenosine monophosphate
ANOVA	Analysis of variance
ASC	Apoptosis-associated speck-like protein containing a CARD
ATP	Adenosine triphosphate
BLAST	Basic local alignment search tool
bp	Base pair
BSL	Biohazard safety level
CD	Cluster of differentiation
CDM	Chamberlain's defined medium
CFU	Colony forming unit
cGMP	Current good manufacturing practices
DMEM	Dulbecco's modified eagle medium
DNA	Deoxyribonucleic acid
EDTA	Ethylenediaminetetraacetic acid
ELISA	Enzyme-linked immunosorbent assay
ERK	Extracellular signal-regulated kinase
FBS	Fetal bovine serum
Fc	Fragment crystallizable
FCP	*Francisella* containing phagosome
FCV	*Francisella* containing vacuole
FDA	Food and Drug Administration
FPI	*Francisella* pathogenicity island
fpt	*Francisella* phagosomal transporter
g	gram

GBP	Guanylate binding proteins
GMP	Guanosine monophosphate
HEPES	4-(2-hydroxyethyl)-1-piperazineethanesulfonic acid
hpi	hours post infection
IACUC	Institutional Animal Care and Use Committee
I.D.	Intradermal
IFN	Interferon
Ig	Immunoglobulin
IL	Interleukin
I.N.	Intranasal
I.P.	Intraperitoneal
IRAK	Interleukin-1 receptor-associated kinase
I.T.	Intratracheal
kB	Kilobase
LAMP	Lysosomal associated membrane protein
LB	Luria-Bertani broth
LD_{50}	Lethal dose, 50%
LDH	Lactate dehydrogenase
LPS	Lipopolysaccharide
LVS	Live vaccine strain
M	Molar
MAPK	Mitogen activated protein kinase
MDM	Monocyte-derived macrophage
MFS	Major facilitator superfamily
MHA	Mueller Hinton agar
MHB	Mueller Hinton broth
µL	Microliter

mL	Milliliter
NHP	Non-human primate
nM	Nanomolar
nm	Nanometer
MIP	Macrophage inflammatory protein
MOI	Multiplicity of infection
mROS	Mitochondrially-derived reactive oxygen species
NADPH	Nicotinamide adenine dinucleotide phosphate
NF-κB	Nuclear factor kappa-light-chain-enhancer of activated B cells
OD_{600}	Optical density at 600 nanometers
PCR	Polymerase chain reaction
PBS	Phosphate buffered saline
Pht	Phagosomal transporter
PI3K	Phosphoinositide 3-kinase
PMA	Phorbol 12-myristate 13-acetate
RPM	Revolutions per minute
RPMI	Roswell Park Memorial Institute
Scarif.	Scarification
STING	Stimulator of interferon genes
TBST	Tris-buffered saline with Tween 20
TGF	Transforming growth factor
TLR	Toll-like receptor
TNF	Tumor necrosis factor
TRAF	TNF receptor associated factor
UMB	University of Maryland, Baltimore
VIC	Voltage-gated ion channel
WT	Wild-type

Chapter 1 – Introduction

Francisella tularensis Background and History

The Gammaproteobacterium *Francisella tularensis* is a non-motile coccobacillus that causes the zoonotic disease tularemia [227, 206]. Though first isolated from ground squirrels in 1911 in Tulare County, California, the bacterium would not be linked to human disease until 1914 [227]. Edward Francis, among the earliest to work with the bacterium in earnest, and for whom the genus is named, proposed naming the illness caused by the bacterium "tularemia" in 1925 [220, 56]. Though the exact taxonomic location of the bacterium in relation to the other gammaproteobacteria has been controversial, the closest pathogenic relatives to *Francisella* are *Coxiella burnetii* and *Legionella pneumophila* [216]. Two species are contained within the genus *Francisella*, *F. philomiragia*, and *F. tularensis*, which itself contains five recognized subspecies: subspecies *tularensis* (also known as Type A), subspecies *holarctica* (also known as Type B), a variant of subspecies *holarctica* unique to Japan, subspecies *novicida*, and subspecies *mediasiatica* [132, 63]. Of these five, only two subspecies, *tularensis* and *holarctica*, are known to be pathogenic to humans and share a sequence identity of 98-99% [103]. The subspecies of *Francisella* are found primarily in the Northern hemisphere. The type B strain, subspecies *holarctica*, is found across both the Eurasian and North American landmasses, while the Type A strain, except in one instance [85], has largely been isolated in North America [150]. Subspecies *holarctica* is the basis for what is termed the "live vaccine strain" (LVS), an attenuated strain created in the Soviet Union by serial passage that was transferred to the United States in 1956. *F. tularensis*

LVS was tested extensively in clinical trials, and is commonly used as a laboratory model due to its lethality in mice and BSL-2 designation [200].

The pathogenic strains cause various forms of disease, which are determined by the route of infection. Ulceroglandular tularemia, the most common form of the disease, results from cutaneous exposure, most often from insect bites or direct contact with an infected animal, including rabbits, muskrats, and voles [142]. Outbreaks in humans often occurs in tandem with outbreaks in nearby animal populations, though it is unlikely that animal populations are the natural reservoir. There is much evidence that *Francisella* can persist in waterways, likely in association with amoebae [15, 1, 59]. After cutaneous exposure, incubation is typically 2-6 days, with onset marked by the appearance of a painless ulcer and flu-like symptoms including chills, fever, headache, and malaise [148]. While debilitating, the ulceroglandular form of tularemia caused by either Type A or Type B *F. tularensis* is rarely fatal, carrying a mortality rate below 5% [78, 65].

F. tularensis can also be acquired via ingestion and even the oculoglandular route [213, 150, 63], but the most lethal form of infection occurs following inhalation, leading to respiratory, also referred to as typhoidal disease [200]. Infection via the respiratory route with an inoculum as low as 10 bacteria of the highly virulent Type A strain often leads to a debilitating disease characterized by fever, chills, systemic soreness, and an unproductive cough [65, 128]. Bacteria spread systemically via the lymphatic system and form foci of infection in such diverse organs as the spleen, liver, kidneys, and intestines [148, 63]. Often, the draining lymph nodes become swollen and palpable [150, 65]. If left untreated, respiratory tularemia has a mortality rate approaching 50% [65, 63, 150].

Perhaps because of its high level of virulence and ability to infect via the aerosol route at a low inoculum, *F. tularensis* has a history of weaponization that spanned the middle of the 20th century [55]. The Japanese Empire, operating in Manchuria in the 1930's through to the end of the Second World War, experimented with *F. tularensis*¸ as well as several other infectious agents, as potential biological weapons [90]. Offensive use of *F. tularensis* may have also occurred in the West during the Second World War as well, with a documented tularemia outbreak, suspected to be intentional by the Soviets [3], affecting thousands of German and Soviet soldiers [52]. After the Second World War, both the Soviet Union and the United States developed *F. tularensis*, among other agents, for use as biological weapons, until offensive biological research was ended in the U.S. by President Richard Nixon in 1969 [89]. Over a century after its initial isolation, and after decades of weapons development research and parallel vaccine development efforts throughout the middle of the 20th century, there still exists no licensed vaccine against *F. tularensis*.

The Intracellular Lifecycle of *Francisella tularensis*

The ability to enter, survive, and replicate within mammalian cells is thought to be the key to virulence of *F. tularensis* [31]. Both clinically relevant subspecies of *F. tularensis* are able to gain entry and proliferate within a variety of cell types, including macrophages, neutrophils, hepatocytes, lung epithelial cells, and even erythrocytes [92, 130, 87, 150]. Though *F. tularensis* can find its way into a myriad of cell types and replicate, much work concerning the intracellular lifecycle utilizes macrophages, as it is believed survival and replication in this cell type is critical to pathogenesis [71, 69]. It is within these cells that a well characterized replication cycle, as shown in Figure 1.1, has

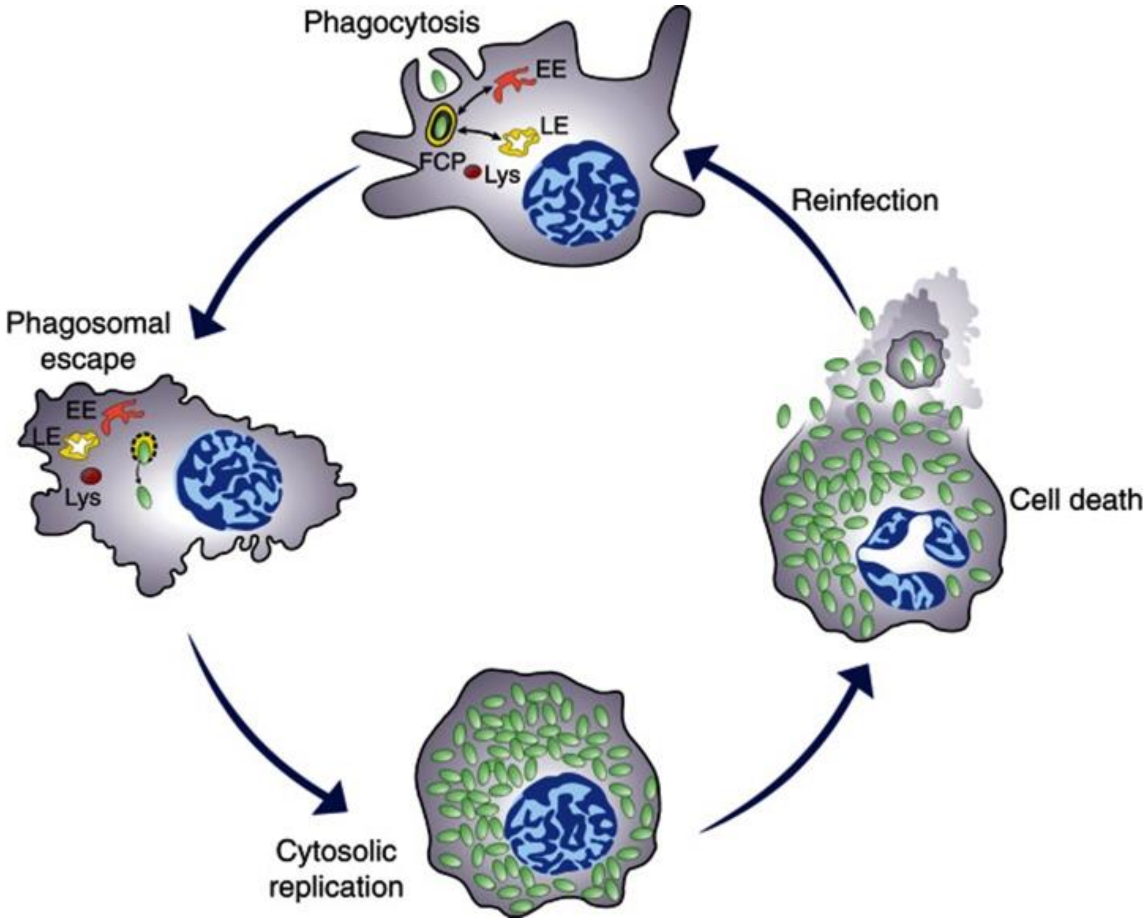

Figure 1.1. The intracellular lifecycle of *Francisella tularensis*. Image reprinted with permission from Cold Spring Harbor Press: Cold Spring Harbor Perspectives in Medicine, 1-14 (2013). EE – early endosome; LE – late endosome; Lys – lysosome.

been defined which includes internalization into a phagosome, escape from the phagosome into the cytosol, replication in the cytosol, and eventual lysis of the host cell and release of the bacteria.

Bacteria not opsonized by complement are thought to rely upon the mannose receptor [193, 75] for entry into macrophages, though other, as yet unknown, receptors may play a role [24]. Bacteria opsonized by complement, which greatly enhances bacterial uptake into phagocytes, rely heavily upon complement receptor 3 [8, 10], though other receptors and molecules, such as scavenger receptor A [158], nucleolin [9], Fcγ receptor, and lung surfactant protein A [8] are involved to varying degrees. Though non-opsonized entry may be more favorable to the bacterium, as evidenced by the fact that opsonized Type A *F. tularensis* proliferated to a diminished degree compared to non-opsonized bacteria within mouse bone marrow macrophages (BMDMs) [75], complement opsonization most commonly precedes uptake during natural infection.

Interestingly, internalization of the bacteria requires lipid rafts in mouse macrophage cell line studies, and components of lipid rafts, namely cholesterol and caveolin-1, are present in the *Francisella* containing phagosome (FCP) [211]. It may be that *F. tularensis* targets receptors clustering in these nanodomains, as depletion of lipid rafts abolishes bacterial entry [31]. The Syk tyrosine kinase and ERK MAP kinase pathways were also found to be indispensable for bacterial internalization [152]. Though Syk is upstream of both the Akt/PI3K and the ERK pathways, only inhibition of ERK decreases phagocytosis of *F. tularensis* in macrophages, demonstrating that the bacteria rely upon a signal transduction system flowing from the membrane, through Syk, to the ERK pathway [152].

After phagocytosis, *F. tularensis* resides in the phagosome, the initial compartment of the endocytic pathway. The newly formed endosome begins a normal maturation process, acquiring both early and late endosomal markers such as LAMP-1, CD63, and Rab7 [35, 186], but fusion with the lysosome is prevented, and the FCP never gains markers, like cathepsin D, of an active, bacteriocidal phagolysosome [35]. *F. tularensis* is also able to inhibit the respiratory burst, furthering its chances of survival by preventing NADPH oxidase from assembling onto the phagosome [130]. Acidification of the FCP in a vacuolar ATPase (v-ATPase) -dependent manner may serve as a trigger for *F. tularensis* to begin escaping from the phagosome into the cytosol [185], though controversy still prevails concerning the necessity of this process for optimal escape. Interestingly, acidified FCPs are found primarily in studies using non-opsonized bacteria, whereas complement-opsonized bacteria tended to display non-acidified phagosomes, demonstrating the possible different fates that result depending on the method of entry [24]. Regardless of the method of entry and whether the FCP requires acidification or not, it has been established that induction of genes within the vital *Francisella* pathogenicity island (FPI), a locus of virulence genes crucial for escape from the phagosome and survival in the host cell, begins while the bacterium is in the phagosome [144, 32].

Phagosomal escape, a common trait found across all subspecies of *F. tularensis*, is critical, as replication can only proceed once the bacterium has entered the cytosol [116, 11]. For this reason, escape-deficient strains are avirulent *in vivo*, underscoring the critical importance of this step to pathogenesis [21, 209, 120]. While exact kinetics for escape remain controversial, and differences have been noted depending on cell type, bacterial strain, and technical details, it is accepted that *F. tularensis* reaches the cytosol between 1 and 8 hours post-phagocytosis [80, 26]. Opsonization state again appears to play a key role at the stage of escape, as opsonized bacteria escape at a slower rate than non-opsonized bacteria [32, 130, 194]. Unlike other Gram negative intracellular pathogens such as *Listeria monocytogenes* and *Shigella flexneri*, *F. tularensis* does not encode any sort of phospholipase or hydrolase normally associated with the degradation of vesicular membranes [109]. Instead, *F. tularensis* employs a Type VI secretion system encoded on the FPI to export numerous gene products, many also encoded on the FPI, into the cytosol to facilitate phagosomal escape [144]. Other genes located outside the FPI contribute to escape to varying degrees and are diverse in function, including genes for uracil biosynthesis [194], acid phosphatases [140, 141], hypothetical genes of unknown function [224, 163, 165], and, intriguingly, the major facilitator superfamily (MFS) isoleucine transporter *fptB* [77].

The FPI is an approximately 30 kb locus that includes 17 genes that, in both the Type A and Type B strains, but not *F. novicida*, is duplicated in the genome [144]. The genes of the FPI are primarily concerned with phagosomal escape, having little to no effect on the bacteria once replication begins in the cytosol, as evidenced by direct microinjection of various FPI mutants into host cytosols [137]. The FPI gene *iglC* is secreted into the cytosol via the Type VI secretion system and features prominently in the degradation of the FCP membrane, as disruption of this gene greatly impedes bacterial escape [187]. Other genes from the FPI, including *pdpA* [192], Type VI secretion system components *iglJ*, *vgrG*, and *dotU* [19] [49], the regulators *migR* and *mglA* [187, 22], *iglI* [120], and *fevR* [20] all play crucial, if still incompletely defined, roles in phagosomal escape. The wide assortment of genes, both within and outside of the FPI, demonstrates the importance of phagosomal escape in the replicative lifecycle of *Francisella*, and that coordination of escape is multifaceted, requiring input from many varied factors like nutrition acquisition, metabolic status, and environmental cues.

Once released to the cytosol, *F. tularensis* begins a period of rapid replication utilizing nutrients from the host. While a common misconception that the cytosol is a hospitable environment, the cell's interior is actually rather nutritionally restrictive, requiring special adaptation from intracellular bacteria to prosper in this compartment [147]. Access to nutrients is further hindered in professional phagocytes such as macrophages, where amino acid levels fluctuate, with several becoming scarcer after activation [146]. Unstable amino acid levels are an acute concern to *F. tularensis*, as amino acids are the primary sources of carbon and energy during the intracellular stage of the lifecycle [184]. Mammalian cells are auxotrophic for 9 amino acids: histidine, lysine, methionine, phenylalanine, tryptophan, leucine, isoleucine, valine, and threonine, but cysteine, while only semi-essential, is most limited in supply inside the host [161]. *F. tularensis* is auxotrophic for cysteine, among other amino acids, and requires high levels of it to convert to pyruvate and funnel into the Krebs cycle [184]. To counteract the limited quantities in the host, *F. tularensis* cannibalizes host glutathione, the most abundant source of cysteine in the cell, to boost cysteine levels [4, 133]. The γ-glutamyl-transpeptidase is utilized by *F. tularensis* to break down glutathione and is a potent attenuation target, signifying the importance of cysteine metabolism to *F. tularensis* [94].

Type A *F. tularensis* is predicted to be auxotrophic for 6 amino acids, specifically arginine, histidine, lysine, tyrosine, methionine, and cysteine, meaning the bacterium overlaps auxotrophies with the host cells at four amino acids: histidine, lysine, methionine, and cysteine [133, 184]. *F. tularensis* has been demonstrated to utilize host autophagy machinery in order to boost general amino acid availability in host cells [26, 45, 204]. The targeted depletion of glutathione is believed to be the trigger for general host autophagy, though the process is non-canonical, as autophagic vesicles formed during *F. tularensis* infection lack the traditional autophagy marker ATG5 [204, 184]. *F. tularensis* has been observed to re-enter the endocytic system late during replication via autophagy, forming non-degradative *Francisella*-containing vacuoles (FCVs) by 20 hours post-infection [26]. Though not all intracellular bacteria are observed to be in vesicles at later time points [26], autophagy markedly affects replication numbers. Inhibition of autophagy by chemical inhibitors such as bafilomycin A1, chloramphenicol, or 3-methyladenine drastically reduces intracellular bacterial numbers [204]. Similarly, radiolabeled, host-derived amino acids are demonstrated to be transported into *F. tularensis* and utilized in new protein products at a significantly lower rate when autophagy is inhibited, demonstrating that *F. tularensis* actively harvests amino acids from the autophagy machinery [204].

The increase in amino acid levels engendered by autophagy would be wasted without suitable transporters to take up the freshly liberated nutrients. The Type A and Type B strains of *F. tularensis* are predicted to have 182 and 210 transporters of all types, respectively [107], representing approximately 12% of the protein coding sequences in either genome. While deletion of nutrient transporters is a largely unexplored endeavor in the *Francisella* field, and is the focus of this study, some prior work has demonstrated the importance of amino acid transporters to the cytosolic replication of *F. tularensis*. We previously demonstrated that targeted single deletion of 3 MFS transporters in the LVS background severely diminished intracellular replication [128]. Not unexpectedly, two of the three transporters deleted, *fptB* and *fptE*, are high affinity amino acid transporters, transporting isoleucine and asparagine, respectively [76, 77]. As an intracellular pathogen, *F. tularensis* must rely upon a multitude of high affinity transporters to scavenge nutrients in the challenging environment of the mammalian cytosol [133].

The end of the *F. tularensis* replication cycle is a topic that has received little attention, and thus, minimal mechanistic information has been revealed. It is known that *F. tularensis* subspecies *holarctica* and *novicida*, via interactions with the AIM2/ASC inflammasome complex, trigger pyroptotic cell death in an attempt by the host cell to deprive *F. tularensis* of its privileged replicative niche [126, 98]. Evidence exists, on the other hand, that the immunosuppressive *F. tularensis* Type A strain avoids detection by AIM2/ASC [44], and instead, triggers cell death in a caspase-3-dependent manner [228]. *F. tularensis* is released from dying cells for subsequent re-infection of neighboring cells. One report provides evidence that *F. tularensis* may additionally be spread cell to cell via trogocytosis, the direct cell-to-cell transfer mechanism that exchanges membrane and cytoplasm between immune cells [205]. Trogocytosis has been documented to be an important boost to the immune response by increasing and diversifying signaling in many diverse circumstances, including tissue transplantation, vaccination, and cancer response [231, 115, 33]. It is likely that *F. tularensis* is an unwitting beneficiary of this behavior, allowing for transfer of bacteria to other cells as early as 6 hours post-infection [205]. Detailed analysis of the exact escape processes and molecular mechanisms *F. tularensis* utilizes to leave the host and spread remains a gap in the knowledge of the *Francisella* lifecycle.

The Immune Response to *Francisella tularensis* Infection

The interaction of *F. tularensis* with the immune system begins at the cell surface during phagocytosis, as shown in Figure 1.2, when the Toll-like receptor heterodimer TLR2/6 recognizes lipoproteins on the bacterial cell surface [40, 102]. This triggers a signaling cascade dependent upon MyD88, IRAK4/1, and TRAF6 to ultimately release NFκB for nuclear translocation, and the transcription of multiple pro-inflammatory genes [113]. This early innate recognition allows for production of important pro-inflammatory cytokines like pro-interleukin-1 (IL-1β), tumor necrosis factor-α (TNF-α), interleukin-12 p40 (IL-12p40), and costimulatory markers including CD80/86 by 2 hours post infection [102, 38]. Such early signaling is critical, as removal of TLR2 significantly hastens mortality in mice [121]. To limit its visibility to TLR2 and dampen the induced response, *F. tularensis* minimizes exposure of its lipoproteins by actively repressing their production during the first hours of infection [97]. Conversely, more robust TLR2-dependent cytokine production is observed if *F. tularensis* are retained in the phagosome, prolonging the exposure of the bacterium to the TLR2-sensing machinery, as demonstrated by FPI mutant strains [38]. Unlike many other Gram-negative bacteria, *F. tularensis* does not induce a strong endotoxin response through TLR4 due to the unique tetraacylated structure of the lipid A component of its lipopolysaccharide (LPS) [86]. The long length of its acyl chains and unusual structure of its core sugars inhibits interaction between *Francisella* lipid-A and the TLR4/MD2/CD14 complex [149].

Upon escape from the phagosome, *F. tularensis* begins replicating in the cytosol. In this cellular compartment, *F. tularensis* induces the production of Type I interferon. In the cytosol, *F. tularensis* interacts with the DNA sensors cyclic GMP-AMP (cGAS) and

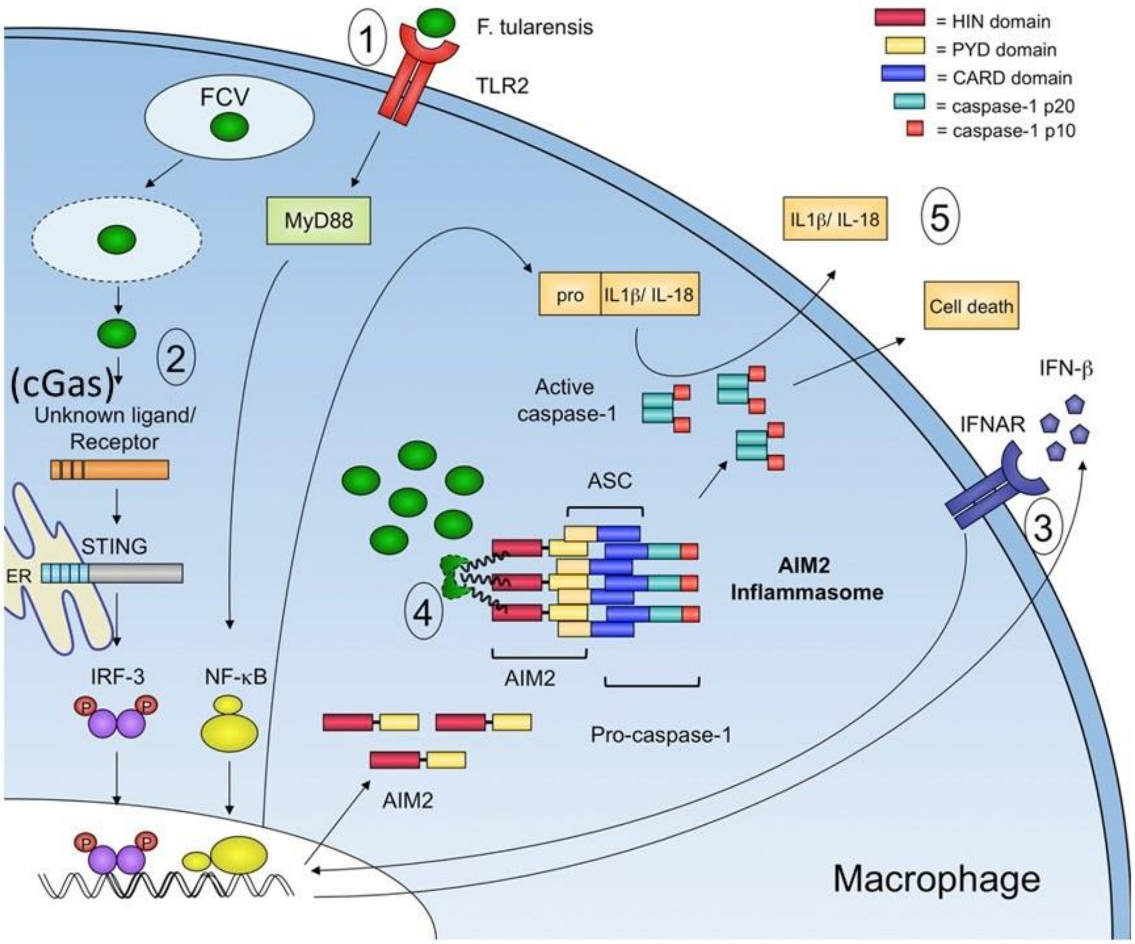

Figure 1.2. The early innate immune response to *Francisella tularensis*. Image modified from Jones JW, Broz P, Monack DM. 2011. "Innate Immune Recognition of Francisella Tularensis: Activation of Type-I Interferons and the Inflammasome". Frontiers in Microbiology 2:16.

Ifi204, which signal through STING for the production of Type I interferon [122, 207]. Autocrine and paracrine signaling through the interferon receptor (IFNAR) leads to the upregulation of the "absent in melanoma 2" (AIM2) inflammasome complex [66, 169], and the IRF1-dependent upregulation of guanylate binding proteins (GBPs) [122]. Via an as yet undefined process, though possibly requiring the presence of mitochondrially-derived reactive oxygen species (mROS) [44], GBPs facilitate the killing of a small number of cytosolic *F. tularensis* and their subsequent release of double stranded DNA to the cytosol [98], allowing for recognition by AIM2/ASC, and for oligomerization of this inflammasome [122, 136, 126]. Activation of the inflammasome leads to autocatalysis of caspase-1, and the subsequent processing of pro-IL-1β and pro-IL-18 to their active forms for subsequent release [169]. Cell death via apoptosis/pyroptosis mediated by AIM2/ASC defines the end stages of the initial cellular response to *F. tularensis* [66, 159, 156].

F. tularensis spends the majority of its time within cells, thus a cell-mediated, Th1-dependent immune response leading to the production of interferon-γ (IFN- γ) has been found to be important for host survival [134]. IFN-γ-stimulated macrophages are able to control intracellular *F. tularensis* in a nitric oxide-dependent manner [160, 70, 118], but to arrive at this effective immune response requires tight interplay between the innate and adaptive arms of the immune system. In mice, it has been shown that IL-1β and IL-18 secreted in the first 72 hpi lead to *F. tularensis*-specific anti-LPS IgM production from B1-a cells and IFN-γ from an as yet unknown source, respectively [51]. The degree to which protective immunity requires either T cells or B cells, or what combination of both, is still unresolved. Adoptively transferred splenocytes from immunized mice are able to protect mice from *F. tularensis* challenge, but this effect is lost when T cells are depleted [71]. However, other work using athymic mice was able to demonstrate a protective, specific response against *F. tularensis* challenge after prior priming with LVS, indicating a humoral path to protection [62]. It is commonly held that an effective response is driven through IFN-γ and TNF-α, and that IgG, but not IgM, mediates bacterial clearance [173, 201].

F. tularensis utilizes multiple survival and evasion strategies to subvert the immune response. The aforementioned atypical LPS produced by *F. tularensis* gives rise to much more limited visibility to the innate immune system by abolishing TLR4 signaling. *F. tularensis*, and more specifically the Type A strain, actively antagonizes the immune system as well, by making infected macrophages unresponsive to subsequent *Escherichia coli* LPS exposure, for example [214]. Infection with the Type A strain can attenuate an ongoing immune response in a dose-dependent fashion, dampening cytokine transcription and secretion within a couple of hours of entrance into the cell [79]. Further evidence has demonstrated signatures of aberrant activation of innate immune cells, whereby infected cells secreted significantly less TNF-α and interleukin-6 (IL-6), and significantly increased amounts of the immunosuppressive cytokine transforming growth factor-β (TGF-β) compared to cells stimulated with LPS [17, 18]. Furthermore, evidence exists that *F. tularensis* LVS, though not the Type A strain, may induce alternative activation of macrophages, skewing the immune response towards one more favorable to bacterial survival [197, 83]

On a macroscopic, organismal level, *F. tularensis* infection leads to death via sepsis and high levels of inflammation, regardless of the route of infection. [123, 196].

Specifically, high levels of the inflammatory cytokines IL-6 and macrophage inflammatory protein 2 (MIP-2) were correlated with death in mice, while elevated IL-1β and IgM correlated with survival [30]. As observed in mice, the widespread sepsis that characterizes *F. tularensis* infection likely stems from the atypical inflammatory response stimulated by the bacteria, resulting in a subsequent delay in inflammatory, bactericidal cell recruitment [123]. Extensive apoptosis may drive macrophages *in vivo* to skew to an alternative activation state aimed more at clearing debris than combating the bacteria [124]. During lung infection, excessive levels of neutrophil infiltration may drive pathology as well [123].

The Major Facilitator Superfamily of Transporters

Cells of all types employ a multitude of transporters to transfer a wide assortment of substrates across membranes. These transporters fall into 3 broad categories: the primary transporters that rely upon hydrolysis of ATP to drive their substrates across the membrane against its gradient, the secondary transporters which utilize the chemiosmotic gradient of a solute traveling down its gradient to power transport of another molecule against its gradient, and the group translocation transporters that tie movement of their solute to their chemical modification [111]. The major facilitator superfamily (MFS) is the largest group within the secondary transporters category, with 74 recognized families and over 10,000 members [171, 222]. MFS transporters are present in Archaea, Bacteria, and Eukarya, [178], and thus represent an ancient solution to the problem of specialized substrate transport.

The MFS likely arose through duplication events in primordial voltage-gated ion channel proteins (VIC) where a 2-transmembrane domain channel gained a third transmembrane domain and subsequently underwent 2 rounds of intragenic duplication to give rise to a 12 transmembrane domain protein with homologous halves [93]. Members within the family are capable of symport, antiport, and uniport [125]. As shown in Figure 1.3, transporters within the MFS are structurally defined as containing 12 transmembrane domains, though members have been characterized with 13, 14, 16 and even 24 transmembrane domains, the latter being the result of fusion events resulting in dual substrate transporters [171]. The mechanism of transport for MFS members has been widely characterized and involves minimal movement of the substrates; rather, the protein itself will move around the substrate, alternatively exposing either face of the transporter as it cycles [84].

Despite the ubiquity across all forms of life, involvement in the transport of many of the most basic building blocks critical for the maintenance of life, the MFS includes as many as 17 entire families that remain entirely uncharacterized with not a single member's substrate identified [171]. For the majority of MFS transporters that have been characterized, much of the work thus far has focused on the structural or mechanistic aspects of the transporters. More recently, a role for certain MFS transporters as virulence factors in bacterial pathogens has been recognized, though still understudied [5, 57, 199]. Transporters within the MFS have come into the spotlight in recent years as multidrug efflux pumps contributing to reduced efficacy of many antibiotics [48]. Drug resistance efflux pumps fall into five families, including the MFS, which is known to contain the largest number of drug efflux pumps [28] with the entirety of 2 subfamilies containing drug antiporters [179]. Research into this field is uncovering new members, but with the fast pace at which clinically important pathogens previously thought to be therapeutically

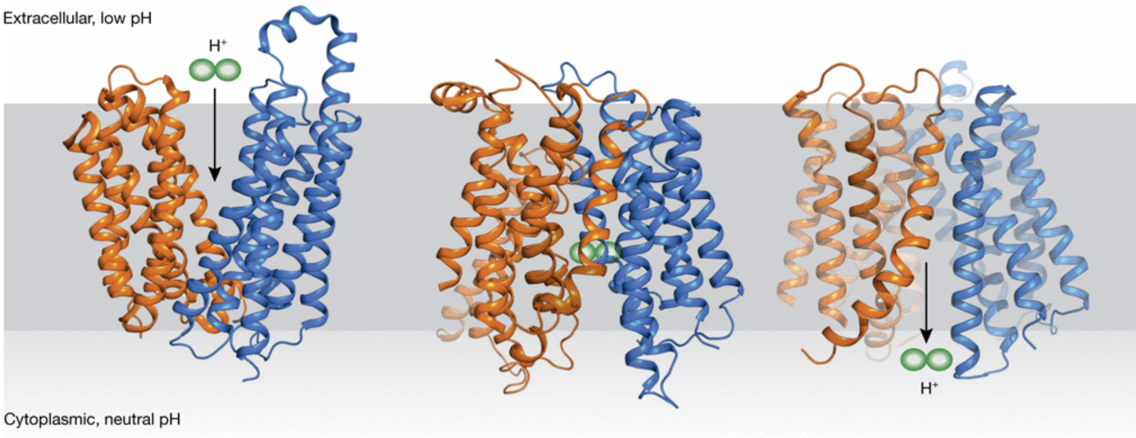

Figure 1.3. The structure and mechanism of action of a major facilitator superfamily transporter. MFS transporters move a substrate against its concentration gradient by tying transport to ions traveling down their gradient. Image reprinted with permission from John Wiley and Sons: Nissen, 2012. The EMBO Journal, 3382–3383 (2012).

controllable, such as *Mycobacterium tuberculosis* [189], *Escherichia coli* [198], and *Pseudomonas aeruginosa* [53], among several others [5], are acquiring resistance, more attention is warranted.

Some examples, such as MdfA of *E. coli* have the ability to transport a very large subset of drug types both directly out of the cytosol and from the lipid bilayer in a proton gradient-dependent manner [198]. MdfA appears to function in nature by endowing *E. coli* with the ability to thrive in alkaline environments as basic as pH 10 by effecting transport of Na^+ and K^+ ions [112]. A wide variety of antibiotics were found to be substrates of MdfA, including the non-aromatic macrolide erythromycin and uncharged chloramphenicol, as well as fluoroquinolone drugs, aminoglycosides like neomycin and kanamycin, and lipophilic compounds like ethidium bromide, rhodamine, tetracycline and puromycin [57]. Several of these compounds were, and are still, of clinical or agricultural importance. Curiously, no single amino acid residue in the entire sequence of MdfA is irreplaceable in terms of drug transport, implying a robust and varied binding and transport mechanism [199]. The gene encoding MdfA is present on mobile conjugative plasmids, and has been found everywhere from meat in marketplaces to patients in hospital intensive care units and is considered a prototypical example of a multidrug resistance transporter [230, 221].

A largely understudied aspect of MFS transporters focuses on their involvement in pathogenesis. All bacteria require carbon in some form from which they can extract energy, synthesize new molecules, and reproduce. Pathogenic bacteria rely on taking these resources to at least some degree from the host they are parasitizing [203]. Nutrient transporters in the MFS have been found to be essential to virulence. *Legionella* *pneumophila* relies upon amino acids as a primary carbon source for both energy generation and production of other molecules [215, 184]. Accordingly, with such a premium placed on amino acid acquisition from the host, deletion of the threonine transporter in *L. pneumophila*, phagosomal transporter A (PhtA), led to severe attenuation of intracellular growth in macrophages [191]. Other vital members in the Pht family identified thus far in *L. pneumophila* include PhtC and PhtD, both of which are involved in thymidine salvage during invasion [67], and PhtJ, a valine transporter [27]. Many paralogues exist, not just within the Gammaproteobacteria class, which includes important pathogens, such as *Vibrio cholera*, *Escherichia coli*, *Pseudomonas aeruginosa*, the *Salmonella* species, and *Francisella tularensis*, among others, but also within the Alphaproteobacteria class, and *Chlamydia* and *Cyanobacteria* species [27]. Recently, *F. tularensis*, a bacterium with similar nutritional requirements as *L. pneumophila*, was found to contain 9 homologues of PhtA, identified as the *Francisella* phagosomal transporters (*fpt*) [128]. Deletion of three *fpt* members, *fptB*, *fptE*, and *fptG*, in *F. tularensis* LVS resulted in strains that were significantly attenuated and protective to varying degrees when used to vaccinate mice [128]. The substrates for *fptB* (also *ileP*) and *fptE* (also *ansP*) were later identified as isoleucine and asparagine, respectively [76, 77]. Interestingly, *F. tularensis* is not auxotrophic for either of these amino acids, but deleting the transporter for either resulted in reduced intracellular growth [76, 128]. Additionally, the Δ*fptB* strain was delayed in escaping from the phagosome, thus altering significantly the intracellular lifecycle of *F. tularensis* [77].

Francisella tularensis Vaccines

As mentioned previously, no licensed vaccine exists for protection against *F. tularensis* though interest in the creation of one was renewed since the anthrax attacks of 2001 [150]. Historically, vaccination strategies against *F. tularensis* have utilized one of three approaches: killed whole cell formulations, subunit vaccines, and live attenuated strains. Killed vaccines, named "Foshay" vaccines after their inventor, Dr. Lee Foshay, consisted of phenol- or acetone-killed bacteria [72]. Original experiments with this formulation met with mixed success; reductions in ulceroglandular and typhoidal disease incidences were documented in U.S. Army researchers who were administered the vaccine [43], but poor levels of protection were observed in other studies with human immunization and challenge [219, 58]. More recent attempts to develop inactivated *F. tularensis* vaccines have reached similarly poor results. Heat killed *F. tularensis* LVS coupled with IL-12 expressed from a vasicular stomatitis virus vector increased bacterial clearance in mice from *F. tularensis* LVS challenge when compared to non-adjuvented controls, but all protection was lost when challenge utilized the *F. tularensis* Type A strain [110, 12]. The observed inability of these vaccine constructs to induce a cellular immune response, widely considered necessary for successful protection against *F. tularensis*, has reduced enthusiasm for this type of vaccine strategy [223, 212, 63]. Subunit-based vaccine strategies have been similarly disappointing. Low-level protection was observed in mice vaccinated with *Francisella* O-antigen conjugated to bovine serum albumin when challenge consisted of *F. tularensis* LVS or wildtype Type B strains, but no protection was achieved with systemic challenge with the Type A strain [74, 43]. Proteins have been targeted as well, most notably the outer membrane proteins FopA and

Tul4 [81, 73], but these attempts did not outperform LPS-based constructs. Most promising of the recent component vaccine constructs have been those utilizing cationic surfactant vesicles incorporating either *F. tularensis* LVS or SchuS4 components. Most intriguingly, vaccination of mice with SchuS4-derived nanoparticles elicited 66% protection from heterologous intranasal challenge [174], likely pointing the way forward for further development.

The live attenuated vaccine strategy has shown the most promise to date, most notably through the live vaccine strain *F. tularensis* LVS. What would become LVS was developed from several live attenuated vaccine candidate strains derived from *F. tularensis* subspecies *holarctica* produced by the Soviet Union through the 1940’s and 1950’s and transferred to the United States in 1956 [150]. Further passage of that strain in the United States on peptone cysteine agar gave rise to LVS, characterized as having two phenotypic variants, blue and gray-colored colony types [223]. Vaccination of mice with blue colony *F. tularensis* LVS was found to confer full protection against Type A and Type B challenge, while gray colony LVS failed to protect [58]. Human studies undertaken to determine the efficacy of *F. tularensis* LVS were conducted by the U.S. Army under the moniker “Operation Whitecoat” [223]. *F. tularensis* LVS conferred some protection against Type A challenge, especially in comparison to contemporary Foshay vaccines [23], but the efficacy varied via route and dose of vaccination and route and dose of challenge. For example, all individuals vaccinated via inhalation with *F. tularensis* LVS were protected from aerosol challenge with 2.5×10^4 CFU of the Type A strain SchuS4, while only 46% of cutaneously vaccinated individuals developed sickness [91, 131]. While the superiority of aerosol vaccination with *F. tularensis* LVS was ascertained, LVS was found to be more reactogenic when inhaled, and thus, the less efficacious scarification method was the only route of vaccination approved for use [223].

F. tularensis LVS never gained licensure in the United States, largely due to the inability to protect fully against Type A strain challenge, the instability of its colony types, and the lack of understanding (at the time) of the attenuating mechanism behind the strain [180, 127]. Importantly, LVS provides proof-of-principle that a live attenuated strain can provide at least partial protection against aerosol challenge with the highly virulent *F. tularensis* Type A strain. Recently, a batch of *F. tularensis* LVS produced following current good manufacturing practice (cGMP) conditions was found to be entirely of the blue colony type, and was attenuated and immunogenic in rabbits [153]. Trials in humans with this newly manufactured strain demonstrated robust induction of *Francisella*-specific IgA, IgM, and IgG via the scarification route [60, 143], and represent the first steps towards future licensure in the United States. Beyond new attempts to reassess *F. tularensis* LVS, many new live vaccine candidates have been constructed utilizing both the LVS, Type A SchuS4, and subspecies *novicida F. tularensis* backgrounds, with the goal to confer a high level of protection against the virulent *F. tularensis* Type A strain and to qualify for licensure under the FDA's Two Animal Rule [68]. Targeted deletion of genes believed to be important for virulence have produced strains of known origin and rational construction, and have exhibited varying degrees of efficacy in animal models, as work aims to find the ideal balance between immunogenicity and attenuation [127, 162].

F. tularensis LVS has served as the basis for numerous vaccine strain constructs, as it serves as a reliable substitute for the Type A strain in mice. *F. tularensis* LVS is non-lethal in humans and can be handled in a BSL-2 environment, yet it induces a disease similar to that of the Type A strain in humans in mice [71]. The 50% lethal dose (LD_{50}) in mice has been calculated for many routes of challenge [127], making the strain a useful benchmark against which to test the attenuating capacity of new mutations. Furthermore, the 99% genetic identity between *F. tularensis* LVS and the Type A strains allows for LVS to serve as a surrogate before work is attempted in the more virulent Type A strain [103]. *F. novicida* has 98% genetic similarity to the Type A strain, and has also been utilized in this fashion [105]. Several key genes have been targeted for mutation and tested in *F. tularensis* LVS, *F. novicida*, and Type A *F. tularensis*, including the guanosine monophosphate (GMP) biosynthesis genes *guaA* and *guaB* [182, 183], purine biosynthesis genes *purMCD* [154, 155], the aforementioned γ-glutamyl transpeptidase *ggt* [4, 94], capsule biosynthesis gene *capB* [96, 138], the catalase gene *katG* [117], and several others that are summarized more completely in Table 1.1. Protection against the virulent Type A strain in animals has been varied, as the optimal balance between immunogenicity and degree of attenuation remains elusive across the multitude of animal models utilized in the *Francisella* field.

Table 1.1 Summary of published live attenuated *F. tularensis* vaccine strains and their protective ability in animal models.

Base Strain	**Gene Targeted**	**Gene Function**	**Vaccination Dose and Route (CFU)**	**Challenge Dose and Route (CFU)**	**Survival in Animals**	**Citation**
LVS	*guaA*	guanine nucleotide biosynthesis	2.2×10^7 I.P.	2.8×10^5 I.P. LVS	100% BALB/C	[181, 182]
SchuS4			7.0×10^5 I.N.	100 I.N. SchuS4	0% C57BL/6J	
LVS	*guaB*	guanine nucleotide biosynthesis	3.6×10^7 I.P.	2.8×10^5 I.P. LVS	100% BALB/C	[181, 182]
SchuS4			6.0×10^7 I.N.	100 I.N. SchuS4	0% C57BL/6J	
SchuS4	*guaBguaA*	guanine double mutant	1.0×10^8 I.N.	100 I.N. SchuS4	0% C57BL/6J	[182]
LVS	*purMCD*	purine biosynthesis	1.0×10^6 I.N.	5.0×10^3 I.P. LVS	100% BALB/C	[154, 155]
LVS			1.0×10^6 I.N.	100 I.N. SchuS4	100% BALB/C	
SchuS4			1.0×10^4 I.N.	500 I.N. SchuS4	40% BALB/C	
LVS	*capB*	capsule biosynthesis	1.0×10^5 I.N.	10X LD_{50} aerosol	100% BALB/C	[96, 201]
SchuS4			1.6×10^4 SC	100 SC SchuS4	100% BALB/C	
SchuS4	*FTT_1103*	conserved hypothetical lipoprotein	1.3×10^8 I.N.	37 I.N. SchuS4	100% C57BL/6J	[164]
			2.6×10^8 I.N.	68 I.N. SchuS4	50% C57BL/6J	
			1.0×10^8 I.N.	95 I.N. SchuS4	75% BALB/C	
SchuS4	*clpB*	heat shock protein	1.0×10^7 I.D.	105 I.N. SchuS4	100% BALB/C	[82]

Table 1.1 Continued

F. novicida	*iglB*	Type VI secretion system component	1.0×10^{7} I.N.	3×10^{4} I.N. LVS	100% BALB/C	[41]
			1.0×10^{3} orally	25 I.N. SchuS4	67% C57BL/6J	
F. novicida	*iglB:fljB*	*iglB* mutant expressing *S.* Typhi flagellin	1.0×10^{3} orally	8.5×10^{4} I.N. LVS	83% BALB/C	[46]
			1.0×10^{7} orally	1.0×10^{4} I.T. SchuS4	83% Fischer rat	
SchuS4	*iglC*	Type VI secretion system component	1.0×10^{6} I.D.	500 I.D. FSC033	0% BALB/C	[216]
			1.0×10^{7} I.D.	10 aerosol FSC033	0% BALB/C	
F. tularensis subsp. *holarctica*	*iglH*	*Francisella* pathogenicity island (FPI) component	3.0×10^{7} SC	300 SC FSC200	100% BALB/C	[207]
F. novicida	*mglA*	FPI regulator	1.0×10^{5} aerosol	6×10^{2} aerosol *F. novicida*	0% BALB/C	[225]
F. novicida	*iglD*	FPI component	9.7×10^{8} I.N.	1.0×10^{3} I.N. SchuS4	83% Fisher rat, NHP	[34]
			1.0×10^{5} I.D.	500 I.N. SchuS4	80% BALB/C	
			4.8×10^{6} I.N.	1.0×10^{3} I.N. LVS	0% BALB/C	
SchuS4	*ggt*	glutamyl-transpeptidase	8.75×10^{5} SC	100 Scarif. SchuS4	100% BALB/C	[94]
LVS	*sodB*	superoxide dismutase	1.0×10^{4} I.N.	14 I.N. SchuS4	40% C57BL/6J	[7]

Table 1.1 Continued

LVS	*wbtA*	LPS O-antigen biosynthesis	1.0 x 10^6 I.N.	25X LD_{50} I.D./I.N./I.P. LVS	100% BALB/C	[169]
			1.0 x 10^8 I.D.		100% BALB/C	
			1.0 x 10^7 I.P.		100% BALB/C	
LVS	*wtbI*	LPS O-antigen biosynthesis	2.8 x 10^7 I.P.	25X LD_{50} I.D. (LVS)	100% BALB/C	[114]
				25X LD_{50} I.P. (LVS)	60% BALB/C	
LVS	*wzy*	LPS O-antigen biosynthesis	1.5 x 10^7 I.N.	1.0 x 10^5 I.N. LVS	100% BALB/C	[104]
			3.5 x 10^6 I.N.	8 I.N. SchuS4	84% BALB/C	
LVS	*galU*	galactose utilization	1.0 x 10^7 I.N.	5.0 x 10^4 I.N. LVS	100% C57BL/6J	[95]
LVS	*fptB*	isoleucine transporter	3.0 x 10^3 I.P.	1.2 x 10^5 I.P.	100% BALB/C	[128]
	fptE	asparagine transporter	3.0 x 10^3 I.P.	1.2 x 10^5 I.P.	100% BALB/C	
	fptG	MFS transporter	3.0 x 10^6 I.P.	2.0 x 10^6 I.P.	100% BALB/C	
SchuS4	*FTT_1676*	hypothetical membrane protein	10 I.N.	10 I.N. SchuS4	45% BALB/C	[174]
				50 I.D. SchuS4	25% BALB/C	
			50 I.D.	10 I.N. SchuS4	100% BALB/C	
				50 I.D. SchuS4	100% BALB/C	

Table 1.1 Continued

SchuS4	*FTT_0369c*	hypothetical protein	10 I.N.	10 I.N. SchuS4	80% BALB/C	
				50 I.D. SchuS4	50% BALB/C	
			50 I.D.	10 I.N. SchuS4	90% BALB/C	
				50 I.D. SchuS4	100% BALB/C	
SchuS4	*FTT_0369c* + *FTT_1676*	double mutant lacking 2 hypothetical proteins	10 I.N.	10 I.N. SchuS4	10% BALB/C	
				50 I.D. SchuS4	30% BALB/C	
			50 I.D.	10 I.N. SchuS4	65% BALB/C	
				50 I.D. SchuS4	70% BALB/C	
LVS	*FTL_0439*	hypothetical protein	2.3×10^3 I.P.	1.2×10^5 I.P.	100% C57BL/6J	[194]
F. novicida	*pmrA*	orphan response regulator	1.0×10^6 I.N.	1.0×10^6 I.N. *F. novicida*	100% BALB/C	[141]
SchuS4	*fipB* (*dsbA*)	disulfide bond formation	1.3×10^8 I.N.	37 I.N. SchuS4	100% C57BL/6J	[164]
SchuS4	*dsbB*	disulfide bond formation	2.0×10^3 I.N.	13 I.N. SchuS4	0% C57BL/6J	[162]

Abbreviations: I.N. – intranasal, I.P. – intraperitoneal, I.D. intradermal, Scarif. – scarification, I.T. – intratracheal

Project Background

The ubiquity of MFS transporters in all domains of life has demonstrated the necessity and adaptability of members within this family to transport many important substrates across many species, including numerous pathogenic species [139, 171, 107]. As such, they are potentially important targets of exploitation for vaccine and small molecule therapies that have remained largely understudied. Intracellular bacteria, including facultative ones like *F. tularensis*, have been demonstrated to undergo genomic reductions, with transporter, biosynthesis, and metabolism genes being shed at a higher than random rate [135]. There is an implied necessity for transporter-encoding genes that remain in these pathogens, making them especially intriguing targets. Previous work in *L. pneumophila*, another intracellular bacterium within the Gammaproteobacteria class that is closely related to *F. tularensis*, demonstrated the value of targeting MFS transporters in facultative intracellular pathogens. Deletion of *phtA* (phagosomal transporter A), a threonine transporter, elicited a strong intra-macrophage growth defect, as well as greatly altering the replicative cycle for *L. pneumophila* [191]. A similar necessity for replication was demonstrated for *phtC* and *phtD*, other members within the phagosomal transporter family responsible for thymidine salvage [67].

A BLAST search of the *F. tularensis* Type A genome SchuS4 using *phtA* as the probe identified nine homologous genes, all of which have highly similar (≥98%) homologs in LVS [128]. As shown in Table 1.2, previous work in our lab endeavored to ascertain if these genes were necessary for intracellular replication and virulence. Eight of the nine identified *Francisella* phagosomal transporters (*fpt*) were successfully deleted in the *F. tularensis* LVS background. The loss of three of these eight, *fptB*, *fptE*, and *fptG*

Table 1.2. Summary of *fpt* family transporters in *Francisella tularensis* and their deletion phenotypes in *F. tularensis* LVS [128] (*unpublished results).

Strain	**LVS Gene ID**	**SchuS4 Gene ID**	**Altered Replication *in vitro***	**Attenuation in BALB/c mice**	**Highest dose tested (CFU)**	**Survival**
LVS	--	--	No	No	5.0×10^2	0/4
LVSΔ*fptA*	*FTL_1673*	*FTT_0104c*	No	Yes*	3.0×10^3	4/4
LVSΔ*fptB*	*FTL_1803*	*FTT_0056c*	Yes	Yes	3.0×10^5	2/4
LVSΔ*fptC*	*FTL_0946*	*FTT_0671*	No	No*	3.0×10^3	0/4
LVSΔ*fptD*	*FTL_1806*	*FTT_0053*	N/A	N/A	N/A	NA
LVSΔ*fptE*	*FTL_1645*	*FTT_0129*	Yes	Yes	3.0×10^4	2/4
LVSΔ*fptF*	*FTL_1647*	*FTT_0127c*	No	Yes*	6.0×10^3	4/4
LVSΔ*fptG*	*FTL_0443*	*FTT_1291*	Yes	Yes	3.0×10^6	4/4
LVSΔ*fptH*	*FTL_1573*	*FTT_0488c*	No	No*	5.0×10^3	1/4
LVSΔ*fptI*	*FTL_1528*	*FTT_0708*	No	No*	4.0×10^3	0/4

was found to cause significant alterations to the intracellular replication cycle of *F. tularensis* LVS. Deletion of *fptB* and *fptG* severely reduced replication in J774.1 macrophage-like cells, while deletion of any of the three greatly reduced replication in HepG2 hepatocyte carcinoma cells [128]. Furthermore, mutants lacking any of *fptB*, *fptE*, or *fptG* were highly attenuated when inoculated via the intraperitoneal route, as compared to WT LVS in BALB/C mice. Most intriguingly of all, when utilized as a vaccine, mice inoculated with these strains survived challenge with 1,000× the lethal dose of LVS, demonstrating their promise as vaccine targets [128].

Given the high level of homology between *F. tularensis* LVS and SchuS4 across the entirety of both genomes, and because we hypothesize that the Type A background will provide a higher level of protection against *F. tularensis* Type A challenge, the next step of development for an *fpt*-based live attenuated vaccine is derivation of *F. tularensis* Type A-based *fpt*-deficient strains. It was hypothesized that deletion of one of the four most promising *fpt* gene targets, *fptB*, *fptE*, *fptF*, or *fptG*, would result in strains with significant alterations to the intracellular replicative lifecycle that would render the strains attenuated for virulence. In addition, alterations in the intracellular lifecycle would reveal important aspects of the host-pathogen interaction. To this end, a suicide plasmid vector system was utilized to create targeted, marker-less deletions in the *F. tularensis* SchuS4 Type A background in the *fptB*, *fptE*, *fptF*, and *fptG* loci.

The four resulting mutant strains were tested for alterations to the replicative lifecycle. For *F. tularensis* SchuS4Δ*fptG*, SchuS4Δ*fptE*, and SchuS4Δ*fptF*, no aberrations were found in replication in Chamberlain's defined medium, a minimal broth medium. *F. tularensis* SchuS4Δ*fptB* was observed to replicate at a slower rate, and this growth attenuation was rescued with an excess of isoleucine, the substrate of the FptB transporter [77]. Two of the four strains, *F. tularensis* SchuS4Δ*fptG* and SchuS4Δ*fptB*, were delayed in cellular escape from macrophages, and in the case of SchuS4Δ*fptG*, hepatocytes. Additionally, *F. tularensis* SchuS4Δ*fptB* was found to be attenuated for growth in macrophages. The host innate immune response was found to be altered with regard to both strains that had altered replication mechanics. Both *F. tularensis* SchuS4Δ*fptB* and SchuS4Δ*fptG* were attenuated in the C57BL/6J mouse model, and ultimately, *F. tularensis* SchuS4Δ*fptB* was found to confer modest protection against virulent Type A *F. tularensis* challenge. Further work is needed in order to elucidate the molecular mechanism driving the escape delay phenotype uncovered by *F. tularensis* SchuS4Δ*fptG* and SchuS4Δ*fptB*, but a possible link to autophagy was made utilizing the vesicle acidification/autophagy inhibitor bafilomycin A1 in the context of SchuS4Δ*fptG* infection. A deeper investigation into the molecular mechanisms of the immune response engendered by *F. tularensis* SchuS4Δ*fptB* is also warranted, as vaccination with this strain was never able to protect fully against any dose of WT challenge. Over the course of this study, it has been demonstrated that members of the *Francisella* phagosomal transporters are important determinants of virulence and play a vital role in the timely progression of *F. tularensis* through its intracellular replication cycle.

Hypothesis: The central hypothesis of this work is that members of the *fpt* family are vital components of the intracellular pathogenic lifecycle of *Francisella tularensis*, and as such, are valuable targets for the development of a live attenuated vaccines derived from the virulent Type A strain.

<u>Aim I:</u> Construction and *in vitro* characterization of single knockout *fpt* Type A strains.

Deletion mutants will be evaluated in both cell-free and intracellular environments. Standardized growth curves in minimal defined media will ascertain if any of the *fpt* genes are necessary for *in vitro* replication. Then, gentamicin protection assays will determine the abilities of the mutants to replicate, survive, and escape from relevant model cell types, as intracellular proliferation is a key determinant of virulence for *F. tularensis* [4, 133]. In the course of the gentamicin protection assays, the early *in vitro* cytokine response will be examined both at the level of transcription, and cytokine secretion. Early innate immune responses are important determinants of the success of the overall response to *F. tularensis*, and guide both survival, and vaccine efficacy [51, 127, 61].

<u>Aim II:</u> Characterization of attenuation and the protective capacity of Type A-based *fpt* knockout mutants in C57BL/6J mice.

Type A *F. tularensis* causes a lethal infection in mice, and C57BL/6J strain mice are exceptionally susceptible with as few as ≤ 10 CFU being lethal [29, 167], making them a rigorous background upon which to test for attenuation and the protective abilities of *fpt* mutant strains. Both male and female mice will be utilized, to control for the possibility of gender bias [210]. To ascertain an LD_{50}, mice will be inoculated with increasing doses of an *fpt* mutant strain, and will be monitored for survival and clinical signs of sickness such as weight loss, lethargy, and ruffling of fur. Should a strain be sufficiently attenuated, the protective capacity of this strain will be tested.

<u>Aim III:</u> Determination of the role of FptG in virulence and the investigation of the importance of autophagy in the host escape delay phenotype of *F. tularensis* SchuS4Δ*fptG*.

To date, the substrate transported by FptG has yet to be identified. Due to the genetic identity between *F. tularensis* LVS and SchuS4 at the *fptG* locus, LVSΔ*fptG* will be utilized in supplemented minimal media growth curves to ascertain the nature of the substrate for *fptG*. Findings in the *F. tularensis* LVS background will be translated to the SchuS4 background for further confirmation. Furthermore, *F. tularensis* SchuS4Δ*fptG* exhibits no replicative defect, but instead a significant delay in escape from the host's cytosol in multiple cell types, a novel phenotype in *Francisella*. Investigations utilizing gentamicin protection assays supplemented with the autophagy inhibitor bafilomycin A1 will aim to identify if the escape delay phenotype relies upon *Francisella's* induction of autophagy [26, 45, 204].

At the end of these studies, we expect to have identified *Francisella* phagosomal transporters that are required for normal intracellular lifecycle progression, pathogenesis, and virulence. On the weight of prior studies in *F. tulanrensis* LVS, it is expected that several, if not all, mutants will exhibit some sort of *in vitro* deficiency, and will be both variably attenuated and protective in *in vivo* studies. Ultimately, the viability of targeting *fpt* genes, and the viability of targeting nutrient transporters in general, will be tested in the virulent Type A background of *Francisella tularensis*.

Chapter 2 – Materials and Methods

Bacteria and Growth Conditions

Bacterial strains utilized in this study are listed in Table 2.1. *F. tularensis* SchuS4 was obtained from BEI Resources (Manassas, VA) and preserved in supplemented Mueller Hinton broth (BD Microbiology Systems, Sparks, MD) with 15% glycerol and stored at -80° C for long-term storage. *F. tularensis* LVS was obtained from the ATCC (Manassas, VA), and was kindly provided by Dr. Karen Elkins (CBER/FDA, Rockville, MD). LVS was maintained for long term storage as outlined above. Working bacterial stocks for use in *in vitro* and *in vivo* experiments were prepared in supplemented Mueller Hinton broth using bacteria concentrated from a supplemented Mueller Hinton agar plate. Bacteria were re-suspended to a concentration of approximately OD_{600nm} 0.6 and aliquoted for storage at -80° C.

Mueller Hinton broth (MHB) is supplemented with 1% Isovitalex (BD, Sparks, MD), 0.25% ferric pyrophosphate (Sigma, St. Louis, MO), 0.1% glucose, 0.105 g hydrous $MgCl_2$ (Sigma, St. Louis, MO), and 0.09 g CaCl2·2H2O (Sigma, St. Louis, MO). Mueller Hinton Agar (MHA) was supplemented with 1% Isovitalex (BD, Cockeysville, MD), 0.25% ferric pyrophosphate (Sigma, St. Louis, MO), 0.1% glucose, 10% defibrinated sheep blood (Lampire Biological, Pipersville, PA), 1.6% granulated agar (BD Bioscience, Sparks, MD), 1% bacto-tryptone (BD Bioscience, Sparks, MD), and 0.5% NaCl (Sigma, St. Louis, MO). Liquid cultures were grown on a shaker at 37° C and 5% CO_2. Solid cultures were grown in an incubator at 37° C and 5% CO_2. Selection parameters for co-integrants utilized kanamycin (Sigma, St. Louis, MO) at a final culture

Table 2.1: *F. tularensis* LVS and SchuS4 strains utilized in this study

Strain	**Characteristic**	**Source**
LVS	attenuated Type B vaccine strain	CBER/FDA
LVSΔ*fptB*	LVS strain lacking FTL_1803	Laboratory collection [128]
LVSΔ*fptC*	LVS strain lacking FTL_0946	Laboratory collection [128]
LVSΔ*fptE*	LVS strain lacking FTL_1645	Laboratory collection [128]
LVSΔ*fptF*	LVS strain lacking FTL_1647	Laboratory collection [128]
LVSΔ*fptG*	LVS strain lacking FTL_0443	This Study
LVSΔ*fptB*Δ*fptC*	LVS strain lacking FTL_1803 and FTL_0946	This Study
LVSΔ*fptF*Δ*fptE*	LVS strain lacking FTL_1647 and FTL_1645	This Study
SchuS4	Wildtype Type A *Francisella tularensis*	BEI
SchuS4Δ*fptB*	Type A strain lacking FTT_0056c	This Study
SchuS4Δ*fptE*	Type A strain lacking FTT_0129	This Study
SchuS4Δ*fptF*	Type A strain lacking FTT_0127c	This Study
SchuS4Δ*fptG*	Type A strain lacking FTT_1291	This Study
SchuS4Δ*fptG*Comp	*Trans*-complement of *fptG*	This Study
SchuS4Δ*fptB*Comp	*Trans*-complement of *fptB*	This Study

concentration of 10 µg/mL or sucrose at 0.5 M solubilized in MHB or at 8% volume in MHA.

<u>Targeted Deletion of Genes in *F. tularensis*</u>

F. tularensis SchuS4 or LVS was transformed via electroporation. First, competent cells were produced by resuspending a fully grown MHA plate of WT *F. tularensis* into 2 mL of 0.5 M sucrose in PBS (Corning, Manassas, VA) distributed in to 4 1.5 mL Eppendorf tubes. Bacteria were pelleted via centrifugation at 5,000 RPM (1,400 × g) for 15 minutes, and supernatants were discarded. Pellets were re-suspended with fresh 0.5 M sucrose via pipetting. Pelleting and resuspension steps were repeated a total of 3 times, before resuspending at a final volume of 50 µL per tube and combining into one tube. At this stage, the desired suicide plasmid (Table 2.2), approximately 150 µL in volume prepared from a 500 mL LB broth culture of DH5α *E. coli* (Qiagen Midi-Prep, Germantown, MD), was mixed thoroughly among the bacteria with gentle pipetting, then the entire mixture transferred to a 0.2 cm electroporation cuvette (BioRad, Hercules, CA). Bacteria were pulsed 3× at 1,750 KV, 25 µF, and 600Ω. After electroporation, bacteria were recovered using MHB, and allowed to incubate at 37° C and 5% CO_2 shaking at 150 RPM for approximately 1 hour. To begin selection for co-integrant strains, the bacterial suspension was plated on MHA plates containing kanamycin and allowed to incubate at 37° C and 5% CO_2 for no less than 5 days. Co-integrant strains were confirmed by replica plating to fresh kanamycin-containing MHA plates and PCR.

Once co-integration was confirmed, counter-selection was begun to find double-recombinants. Counter-selection was begun by first plating the confirmed co-integrant to

Table 2.2: Plasmids utilized in the construction of *F. tularensis* LVS and SchuS4 deletion mutants

Plasmid	**Characteristics**	**Source**
pFT893Δ*fptB*	Suicide plasmid for FTT_0056c/FTL_1803	[128]
pFT893Δ*fptG*	Suicide plasmid for FTT_1291/FTL_0443	[128]
pFT893Δ*fptE*	Suicide plasmid for FTT_0129	[128]
pFT893Δ*fptF*	Suicide plasmid for FTT_0127c	[128]
pFT893Δ*fptA*	Suicide plasmid for FTL_1673	[128]
pFT906*fptG*	Trans-complement plasmid of *fptG*	[128]
pFT906*fptB*	Trans-complement plasmid of *fptB*	[128]

a kanamycin-free MHA plate and allowing 2-3 days of growth. A swab was taken through the thickest growth and re-suspended into MHA containing 10% sucrose. Double- recombinant strains have lost the plasmid and the corresponding *sacB* selection marker, and will thus be unaffected by the presence of high levels of sucrose, while plasmid containing bacteria will be severely affected. Sucrose curing was allowed to occur overnight at 37° C and 5% CO_2 while shaking at 150 RPM. The sucrose culture was then diluted out to 10^{-4}, and the entirety of all dilutions were plated to MHA plates containing 8% sucrose. Colonies formed on sucrose plates were re-plated to fresh sucrose plates, and were screened for loss of the target gene via PCR using primers outlined in Table 2.3.

Table 2.3: DNA primers utilized in the construction and characterization of *fpt* mutant strains

Primer	Sequence	Function	Strain
Fpt_G Forward	TCTAGGTGGTGTCACCAAAC	External primers *fptG*	LVS, SchuS4
Fpt_G Reverse	AGCAAACCGCTATGGTATCC	External primers *fptG*	LVS, SchuS4
Fpt_B_SchuS4_F	CCCTGGACTGAACTGCTTAT	External primers *fptB*	LVS, SchuS4
Fpt_B_SchuS4_R	CGGTTAGGCATCTACAAGGA	External primers *fptB*	LVS, SchuS4
Fpt_F_SchuS4_F	TGTTCCGCCGTAAATCTCAAGC	External primers *fptF*	SchuS4
Fpt_F_SchuS4_R	GAACCAGTTAGCGCGTTAGATGTG	External primers *fptF*	SchuS4
SchufptE_F	GGCGCACAATATCGTACTCAAC	External primer *fptE*	SchuS4
SchufptE_R	TTTGATCTGGCTTAACGCGGCCAAAC	External primer *fptE*	SchuS4
Fpt_A Forward	GGTTGTTGGCGTAATACC	External primer *fptA*	LVS
Fpt_A Reverse	GCGATTGGAGATGATAGC	External primer *fptA*	LVS
Fpt_C forward	AAAGCTAAGCTAGCGAC	External primer *fptC*	LVS
Fpt_C reverse	TAGAGCTGCTGCACTTGG	External primer *fptC*	LVS
SchuS4_inB_F	TTTGCCTTTGCCGCAAGCTTTC	Internal primer *fptB*	SchuS4, LVS
SchuS4_inB_R	CCAATAATTGGTGAGCCGATAGCC	Internal primer *fptB*	SchuS4, LVS
SchuS4_inG_F	CCGCTTTCATGTGGTCATATGC	Internal primer *fptG*	SchuS4, LVS
Schus4_inG_R	GCAACTAATGCCCATGTTGGAG	Internal primer *fptG*	SchuS4, LVS
LVS_inF_F	ATGGGCTGGCTTACTCTATACG	Internal primer *fptF*	SchuS4, LVS
LVS_inF_R	TCGCCACTATCAATAGCGAGTC	Internal primer *fptF*	SchuS4, LVS
LVS_inE_F	GCAAGTCCTGCATAATGCACTGAG	Internal primer *fptE*	SchuS4, LVS
LVS_inE_R	TGGGCTTATGTGGCATCACAAC	Internal primer *fptE*	SchuS4, LVS
LVS_inA_F	CCTAAAGTTCTGGGCTGCAAG	Internal primer *fptA*	LVS
LVS_inA_R	TACTCTCGCTGTTGCTGATCC	Internal primer *fptA*	LVS

Table 2.3 Continued

LVS_inC_F	ACACTGAAAGTGGCTGCTGATG	Internal primer *fptC*	LVS
LVS_inC_R	AGGAAGGACCTCCAACTGCTATAC	Internal primer *fptC*	LVS

Bacterial Growth Curves

The impact of the deletion of *fpt* genes on the replication rate of the *F. tularensis* Type A strain was first assessed in broth culture. Growth curves were performed in Chamberlain's Defined Medium [25] (CDM) (Teknova, Hollister, CA), and either WT *F. tularensis* or an *fpt* mutant were grown from a starting OD_{600} approximately 0.1. Cultures were grown at 37° C and 5% CO_2 while shaking at 150 RPM, and OD_{600} readings were taken every 1.5 hours over the course of 7.5 hours.

Supplementation experiments utilizing either *F. tularensis* LVS and LVSΔ*fptG* were undertaken using CDM supplemented with either 0.5% casamino acids (Fisher Scientific, Pittsburgh, PA), 3 mM methionine (Sigma, St. Louis, MO), 2X glucose (Sigma, St. Louis, MO), 5X thiamine (Sigma, St. Louis, MO), 4X calcium pantothenate (TCI America, Portland, OR), or 3X spermine phosphate hexahydrate (Santa Cruz Biotechnology, Dallas, TX). Experiments using *F. tularensis* SchuS4Δ*fptB* included 3 mM isoleucine supplementation(Acros Organics, Geel, Belgium). Experimental time courses and setup for all supplementation assays were as outlined above.

To assess the impact of a second *fpt* deletion from the *F. tularensis* LVS genome, *F. tularensis* strains LVS, LVSΔ*fptF*Δ*fptA*, and LVSΔ*fptC*Δ*fptB* were grown in a 96 well flat-bottom plate in 100 µL of MHB over 25 hours in a Tecan m200 Pro set to rock at 100 RPM, and maintain 37° C and 5% CO_2. Strains were plated in decuplicate.

Intracellular Replication and Escape Assays

The ability of *F. tularensis* Type A strain-derived *fpt* mutant strains to replicate and spread cell-to-cell was evaluated in THP-1 human macrophage-like cell line and HepG2 human hepatocyte carcinoma cell line cells (ATCC, Manassas, VA), as well as in C57BL/6J mouse bone marrow derived macrophages (BMDMs) and human monocyte derived macrophages (MDMs). *F. tularensis* LVS-derived *fpt* single and double mutant strains were evaluated in the RAW 264.7 macrophage-like cell line (ATCC, Manassas, VA).

THP-1 cells were cultivated in Roswell Park Memorial Institute 1640 medium (RPMI 1640) (Cellgro, Manassas, VA) supplemented with 10% FBS (Sigma, St. Louis, MO), and 0.1% 1000× 2-mercaptoethanol (Gibco, Gaithersburg, MD) and maintained at 37°C in 5% CO_2. Three days before the beginning of an assay, THP-1 cells were seeded at a density of 1×10^6 cells per well in 12-well plates (Corning Costar, Corning, NY) and differentiated using phorbol myristate acetate (PMA) (Sigma, St. Louis, MO) at a concentration of 50 ng/mL for 24 hours. Media was then changed to RPMI 1640 supplemented as described above.

For assays to assess bacterial replication, cells were infected at a multiplicity of infection (MOI) of 100 with either *F. tularensis* SchuS4 or an *fpt* mutant for a period of 2 hours. Following the 2 hour infection, cells were washed twice with PBS and incubated in RPMI 1640 containing 50 μg/mL gentamicin (Gibco, Gaithersburg, MD) for 1 hour. At 3 hours post infection (hpi), cells were washed again 2X with PBS, and placed into fresh RPMI 1640 lacking gentamicin. Bacterial replication was assayed at 3, 24, and 48 hours post-infection by lysing cells with a 0.02% SDS in PBS solution, followed by serial dilution and plating on MHA. Supernatants were saved for downstream analyses.

For assays to assess bacterial escape kinetics, the infection and washing steps were repeated as shown above through 3 hpi. Instead, gentamicin containing media was not washed off cells, and thus cells were left for the duration of the assay in 50 μg/mL gentamicin. CFU were sampled as described above in either 3, 24, and 48 hour time courses, or 3, 9, 15, 21, 27, and 33 hour time courses. Supernatants were saved for downstream analyses.

HepG2 cells were cultured in Eagle's Minimal Essential Medium (EMEM) (Cellgro, Manassas, VA) supplemented with 10% FBS and maintained at 37°C in 5% CO_2. One day prior to the start of an assay, HepG2 cells were seeded at a density of 1×10^6 per well in a 12 well plate and infected at an MOI of 300 at the start of the assay. Infection and washing protocols are as described above for both replication and escape kinetics assays with time points for CFU sampling at 3, 24, and 48 hpi.

RAW264.7 mouse macrophage-like cells were cultured in Dulbecco's Modified Essential Medium (DMEM) (Cellgro, Manassas, VA) supplemented with 10% FBS and were maintained at 37°C in 5% CO_2. One day prior to the start of an assay, RAW264.7 cells were seeded at a density of 1×10^6 per well on a 12 well plate, and at assay start, were infected at an MOI of 100 with either *F. tularensis* LVS or an *fpt* mutant strain. Infection and washing protocols are as described above for both replication and escape kinetics assays with time points for CFU sampling at 3, 24, 48, and 72 hpi.

Bone marrow derived macrophages (BMDMs) were extracted from femurs taken from 6-8 week old C57BL/6J mice (University of Maryland, Baltimore, Veterinary Resources Breeding Facility) and flushed with DMEM supplemented with 10% low endotoxin FBS (Gemini Bioproducts, West Sacramento, CA), 30% L929 supernatants, 1% non-essential amino acids (ThermoFisher Scientific, Waltham, MA), 1% HEPES (ThermoFisher Scientific, Waltham, MA)), and 1% penicillin/streptomycin (ThermoFisher Scientific, Waltham, MA). Cells were passed through a 70 µm nylon mesh (Fisher Scientific, Pittsburgh, PA) to remove debris and were placed into a T175

(Corning) flask for culture and differentiation. Fresh media was replaced on the day after extraction, and every other day subsequently for at least 1 week. The day before an assay, cells were scraped gently, centrifuged at 1,100 RPM (125 × g) for 10 minutes, and re-suspended at a concentration of 5×10^5 per milliliter in complete media lacking penicillin/streptomycin. Cells were plated in a 24 well plate (Corning Costar, Corning, NY). At time of infection, cells were infected with an MOI of 10. Infection and washing protocols are as described above for replication kinetics assays with time points for CFU sampling at 3, 8, and 24 hpi. Supernatants were saved for downstream analyses.

Monocyte-derived macrophages (MDMs) were isolated from 100 mL whole human blood obtained in EDTA tubes (BD Microbiology Systems, Sparks, MD) from normal, healthy volunteers by the University of Maryland, Baltimore Center for Vaccine Development clinical staff. Blood was diluted 1:2 in PBS before being added to 15 mL of ficoll (GE Healthcare, Laurel, MD) in SepMate tubes (Stem Cell Technologies, Cambridge, MA). SepMate tubes were spun at 1,200 xg for 15 minutes at room temperature. Red blood cells were depleted using ACK lysis buffer (Gibco, Gaithersburg, MD). Isolated MDMs were cultured for one week before the start of an assay in T75 flasks (Costar, Corning, NY) with RPMI 1640 supplemented with 10% low endotoxin FBS (Gemini Scientific, West Sacramento, CA), 1% non-essential amino acids (ThermoFisher Scientific, Waltham, MA), 1% HEPES (ThermoFisher Scientific, Waltham, MA), and 1% sodium bicarbonate (ThermoFisher Scientific, Waltham, MA). Media was changed daily. Two days before the start of an assay, cells were scraped from the flask, enumerated, and plated at a density of 5×10^5 cells per well in a 24 well plate (Costar, Corning, NY). At time of infection, cells were infected with an MOI of 10.

Infection and washing protocols are as described above for replication kinetics assays with time points for CFU sampling at 3, 8, and 24 hpi. Supernatants were saved for downstream analyses.

Complementation of *fpt* Mutant Strains

Plasmids containing either *fptB* or *fptG* under the control of the *F. tularensis guaB* promoter (Table 2.3) were electroporated into the *F. tularensis* SchuS4 mutant strain as described previously. Complemented strains were evaluated in the THP-1 infection model described previously.

Quantification of Host Cell Membrane Permeability

In order to assess changes to host cell membrane permeability during the course of infection with *F. tularensis* SchuS4 or *fpt* mutants, the levels of lactate dehydrogenase (LDH) released to the supernatants was quantified. LDH release was measured using a Cytotox 96 (Promega, Madison, WI) kit carried out according to the manufacturer's protocol. Briefly, 50 µL of cell-free supernatants were plated in triplicate to a flat-bottom 96 well plate and were combined with 50 µL of reagent solution. The plate was shielded from light and allowed to incubate at room temperature for 30 minutes. Next, 50 µL of stop solution is added to each well to end exposure. Measurement of samples was done using a VersaMax plate reader (Molecular Devices, Sunnyvale, CA) at 490 nm wavelength. Where appropriate, the following equation was utilized to calculate percent cytotoxicity:

$$\text{Percent Cytotoxicity} = 100 \times \frac{\text{Experimental LDH Release }(\mathbf{OD}490)}{\text{Maximum LDH Release }(\mathbf{OD}490)}$$

Maximum LDH release was achieved by incubating control cells with a 0.02% SDS in PBS solution for 1 hour at room temperature.

Quantification of Cytokine Protein Secretion

IL-1β and TNF-α protein levels in THP-1 assay supernatants were measured by ELISA (R&D Systems, Minneapolis, MI). Supernatants were collected at 3, 9, 15, 21, 27, and 33 hours post-infection and stored at -80° C before sterilization and removal from the BSL-3. Per the manufacturer's guidelines, a high binding 96 well plate was coated with 100 µL capture antibody diluted in PBS and allowed to incubate overnight at room temperature. This solution was then discarded and plates were washed 3X with 150 µL of wash buffer per well (0.05% Tween 20 in PBS), before being blocked with 100 µL of reagent diluent (1% BSA in PBS) per well for two hours at room temperature. After blocking, plates were washed as previously described, and 100 µL of supernatant samples were added in duplicate and allowed to incubate at room temperature for 2 hours. Plates were washed as previously described, and 100 µL of detection antibody was added per well and allowed to incubate at room temperature for 2 hours. Plates were washed again as previously described, before the addition of 100 µL per well diluted Streptavidin-HRP. ELISA plates were allowed to incubate for 20 minutes at room temperature with Streptavidin-HRP before being washed once again. After washing, 100 µL per well of substrate solution (KPL, Gaithersburg, MD) was added to each well, and allowed to incubate, shielded from light, at room temperature for 20 minutes. After incubation, 50 µL per well stop solution (1 N phosphoric acid) was added to each well before reading at 450 nm with correction for plate imperfections set at 540 nm on a VersaMax plate reader (Molecular Devices, Sunnyvale, CA).

Western Blot Analysis

THP-1 macrophage-like cells were seeded to a 12 well plate as previously described. Sets of 4 wells of cells were then left untreated, or treated with bafilomycin A1 for the periods of time described previously. Cells were then scraped, combined, and lysed in 70% Tergitol buffer (Sigma-Aldrich, St. Louis, MO), then boiled for 10 minutes at 100° C. Samples were then run on a 12% acrylamide gel, and transferred using an iBlot2 dry blot system (ThermoFisher, Waltham, MA). The sample was then blocked in a 5% milk-TBST solution for one hour at room temperature, before being incubated with rabbit anti-LC3 primary antibody (Novus Biologicals, Littleton, CO) overnight at 4° C. The next day, the membrane was washed 3X for ten minutes each at room temperature with 0.05% TBST before incubating for one hour with goat anti-rabbit secondary antibody conjugated to horseradish peroxidase (BioRad, Hercules, CA). The membrane was again washed 3X at room temperature for ten minutes each before being treated with TMB peroxidase substrate (KPL, Gaithersburg, MD) and reading on a BioRad ChemiDoc MP (BioRad, Hercules, CA) at 650 nm.

Loading control was accomplished by stripping the blot of LC3 staining with Restore (ThermoFisher, Waltham, MA) for ten minutes at room temperature and incubating with rabbit anti-β actin (Novus Biologcals, Littleton, CA) overnight at 4° C. The membrane was then washed as described previously, and incubated with anti-rabbit secondary antibody as described earlier. The membrane was measured at 650 nm as previously described.

Determination of Attenuation of *F. tularensis* SchuS4Δ*fptG* and SchuS4Δ*fptB*

Alterations to the virulence of *F. tularensis* SchuS4Δ*fptG* and SchuS4Δ*fptB in vivo* was determined using the C57BL/6J mouse. Groups of 4 mice were anesthetized with a mix of 80 mg/kg ketamine/10 mg/kg xylazol and were inoculated intranasally (I.N.) with 20 µL doses ranging from 2.0×10^1 through 7.6×10^6 CFU of either *fpt* mutant, or between 1.1×10^1 to 5.4×10^1 CFU of WT *F. tularensis* SchuS4. Mice were checked daily for clinical signs of illness and were weighed every other day during a time course of 14 days. Mouse health was scored based on the following criteria: **Condition 1** – normal activity; mice run freely and energetically around the cage and resist when picked up. **Condition 2** – mice are slower than usual and offer less resistance when picked up. **Condition 3** – mice exhibit a hunched posture, move very slowly, and display ruffled, dull fur and squinted eyes. **Condition 4** – mice are almost entirely sedentary, hunched, and are either unresponsive or barely responsive to prodding. Fur is very ruffled and dull. Mice scored at condition 3 were observed and weighed twice a day, while mice scored at condition 4 were euthanized. A second euthanasia criterion was the loss of > 20% of the original starting body weight. All animal work conformed to the regulations of and were approved by the UMB IACUC.

Determination of Protective Capacity

To test the ability of *F. tularensis* SchuS4Δ*fptB* to protect against virulent WT challenge, groups of 4 mice were inoculated with approximately 1×10^6 CFU SchuS4Δ*fptB* in either a single 20 µL intranasal dose, or prime/boost regimen. Mice receiving a single inoculum were monitored for 28 days before receiving 20 µL intranasal challenge doses ranging between 5×10^1 to $5 \text{ x } 10^2$ CFU. Mice receiving the prime/boost regimen were dosed as described above and monitored for 14 days before receiving a second inoculum of ~1×10^6 CFU SchuS4Δ*fptB*. These mice were then monitored for 28 days before receiving 20 µL intra-nasal challenge doses ranging between 5×10^1 to 1×10^3 CFU. All challenged mice were then monitored and weighed daily for 14 days post-challenge. Mouse health scoring and euthanasia criteria were as described in the attenuation studies. Average day of death for each mouse group was calculated excluding survivors.

Statistical Analysis

Using GraphPad Prism 7.0 (GraphPad Software, San Diego, CA), two-way analysis of variance (ANOVA) with Tukey's post-hoc was performed to assess statistical significance between bacterial CFU counts, calculated bacterial doublings, LDH release levels, and cytokine ELISAs ($p < 0.05$). One-way ANOVA with Tukey's post-test was performed to assess statistical significance between *F. tularensis* LVS OD_{600} readings in MHB broth curves. Bacterial doublings were calculated utilizing the formula:

$$(\log_{10}T_n - \log_{10}T_{(n-1)}) \times 3.32$$

T_n is the number of colony forming units (CFU) at one time point, and $T_{(n-1)}$ is the CFU number at the prior time point [128]. In all instances, WT *F. tularensis* SchuS4, or *F. tularensis* LVS served as the reference strain for all statistical tests. Statistical analyses were performed in conjunction with the Center for Vaccine Development Biostatistics core.

Chapter 3 – Mutagenesis and *in vitro* characterization of *Francisella tularensis* LVS strains lacking *fpt* genes

Generation of *F. tularensis* LVS double mutant strains LVSΔ*fptF*Δ*fptA* and LVSΔ*fptC*Δ*fptB*

Previous studies in this laboratory determined that single deletions of selected *fpt* genes in LVS resulted in growth attenuation [128]. We reasoned, therefore, that a combination of *fpt* deletions would result in further attenuation. To assess the effect of combination deletions on attenuation, double deletion mutants were engineered in the strain *F. tularensis* LVS, targeting *fpt* genes that were only minimally attenuating on their own. For both double mutants engineered, a suicide plasmid vector system dependent upon homologous recombination was utilized to generate a marker-less deletion of a second targeted gene in a pre-existing single deletion mutant strain [128]. The first gene targeted was *fptA*, and deletion of this gene was generated in the *F. tularensis* LVSΔ*fptF* strain. Figure 3.1 is a diagram of one of the suicide vectors utilized and how integration occurs. Following electroporation, co-integrant colonies were selected by growth on kanamycin plates. Co-integration was confirmed by PCR. Counter-selection to cure the plasmid was accomplished in sucrose broth and spread plating on sucrose plates. Genomic preparations of co-integrant and sucrose-cured strains were used as templates in PCR reactions to confirm gene deletion (Fig 3.2). Specifically, two sets of primers were utilized to screen and confirm mutants. One primer pair annealed to the upstream and downstream flanks of the targeted gene, and the second set annealed within the gene itself. As demonstrated in Figure 3.2, upon successful deletion of *fptA* in several selected colonies, a smaller fragment was amplified in lanes 1-5 that corresponds to the size of the deleted gene. Lane 6, containing the co-integrant, exhibited both the larger WT band, and

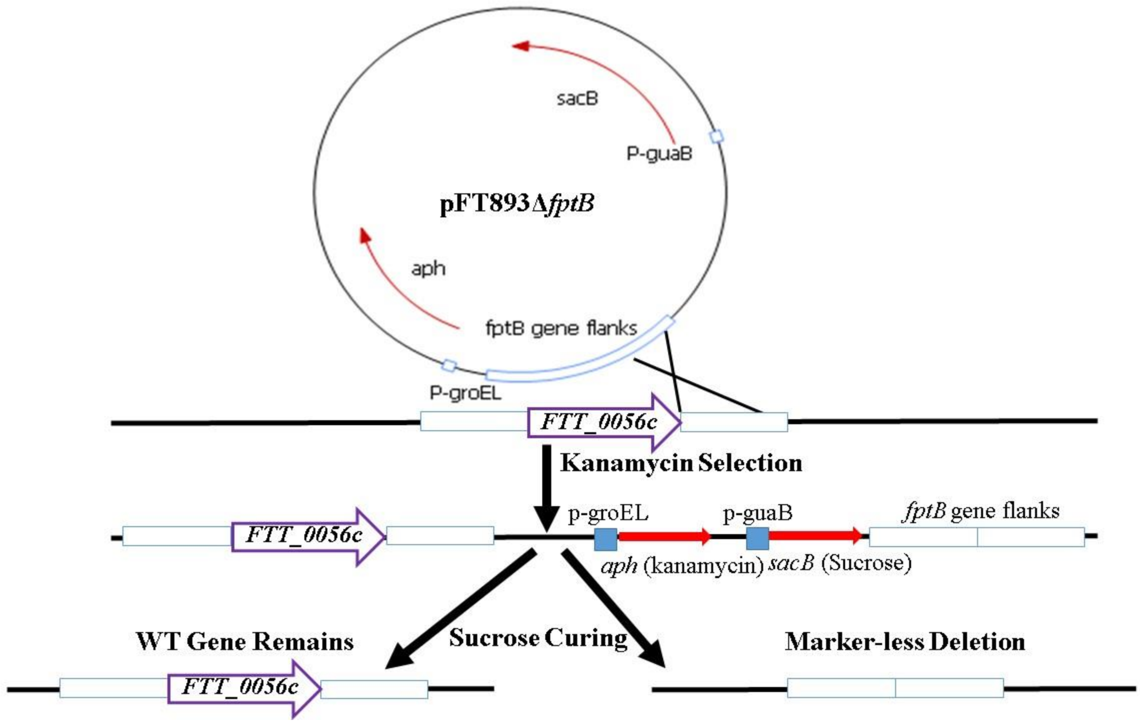

Figure 3.1. Suicide vector utilized in marker-less deletion of *fpt* genes and its integration into the *Francisella* genome. Important elements of the suicide plasmid include the *aph* cassette, allowing for selection with kanamycin for plasmid integration into the chromosome. The *sacB* gene encoding levansucrase allows for the selection of colonies that have recombined to lose the suicide plasmid. The origin of replication for the plasmid is not maintained in *Francisella*. Fragments of ~500 bp encoding the upstream and downstream flanks of the targeted gene were cloned into the suicide plasmid. Electroporation and selection for kanamycin identifies co-integrant strains that have incorporated the plasmid into the genome via homologous recombination. Sucrose curing enriches for strains that have spontaneously lost the suicide plasmid. Resulting sucrose cured, kanamycin-sensitive strains either revert to WT at the selected locus, or harbor marker-less deletions, or are screened by PCR to confirm status of the targeted gene.

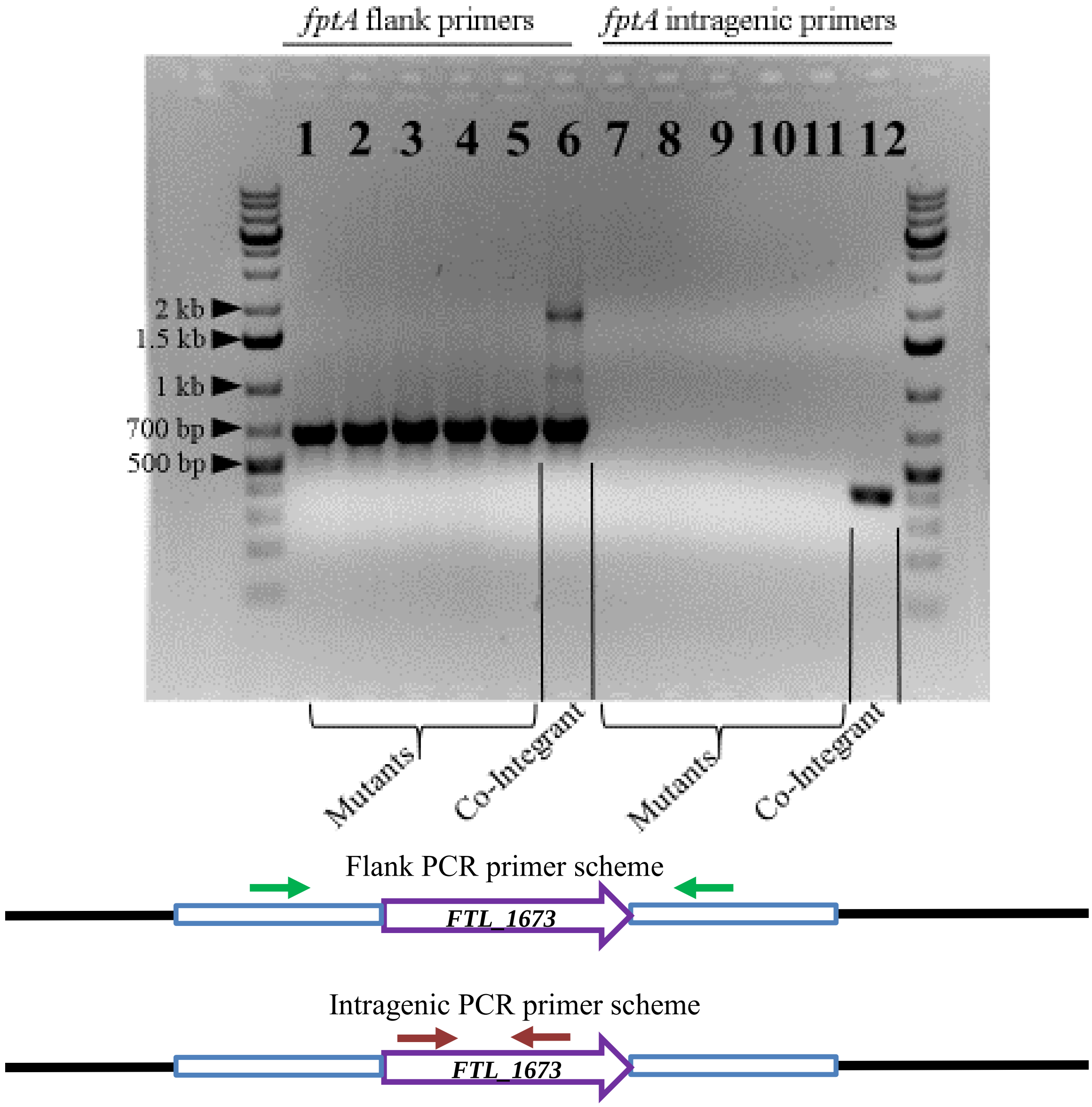

Figure 3.2. Confirmation of deletion of *FTL_1673* (*fptA*). The top panel is a representative gel showing PCR products that confirm the deletion of the *fpt* gene *FTL_1673* (*fptA*) from the *F. tularensis* LVSΔ*fptF* genome. The bottom panel demonstrates the location and orientation of screening primer pairs used to ascertain deletion of *fptA*. Single colony deletion strains (lanes 1-5 and 7-11) or co-integrants (lanes 6 and 12) were used as templates for PCR with primers "Fpt_A_Forward" and "Fpt_A_Reverse" that anneal upstream and downstream of *fptA* (lanes 1-6) or with primers "LVS_inA_F" and "LVS_inA_R" that anneal within *fptA* (lanes 7-12). Band sizes for all lanes under the "*fptA* flank primers" section are as follows: lanes 1-5 show the predicted 671 bp band corresponding to a deletion of the *fptA* gene with PCR primers in the upstream and downstream flanks. Lane 6 exhibits the WT band at 1,903 bp and the smaller band resulting from the the suicide plasmid in the co-integrant strain. Lanes 7-11 exhibit no band, corresponding with the complete absence of the *fptA* gene in the *F.*

tularensis LVSΔ*fptF*Δ*fptA* strains. Lane 12 exhibits the expected 400 bp band of the *fptA* gene present in the LVSΔ*fptF* co-integrant strain.

the deleted band. No bands were amplified in lanes 7-11 of the mutants, as primers originating within the *fptA* gene would be unable to bind, while bands do appear with the co-integrant strain in lane 12.

A second double deletion mutant was generated in the same manner. A pre-existing single mutant strain, *F. tularensis* LVSΔ*fptC,* was electroporated with a suicide plasmid targeting the *fptB* locus. The resulting kanamycin resistant and sucrose-cured colonies were tested by PCR to confirm deletion of *fptB* (Figure 3.3). Primers were located in the upstream and downstream flanks of the *fptB* gene. The reduced size band in lanes 1, 5, 6, 7, 9, and 10 correspond to loss of the *fptB* gene, while the larger band just below 2 kB corresponds to the presence of the WT gene.

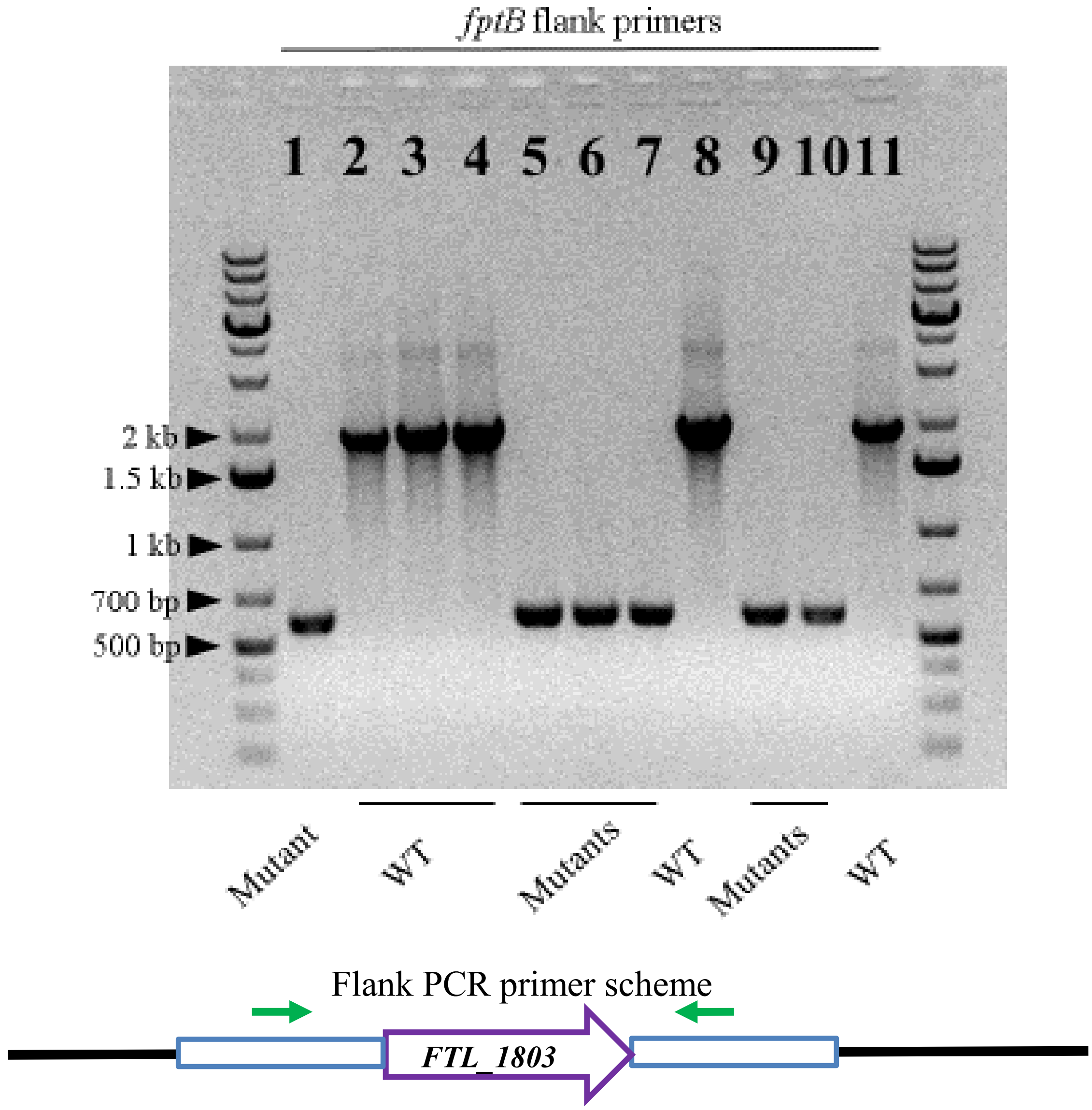

Figure 3.3. Confirmation of the deletion of *FTL_1803* (*fptB*). The top panel is a representative PCR gel of sucrose-cured strains tested for the status of the *fptB* gene. Single colony deletion strains were used as templates for PCR with primers "Fpt_B_SchuS4_F" and "Fpt_B_SchuS4_R" that anneal upstream and downstream of *fptB*. Lanes 1, 5, 6, 7, 9, and 10 exhibit the expected 594 bp band consistent with loss of the *fptB* gene when PCR primers extend from either region flanking the gene. The remaining lanes show bands at 1,918 bp, indicative of the presence of the WT gene. The bottom panel indicates primer locations in this PCR gel.

Evaluation of growth in broth of *F. tularensis* LVSΔ*fptF*Δ*fptA* and LVSΔ*fptC*Δ*fptB*

An initial test of the *in vitro* growth characteristics of the *F. tularensis* LVSΔ*fptF*Δ*fptA* double mutant was performed in Mueller Hinton broth (MHB). *F. tularensis* LVSΔ*fptF*Δ*fptA* replicated at a rate similar to that of both single mutant strains, LVSΔ*fptF* and LVSΔ*fptA*, and all three deletion strains were significantly increased ($p > 0.0001$) from that of parental LVS strain from 12 hours onwards (determined by one-way ANOVA) (Figure 3.4). Despite this, all four strains fit tightly ($R^2 > 0.99$) to a sigmoidal non-linear regression model, indicating a replication rate not deviating from the expected rate.

The replication rate in MHB of *F. tularensis* LVSΔ*fptC*Δ*fptB* was also measured as described above. *F. tularensis* LVSΔ*fptC*Δ*fptB* replicated at a rate similar to that of both the single mutant strains LVSΔ*fptC* and LVSΔ*fptB*, and all three deletion strains were significantly reduced ($p > 0.0001$) compared to parental LVS strain (as determined by one-way ANOVA) (Figure 3.5) . All four strains fit tightly ($R^2 > 0.99$) to a sigmoidal non-linear regression model, indicating a replication rate not deviating from the expected rate.

	LVS	LVS∆*fptF*	LVS∆*fptA*	LVS∆*fptF*∆*fptA*
R square	0.996	0.9951	0.9968	0.9959

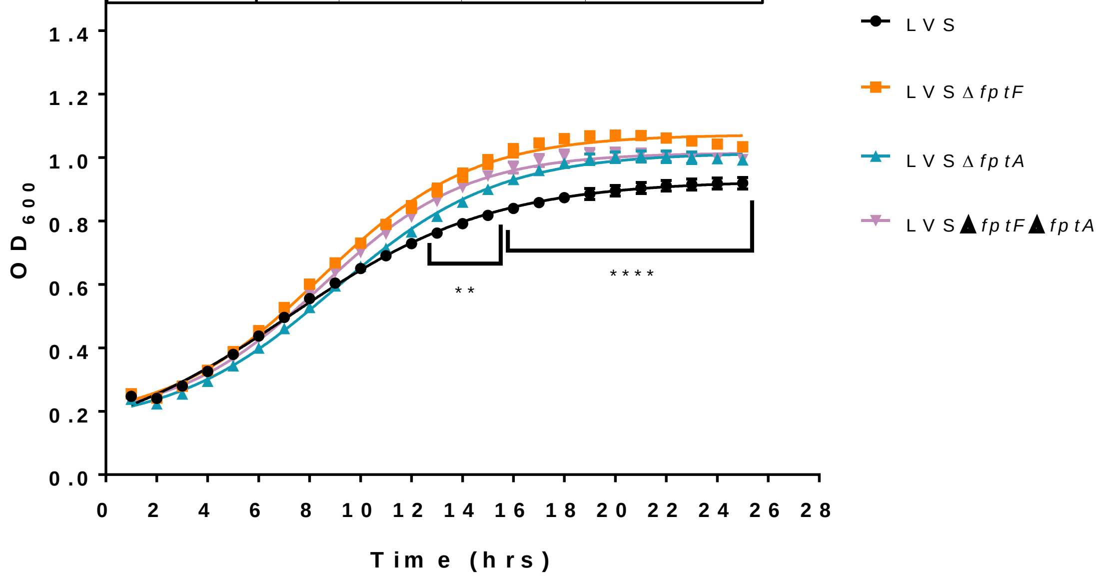

Figure 3.4. Growth of *fpt* double mutant strains compared to parental *F. tularensis* LVS in MHB. Growth of decuplicate samples of each strain was monitored over 25 hours on a Tecan m200Pro, maintaining 37° C, 5% CO_2, and 100 RPM. Data are representative of two independent experiments. ** $p < 0.01$, ****, $p < 0.0001$ (Statistical analyses include a sigmoidal non-linear regression and a non-parametric one-way ANOVA).

	LVS	LVSΔ*fptB*	LVSΔ*fptC*	LVSΔ*fptC*Δ*fptB*
R square	0.9984	0.9981	0.9962	0.9968

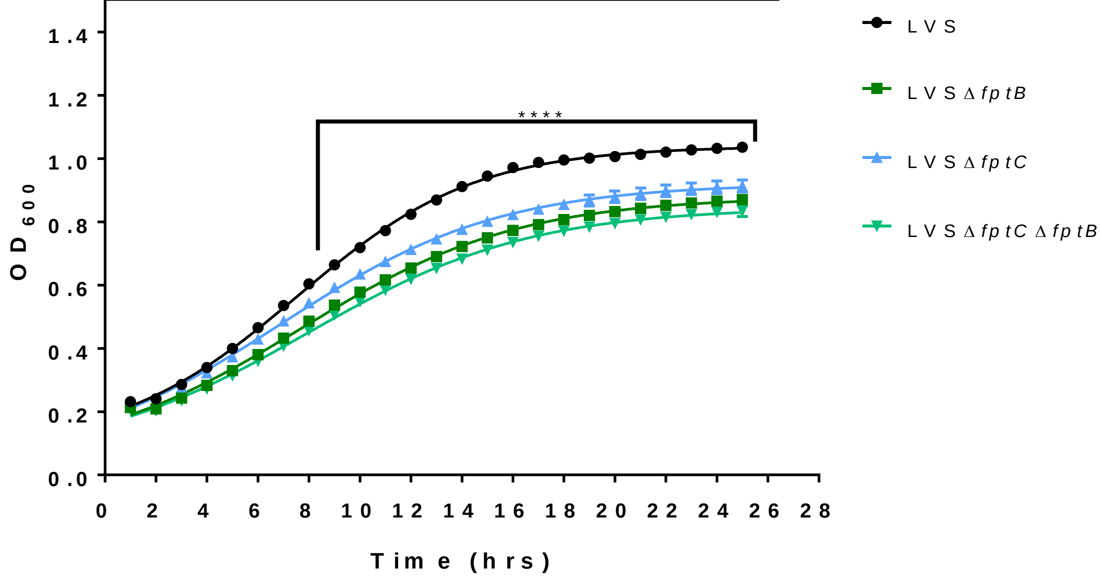

Figure 3.5. Growth of *fpt* double mutant strains compared to parental *F. tularensis* LVS in MHB. Growth of decuplicate samples of each strain was monitored over 25 hours on a Tecan m200Pro, maintaining 37° C, 5% CO_2, and 100 RPM. Data are representative of two independent experiments. ****, $p < 0.0001$ (Statistical analyses include a sigmoidal non-linear regression and a non-parametric one-way ANOVA).

Evaluation of the intracellular replication rates of *F. tularensis* LVSΔ*fptF*Δ*fptA* and LVSΔ*fptC*Δ*fptB*

The ability to enter and replicate in macrophages is a key part of the pathogenesis of *Francisella*. To determine the effects of double mutations on macrophage invasion, double mutant strains were compared to the parental *F. tularensis* LVS strain during invasion of mouse RAW 264.7 macrophage-like cells. In order to examine a single round of entry, replication, and escape only, invasion assays were carried out using a bactericidal concentration of gentamicin, 50 µg/mL, in the tissue culture media throughout the experiment to prevent reinfection. Preliminary studies with LVS demonstrated that 50 µg/mL gentamicin killed 100% of bacteria (Figure 3.6) and allowed quantification of only the first round of cell invasion with no cell-cell spread (Figure 3.7). As shown in Fig. 3.7, the presence of 50 µg/mL gentamicin alters the measured replication rate of *F. tularensis* LVS as early as 24 hpi, with significantly fewer intracellular CFU measured from gentamicin treated cells, suggesting cellular escape has already begun. These conditions allowed for accurate identification of the time of bacterial escape as the point at which intracellular bacterial numbers began to decrease. An additional control confirmed the viability of RAW 264.7 cells in the presence of low (2 µg/mL) or high (50 µg/mL) concentrations of gentamicin through 48 hours of treatment (Figure 3.8).

In previous studies, as shown in Table 1.2, deletion of neither *fptF* nor *fptA* alone in LVS was growth-attenuating in macrophages. The double mutant strains *F. tularensis* LVSΔ*fptF*Δ*fptA* and LVSΔ*fptC*Δ*fptB* were tested in RAW 264.7 cells to determine if the loss of a second *fpt* transporter would result in a growth attenuation phenotype in

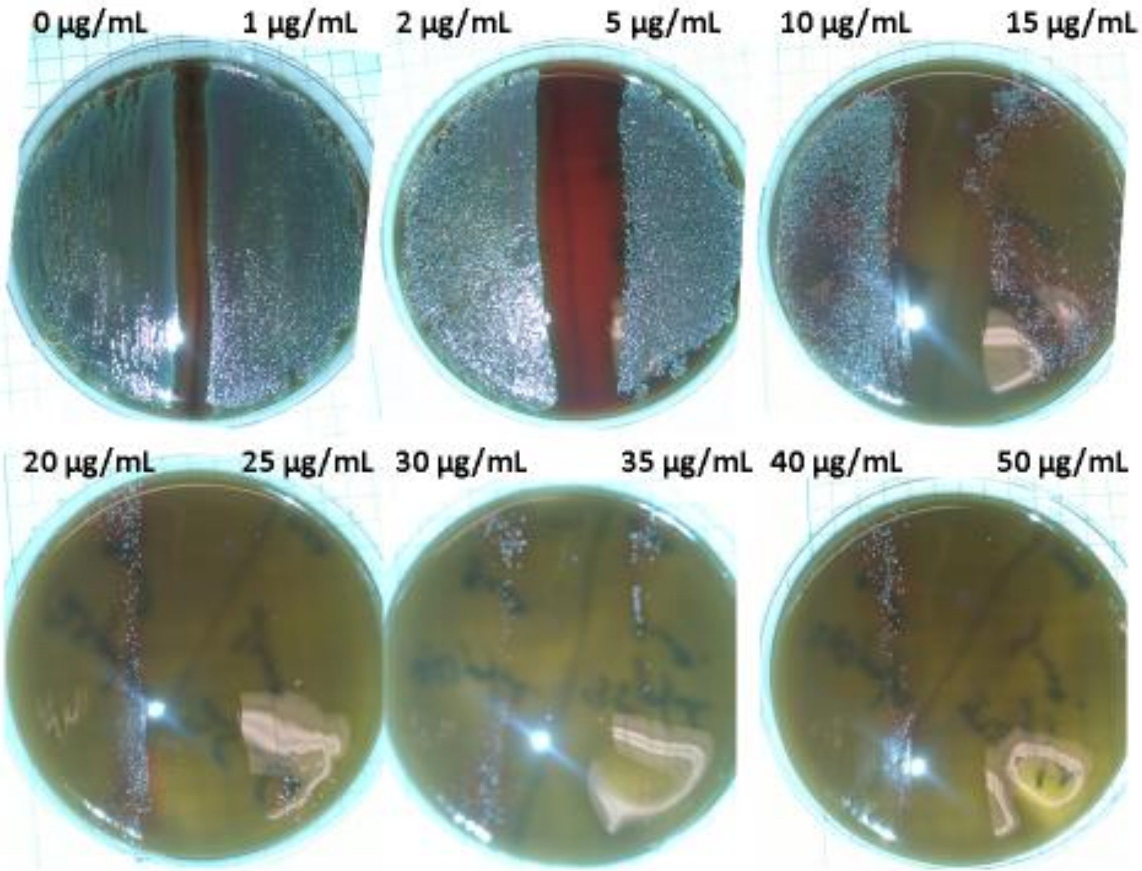

Figure 3.6. Determination of the optimal concentration of gentamicin to eliminate extracellular spread of *F. tularensis*. RAW264.7 macrophages infected with *F. tularensis* LVS were treated with the doses of gentamicin indicated above from 2 hours post infection through 24 hours post infection. At 24 hours post infection, 100 µL of supernatant from each well was carefully aspirated from the top of the well and streaked across half a MHA plate to test for released, viable *F. tularensis* LVS. Data representative of two independent experiments.

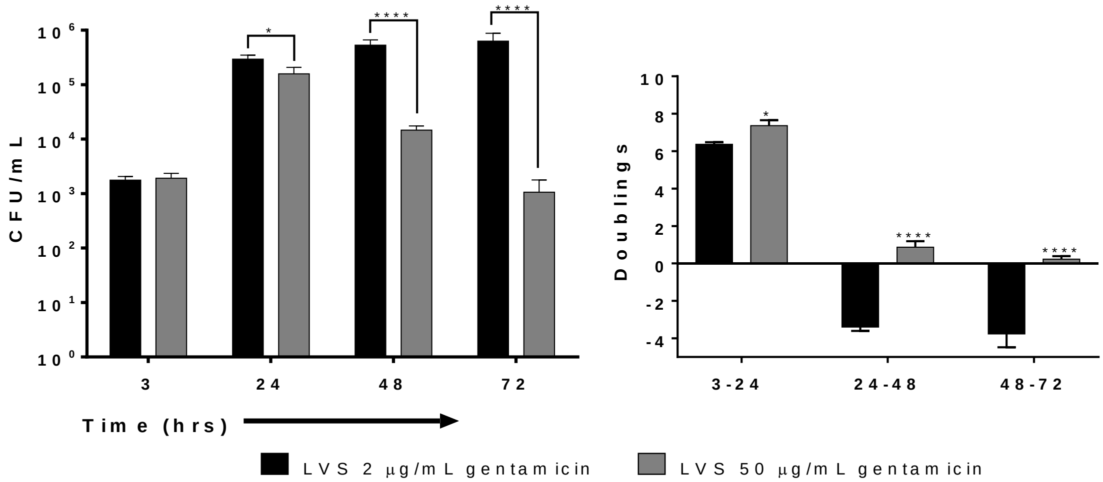

Figure 3.7. Alterations to the observed intracellular CFU and doubling rate of *F. tularensis* LVS in RAW 264.7 macrophage-like cells. RAW 264.7 cells were infected with *F. tularensis* LVS MOI of 10. Intracellular bacteria were enumerated at 3, 24, 48, and 72 hours post-infection and doublings were calculated. A concentration of 50 µg/mL gentamicin was maintained in the media throughout the assay. Data are plotted as the arithmetic mean CFU counts ± standard deviations and consist of one experiment * $p < 0.05$, ****, $p < 0.0001$ (Average CFU and calculated doublings analyzed by two-way ANOVA).

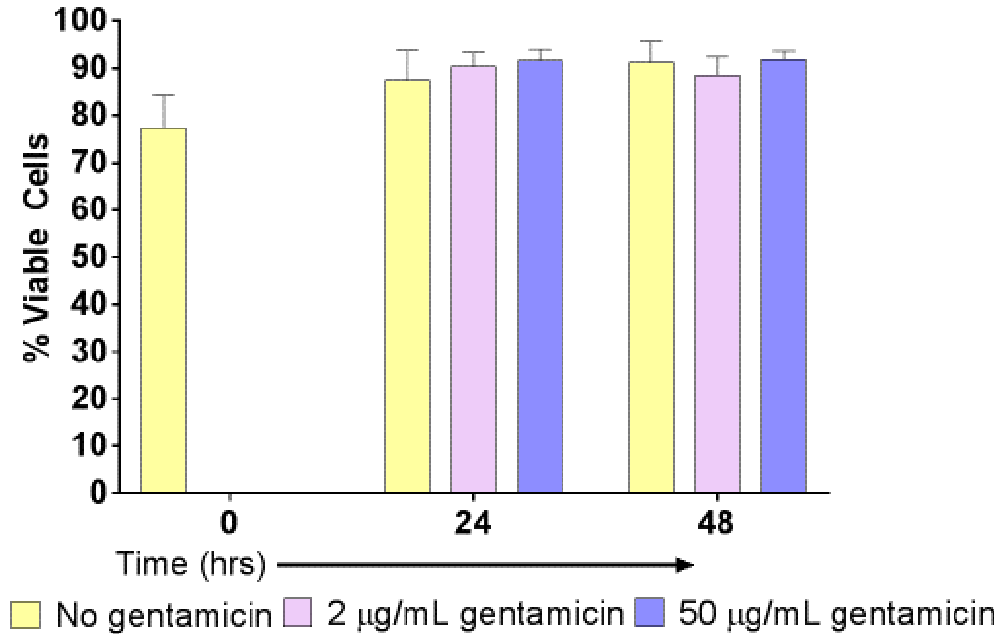

Figure 3.8. Viability of RAW 264.7 cells after long term culture with gentamicin. The viability of RAW 264.7 cells was measured using trypan blue staining at 24 and 48 hours of treatment with gentamicin. Counts were performed on quadruplicate replicates of 2 identical wells containing approximately 1×10^6 cells. Data are plotted as the arithmetic mean live/dead cell counts ± standard deviations and are representative of two experiments of identical design and similar outcome (by one-way ANOVA).

50 µg/mL gentamicin, conditions previously established to limit cell spread. No significant difference between the replication rate of *F. tularensis* LVS and LVSΔ*fptF*Δ*fptA* was observed (Figure 3.9). Calculated doublings were almost identical between *F. tularensis* LVSΔ*fptF*Δ*fptA* and LVS through all experimental replicates, indicating no difference between the strains in terms of replication or cellular escape.

In prior studies, LVSΔ*fptC* had no *in vitro* phenotype, but LVSΔ*fptB* exhibited a profound replication defect (Table 1.2). The double mutant *F. tularensis* LVSΔ*fptC*Δ*fptB* was tested for potential additive *in vitro* attenuation. RAW 264.7 cells were infected with LVSΔ*fptF*Δ*fptA* and parental LVS in 50 µg/mL gentamicin. A significant intracellular replication defect was evident at 24 hpi (Figure 3.10). This phenotype is similar to that observed for *F. tularensis* LVSΔ*fptB* alone; no additive attenuation in intracellular replication was observed.

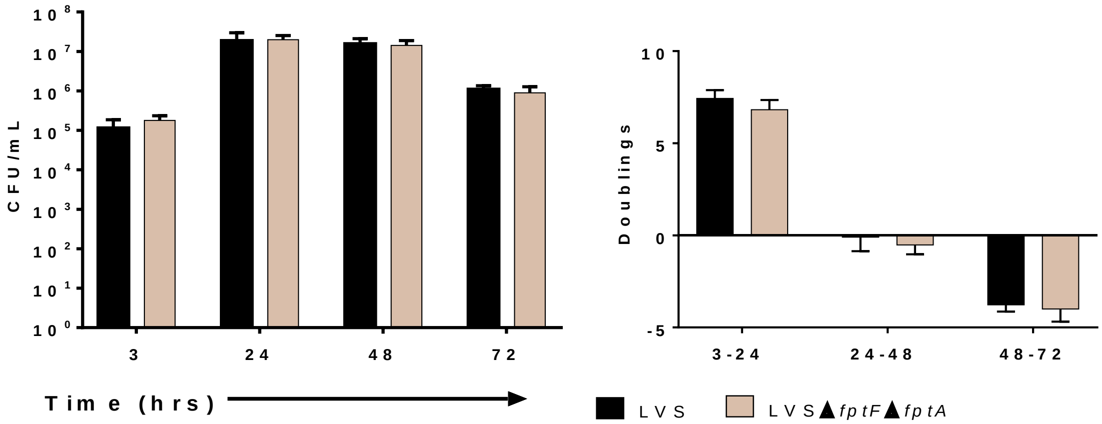

Figure 3.9. Intracellular replication of *F. tularensis* LVSΔ*fptF*Δ*fptA* in RAW 264.7 macrophage-like cells. RAW 264.7 cells were infected with *F. tularensis* LVS and LVSΔ*fptF*Δ*fptA* at an MOI of 80. Intracellular bacteria were enumerated at 3, 24, 48, and 72 hours post-infection and doublings were calculated. A concentration of 50 µg/mL gentamicin was maintained in the media throughout the assay. Data are plotted as the arithmetic mean CFU counts ± standard deviations and consist of two merged experiments of identical design and similar outcome (Average CFU and calculated doublings analyzed by two-way ANOVA).

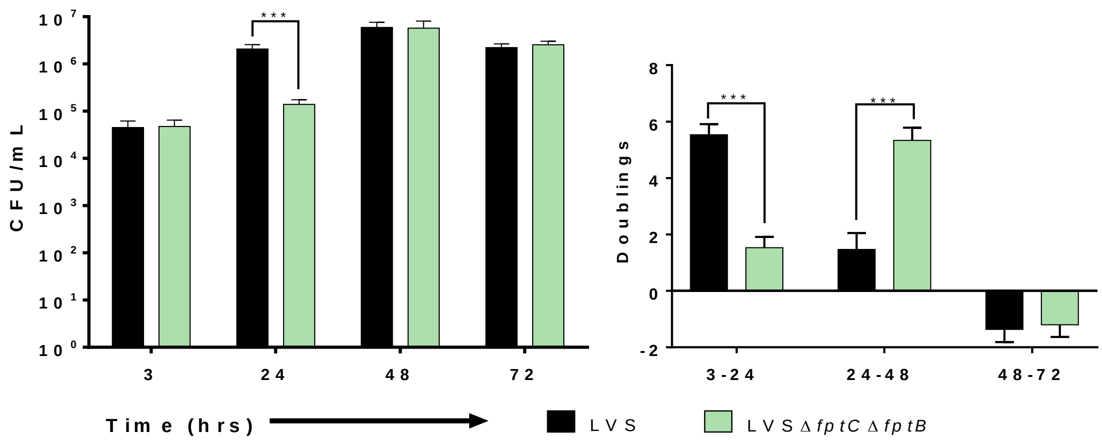

Figure 3.10. Intracellular replication of *F. tularensis* LVSΔ*fptC*Δ*fptB* in RAW 264.7 macrophage-like cells. RAW 264.7 cells were infected with *F. tularensis* LVS and LVSΔ*fptC*Δ*fptB* at an MOI of 80. Intracellular bacteria were enumerated at 3, 24, 48, and 72 hours post-infection and doublings were calculated. A concentration of 50 µg/mL gentamicin was maintained in the media throughout the assay. Data are plotted as the arithmetic mean CFU counts ± standard deviations and consist of two merged experiments of identical design and similar outcome (Average CFU and calculated doublings analyzed by two-way ANOVA)

Evaluation of the initial intracellular replication kinetics of *F. tularensis* LVSΔ*fptG*, LVSΔ*fptB*, and LVSΔ*fptE*

Previous studies measured intracellular replication rates using assay conditions that allowed cell-to-cell spread [128]. Here, we performed assays under conditions that prevent cell-to-cell spread to focus on the initial round of replication only, and allow identification of timing of bacterial escape from host cells. *F. tularensis* strains LVSΔ*fptG*, LVSΔ*fptB*, and LVSΔ*fptE* [128] were tested in RAW 264.7 cells in the presence of 50 µg/mL gentamicin throughout the duration of the assay. *F. tularensis* LVSΔ*fptG* invaded macrophages at a similar rate as parental LVS, as evidenced by similar intracellular numbers at 3 hpi (Figure 3.11). In support of prior findings with this strain [128], *F. tularensis* LVSΔ*fptG* doubled at a rate significantly slower than parental LVS through 48 hpi ($p < 0.001$), with only 3.7 doublings in the first 24 hours compared to 6.2 for WT LVS. Additionally, significantly fewer intracellular CFU were detected at 24 hpi ($p < 0.0001$). Interestingly, *F. tularensis* LVSΔ*fptG* continued to replicate for ~24 hours beyond that of LVS, as evidenced by the positive doubling rate of the mutant at 24-48 hpi and the significant increase in LVSΔ*fptG* intracellular numbers between 24 and 48 hpi ($p < 0.01$). During this same period, LVS exhibited declining intracellular numbers, indicating that this strain had begun escaping its initially infected cell and was killed by the gentamicin in culture. These data suggest a previously unobserved delay in cytosolic escape for *F. tularensis* LVSΔ*fptG* accompanies the reduced intracellular replication phenotype known for this strain.

No significant alteration from prior findings for *F. tularensis* LVSΔ*fptB* was observed in RAW 264.7 cells [128]. With infection at an MOI of 100, *F. tularensis*

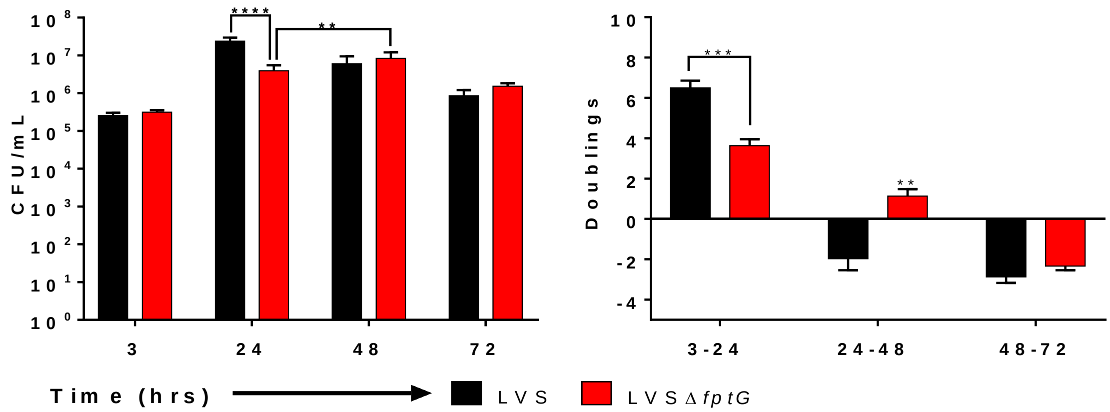

Figure 3.11. Intracellular replication and escape rate of *F. tularensis* LVSΔ*fptG* in RAW 264.7 macrophage-like cells. RAW 264.7 cells were infected at an MOI of 100. Intracellular bacteria were enumerated at 3, 24, 48, and 72 hours post-infection and doublings were calculated based on CFU enumerations. A concentration of 50 µg/mL gentamicin was maintained in the media throughout the assay. Data are plotted as the arithmetic mean CFU counts ± standard deviations and are representative of two experiments of identical design and outcome. **, $p < 0.01$, ***, $p < 0.001$, ****, $p < 0.0001$ (Average CFU and calculated doublings analyzed by two-way ANOVA).

LVSΔ*fptB* invaded at a similar rate as parental LVS, as evidenced by similar 3 hour CFU numbers (Figure 3.12). In line with prior findings [128], *F. tularensis* LVSΔ*fptB* exhibited a severely reduced doubling rate compared to that of parental LVS ($p < 0.001$); approximately 5.8 doublings for LVS compared to 1.7 for LVSΔ*fptB*. Significantly fewer mutant CFU were recovered at 24 hpi compared to LVS ($p < 0.0001$). Interestingly, *F. tularensis* LVSΔ*fptB* appeared to rebound between 24-48 hpi, doubling at almost the same rate LVS had between 3-24 hpi, and significantly higher than the rate of LVS between 24-48 hpi ($p < 0.001$), resulting in equal recovery of CFU from both strains at 48 hpi. These data support the replication defect observed previously with this strain in mouse macrophage cell line cells, but uncover no new phenotypes.

No significant alterations were observed in the replication rate of *F. tularensis* LVSΔ*fptE* in RAW 264.7 cells. Infected at an MOI of 100, *F. tularensis* LVSΔ*fptE* invaded at a similar rate as parental LVS, as evidenced by similar 3 hour CFU numbers (Figure 3.13). Prior findings with this strain reported no defect in replication in macrophages [128]. In support of this, no difference in CFU recovered, or calculated doublings was observed at any time point through 72 hpi *F. tularensis* LVSΔ*fptE* and parental LVS.

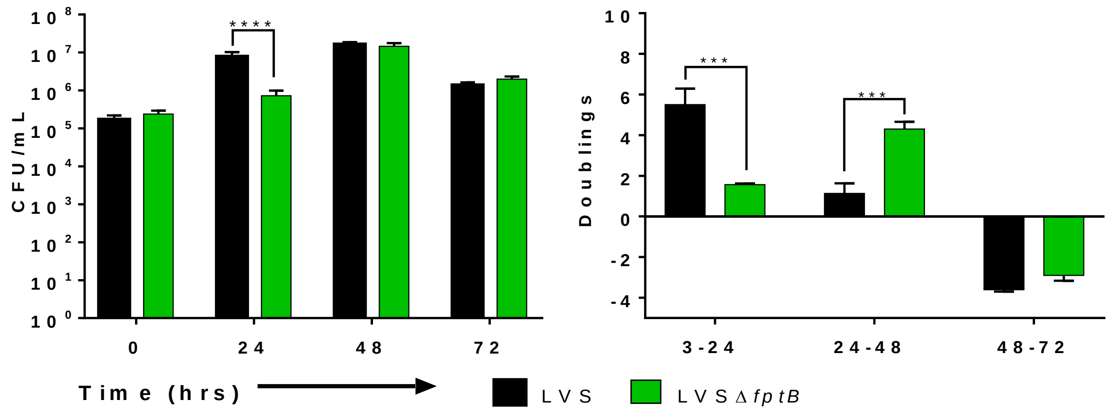

Figure 3.12. Intracellular replication and escape rate of *F. tularensis* LVSΔ*fptB* in RAW 264.7 macrophage-like cells. RAW 264.7 cells were infected at an MOI of 100. Intracellular bacteria were enumerated at 3, 24, 48, and 72 hours post-infection and doublings were calculated based on CFU enumerations. A concentration of 50 µg/mL gentamicin was maintained in the media throughout the assay. Data are plotted as the arithmetic mean CFU counts ± standard deviations and are representative of two experiments of identical design and outcome. **, $p < 0.01$, ***, $p < 0.001$, ****, $p < 0.0001$ (Average CFU and calculated doublings analyzed by two-way ANOVA).

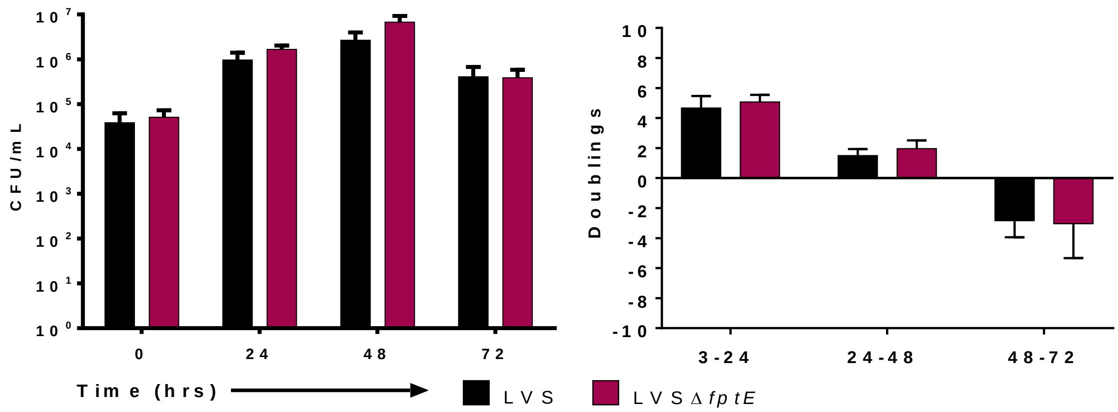

Figure 3.13. Intracellular replication and escape rate of *F. tularensis* LVSΔ*fptE* in RAW 264.7 macrophage-like cells. RAW 264.7 cells were infected at an MOI of 100. Intracellular bacteria were enumerated at 3, 24, 48, and 72 hours post-infection and doublings were calculated based on CFU enumerations. A concentration of 50 µg/mL gentamicin was maintained in the media throughout the assay. Data are plotted as the arithmetic mean CFU counts ± standard deviations and are representative of two experiments of identical design and outcome. **, $p < 0.01$, ***, $p < 0.001$, ****, $p < 0.0001$ (Average CFU and calculated doublings analyzed by two-way ANOVA).

Evaluation of the initial 24 hours of replication of the *F. tularensis* strains LVSΔ*fptG*, LVSΔ*fptB*, and LVSΔ*fptE*

Both *F. tularensis* LVSΔ*fptG* and LVSΔ*fptB* exhibited significantly altered replication cycles compared to WT LVS by 24 hpi. To examine more closely this period of time, and ascertain more precisely when replication begins for each strain, the replication kinetics of all three *fpt* mutants were tracked during the first 24 hpi. Two sets of invasion assays, one covering the period from invasion to 12 hpi, and the second, from 12 to 24 hpi, were carried out under 50 μg/mL gentamicin in RAW 264.7 macrophage-like cells with time points taken for intracellular CFU enumeration every 4 hours. Positive doubling rates were interpreted as replication was outweighing escape or clearance, whereas negative rates were interpreted as clearance or cellular escape was outpacing replication.

Previous assays indicated that *F. tularensis* LVS and LVSΔ*fptE* replicated at a similar pace (Fig. 3.13). Supporting this finding, LVS and LVSΔ*fptE* doubled at a similar rate and elicited similar CFU levels at all time points measured in both the 0-12 hour, and 12-24 hour time courses (Figure 3.14). While no strain doubled at a significantly different rate from any other in the first 12 hpi, only *F. tularensis* LVS and LVSΔ*fptE* exhibited a positive average doubling rate in the first 12 hours. In contrast, *F. tularensis* LVSΔ*fptB* did not yield a positive average doubling rate until 12-16 hpi (Figure 3.14D). Average intracellular CFU numbers (Figure 3.14A) trended downwards through the first 12 hpi, becoming significantly less than parental LVS at 12 hpi ($p < 0.01$). Doublings increased sharply between 16-20 hpi, reaching WT *F. tularensis* LVS levels for 4 hours, before

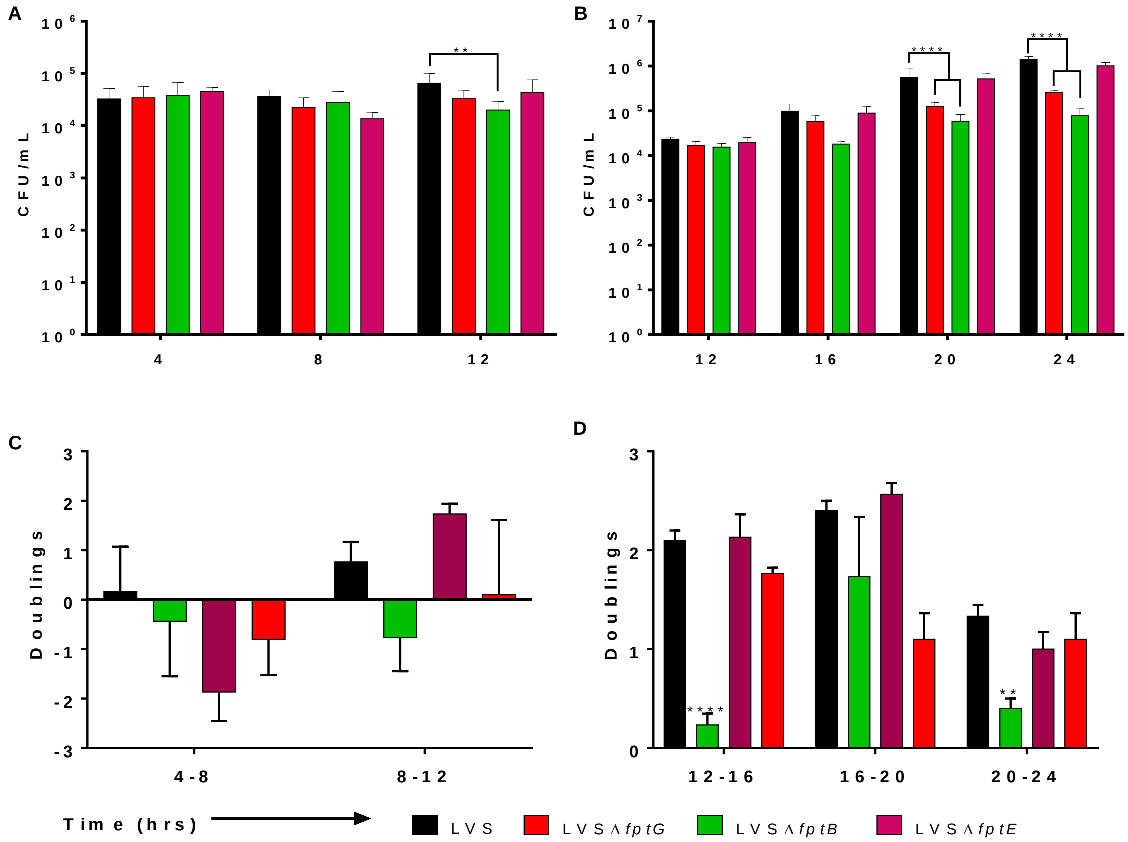

Figure 3.14. Intracellular replication and escape rate of *F. tularensis* LVSΔ*fptG* LVSΔ*fptB*, and LVSΔ*fptE* compared to parental LVS in RAW 264.7 macrophage-like cells. RAW 264.7 cells were infected at an MOI of 100. Intracellular bacteria were enumerated at 3, 24, 48, and 72 hours post-infection and doublings were calculated based on CFU enumerations. A concentration of 50 µg/mL gentamicin was maintained in the media throughout the assay. Data are plotted as the arithmetic mean CFU counts ± standard deviations and are representative of two experiments of identical design and similar outcome. **, $p < 0.01$, ***, $p < 0.001$, ****, $p < 0.0001$ (Average CFU and calculated doublings analyzed by two-way ANOVA).

dropping to significantly less than WT LVS between 20-24 hpi ($p < 0.01$). Significantly fewer intracellular *F. tularensis* LVSΔ*fptB* were quantified at both 20 and 24 hpi ($p < 0.0001$). Taken together, these data demonstrate there is a delay before replication starts for *F. tularensis* LVSΔ*fptB* until between 12-16 hpi.

Similar to *F. tularensis* LVSΔ*fptB*, LVSΔ*fptG* was delayed approximately 12 hours before a positive doubling rate was found between 12-16 hpi (Figure 3.14D). From 12-24 hpi, *F. tularensis* LVSΔ*fptG* replicated at a rate similar to that of LVS. Differences in intracellular CFU are only significant at 20 and 24 hpi ($p < 0.0001$) (Figure 3.14B). Overall, these data indicate that *F. tularensis* LVSΔ*fptG* does not begin replicating until 12-16 hpi.

Summary of Chapter 3

F. tularensis LVSΔ*fptF*Δ*fptA* replicated in MHB broth at a significantly higher rate than parental LVS, while LVSΔ*fptC*Δ*fptB* replicated significantly slower. For both double mutant strains, their replication rates were indistinguishable from that of the parental single deletion mutants. While *F. tularensis* LVS was variable, reaching different maximum OD_{600} values from experiment to experiment, the magnitude of the differences between the strains remained constant. It may be that MHB is too rich a medium to engender consistent OD_{600} values from these strains, complicating comparison and analysis. The findings utilizing *F. tularensis* LVSΔ*fptC*Δ*fptB* and LVSΔ*fptB* are at odds with previously published data [77], which found that *F. tularensis* LVS and subspecies *novicida* mutants harboring a deletion of the *fptB* gene exhibited significant growth defects in CDM, but not MHB. It may be that re-evaluation in CDM, an accepted minimal broth medium for *F. tularensis* replication analysis [25], with either of these double mutant strains would yield consistent, significant growth.

Under conditions that limit intercellular spread in RAW 264.7 mouse macrophage-like cells, *F. tularensis* LVSΔ*fptF*Δ*fptA* doubled at the same rate as WT LVS and was quantified at similar intracellular numbers at all time points measured. This indicates that the combined deletion of both the *fptF* and *fptA* genes is likely not a viable strategy for increasing attenuation. *F. tularensis* LVSΔ*fptC*Δ*fptB* replicated significantly slower than parental LVS in the first 24 hpi, and significantly fewer intracellular bacteria were quantified at this time point, but yielded CFU counts similar to LVS at all other time points. Deletion of the *fptB* gene significantly attenuates growth of *F. tularensis*

LVS and LVSΔ*fptC*, but the double mutant strain did not exhibit doubling values appreciably different from the published single mutant LVSΔ*fptB* strain [128].

Further examination of the strains *F. tularensis* LVSΔ*fptG*, LVSΔ*fptE,* and LVSΔ*fptB* under cell spread-limiting conditions in RAW 264.7 cells demonstrated a previously unreported escape delay, in addition to the replication defect for LVSΔ*fptG* previously described [128]. *F. tularensis* LVSΔ*fptE* exhibited no replication defect in macrophages, supporting prior findings with this strain [128]. *F. tularensis* LVSΔ*fptB* displayed a significant replication defect in the first 24 hpi, similar to previously reported findings [128]. Time course experiments duringthe first 24 of infection further demonstrate that *F. tularensis* LVSΔ*fptE* doubles at a rate similar to WT LVS and is present at similar intracellular numbers at all time points measured, suggesting that asparagine is not a rate-limiting amino acid for *F. tularensis* in mouse macrophages. Both *F. tularensis* LVSΔ*fptB* and LVSΔ*fptG* were delayed approximately 12 hours before replication began, leading to significantly fewer intracellular CFU counts for both strains by 20 hpi. While it cannot be ascertained from this assay, the delay in replication for *F. tularensis* LVSΔ*fptG* may stem from a delay in escaping the phagosome, a phenotype described previously for LVSΔ*fptB* [77].

Chapter 4 – Construction and *in vitro* characterization of two mutant strains of *F. tularensis* SchuS4 lacking *fptF* or *fptE*

Construction of *F. tularensis* SchuS4 single deletion strains SchuS4Δ*fptE* and SchuS4Δ*fptF*

To assess the ability of the MFS transporters FptF and FptE to attenuate WT *F. tularensis* SchuS4, single deletion mutations were introduced into the selected genes as described previously in Chapter 3. As demonstrated in Figure 4.1, the gene *fptF* (*FTT_0127c*) was successfully deleted from the *F. tularensis* SchuS4 genome. Lane 1 demonstrates the predicted, smaller band indicative of a deletion of the *fptF* gene. Lane 2 demonstrates no band, indicating the complete deletion of the *fptF* gene, as the intragenic primers were unable to bind and drive PCR. Both bands in columns 3 and 4 are of the predicted sizes expected from WT *F. tularensis* SchuS4.

Similarly the deletion of the *fptE* gene (*FTT_0129*) was engineered in the SchuS4 background. Figure 4.2 illustrates the successful deletion of the *fptE* gene from the *F. tularensis* SchuS4 genome. Lane 1 under the "SchuS4Δ*fptE*" header demonstrates the predicted band at 699 bp, indicating successful deletion of the *fptE* gene. No bands are found in lanes 2-4 of this section, demonstrating the complete deletion of the *fptE* gene. Lane one under the "SchuS4" heading shows the predicted 1,908 bp band indicative of the full length WT gene. Lanes 2-4, utilizing the intragenic primers, demonstrate the predicted bands at 605 bp, 1,206 bp, and 1,309 bp indicative of the presence of the WT *fptE* gene.

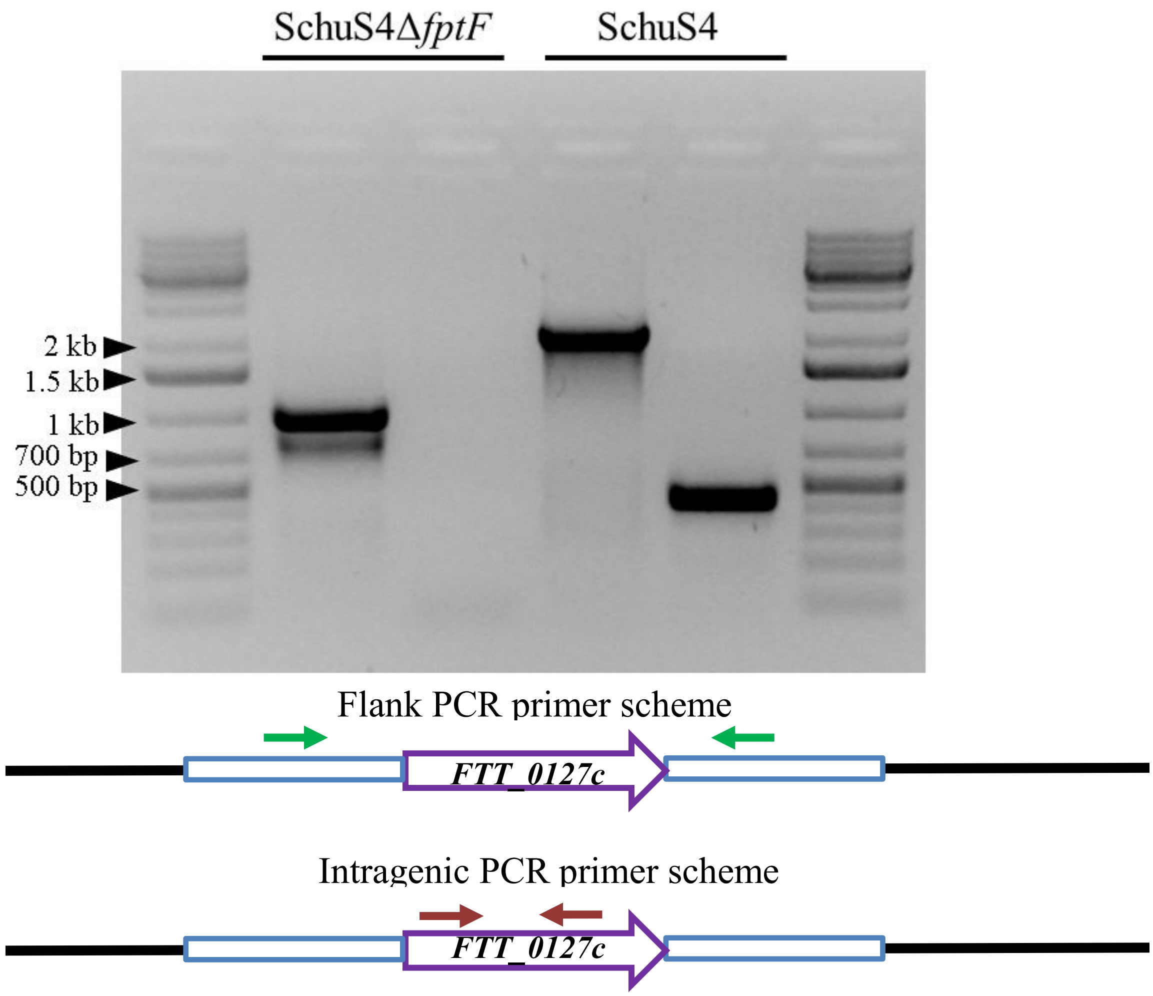

Figure 4.1. Confirmation of deletion of *FTT_0127c* from the SchuS4 genome. Top panel is a representative gel showing PCR products that confirm the deletion of the *fpt* gene *FTT_0127c* (*fptF*) from the *F. tularensis* SchuS4 genome. Bottom panel demonstrates the location and orientation of screening primer pairs used to ascertain deletion of *fptF*. Lanes 1 and 3 represent bands utilizing the primers "Fpt_F_SchuS4_F" and "Fpt_F_SchuS4_R", while lanes 2 and 4 utilized the intragenic PCR primers "LVS_inF_F" and "LVS_inF_R". Lane 1 shows the predicted 983 bp band corresponding to a deletion of the *fptF* gene, while lane 3 exhibits the WT band at 2,131 bp. Lane2 exhibits no band, corresponding with the complete absence of the *fptF* gene in the *F. tularensis* SchuS4Δ*fptF* strain. Lane 4 exhibits the expected 438 bp band indicative of the *fptF* gene present in the WT genome.

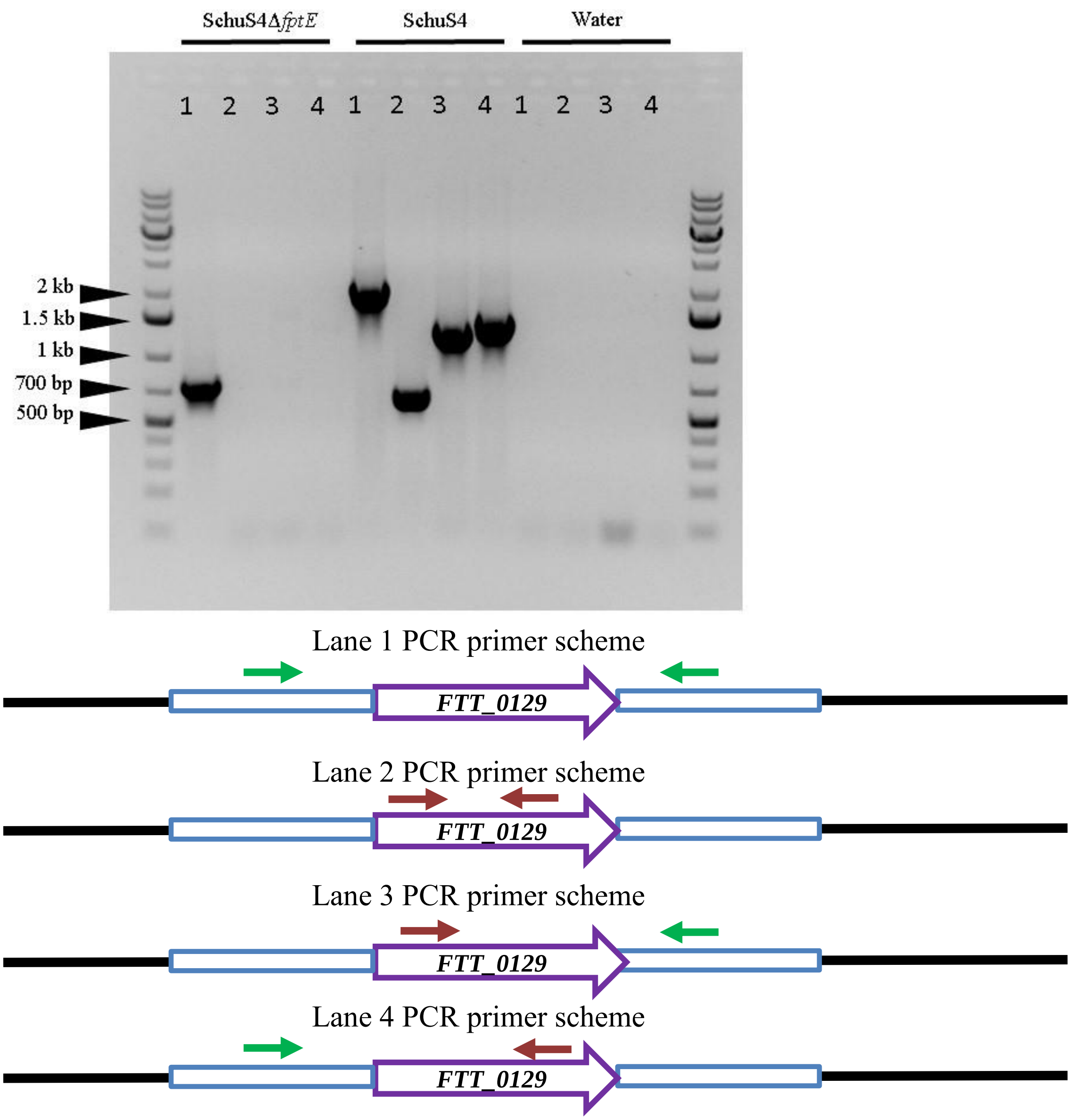

Figure 4.2. Confirmation of deletion of *FTT_0129* from the SchuS4 genome. Top panel is a representative gel showing PCR products that confirm the deletion of the *fpt* gene *FTT_0129* (*fptE*) from the *F. tularensis* SchuS4 genome. Bottom panel demonstrates the location and orientation of screening primer pairs used to ascertain deletion of *fptE*. Lanes 1 represent bands utilizing the primers "SchufptE_F" and "SchufptE_R", while lanes 2 utilized the intragenic primers "LVS_inE_F" and "LVS_inE_R". Lanes 3 utilizes "LVS_inE_F" coupled with "SchufptE_R", and lane 4 utilizes "SchufptE_F" with "LVS_inE_R". Lane 1 under the "SchuS4Δ*fptE*" header shows the predicted 699 bp band corresponding to a deletion of the *fptE* gene, while lanes 2-4 exhibit no bands, demonstrating the complete loss of the *fptE* gene. Lane 1 under the "WT" header exhibits the predicted band at 1,908 bp. Lane 2 exhibits the predicted 605 bp indicating the presence of the WT gene. Lanes 3 and 4 also have the predicted bands of 1,206 and 1,309 bp, respectively, further indicating the presence of the WT gene. No bands are found under the "Water" heading, indicating the specificity of the PCR performed.

Evaluation of growth in broth of *F. tularensis* SchuS4Δ*fptE*

An initial test of the *in vitro* growth characteristics of the *F. tularensis* strain SchuS4Δ*fptE* was carried out in comparison to WT SchuS4 in Chamberlain's Defined Medium (CDM), a minimal medium for *F. tularensis* [25]. *F. tularensis* SchuS4Δ*fptE* did not exhibit any replication defect when grown in CDM through 7.5 hours (Figure 4.3).

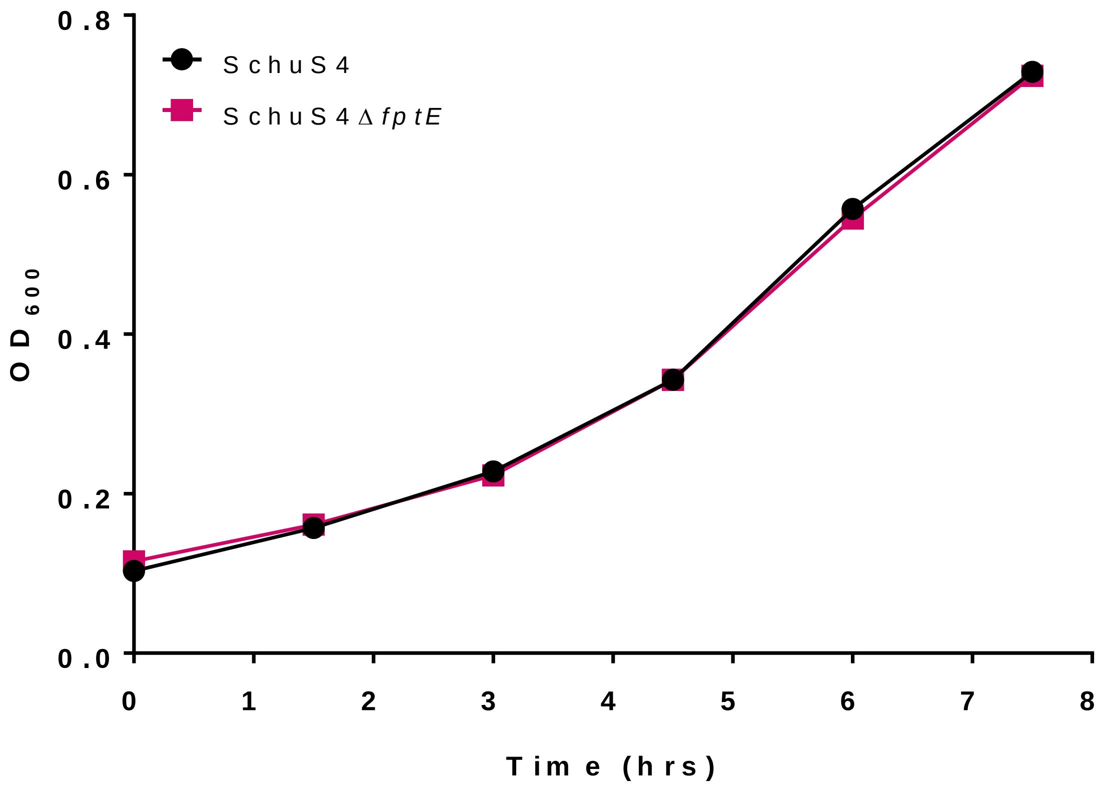

Figure 4.3. Growth of *F. tularensis* SchuS4Δ*fptE* in CDM. Growth kinetics of WT *F. tularensis* SchuS4 and SchuS4Δ*fptE* were examined in CDM. OD_{600} readings were taken every 1.5 hours over a 7.5 hour time course. Data are derived from a single experiment (n = 1).

Evaluation of the initial intracellular replication kinetics of *F. tularensis* SchuS4Δ*fptE* and Schus4Δ*fptF*

Although no alterations to the rate of replication were found in CDM, the *F. tularensis* strains SchuS4Δ*fptE* and Schus4Δ*fptF* were examined in the context of the more physiologically relevant environment of the eukaryotic cell cytosol during intracellular infection. Invasion assays were performed in conditions including 50 µg/mL gentamicin in culture media throughout the experiment to enumerate any changes to the overall replication kinetics and cellular escape rate in both THP-1 human macrophage-like cells, and HepG2 human hepatocyte carcinoma cells.

F. tularensis Schus4Δ*fptF* exhibited no alterations to its replication cycle in either THP-1 macrophages or in HepG2 hepatocyte cells compared to WT. THP-1 cells were infected at an MOI of 100, and HepG2 cells at an MOI of 300, and *F. tularensis* Schus4Δ*fptF* invaded at a similar rate as WT SchuS4, as evidenced by similar 3 hour intracellular bacterial numbers (Figure 4.4). Total intracellular CFU and calculated doublings did not differ significantly from WT *F. tularensis* SchuS4 at any time point measured through to 48 hpi in either THP-1 cells (4.4 A, C) or HepG2 cells (4.4 B, D).

Prior studies in *F. tularensis* LVS demonstrated that loss of the *fptE* gene was growth attenuating in HepG2 cells, with no accompanying change in replication observed in J774A.1 mouse macrophage-like cells [128]. Surprisingly, deletion of the *fptE* gene from the *F. tularensis* SchuS4 genome resulted in no growth attenuation in either THP-1 or HepG2 cells. THP-1 cells were infected at an MOI of 100, and HepG2 cells at an MOI of 300, and *F. tularensis* Schus4Δ*fptE* invaded at a similar rate as SchuS4, as evidenced by similar 3 hour CFU numbers (Figure 4.5). Total intracellular CFU and calculated

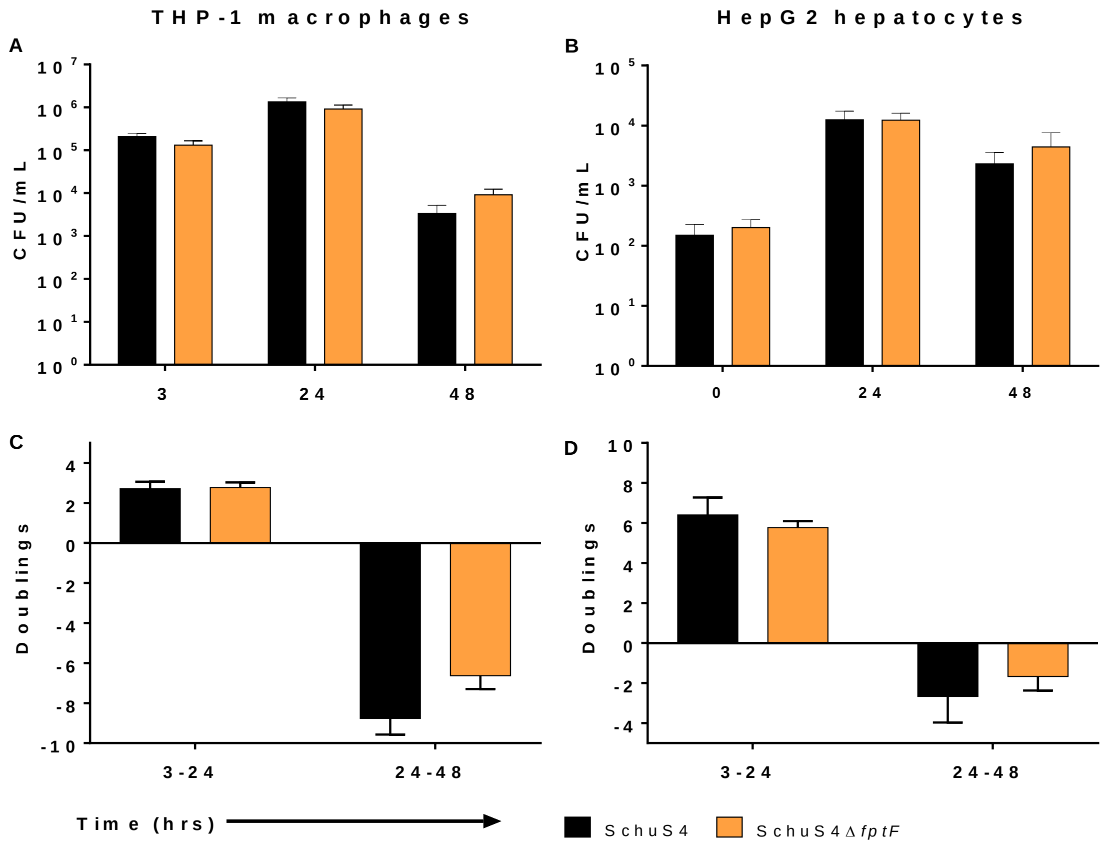

Figure 4.4. Determination of the intracellular replication rate of *F. tularensis* SchuS4Δ*fptF* in THP-1 macrophage-like cells and HepG2 hepatocyte carcinoma cells. THP-1 cells (panels A and C) were infected at an MOI of 100, while HepG2 cells (panels B and D) received an MOI of 300. Intracellular bacteria were enumerated at 3, 24, and 48 hpi and doublings were calculated based on CFU enumerations. A concentration of 50 µg/mL gentamicin was maintained in the media from 3 hpi until the end of the assay. Data are plotted as the arithmetic mean CFU counts ± standard deviations and are representative of two sets of experiments of identical design and outcome (Average CFU and calculated doublings analyzed by two-way ANOVA).

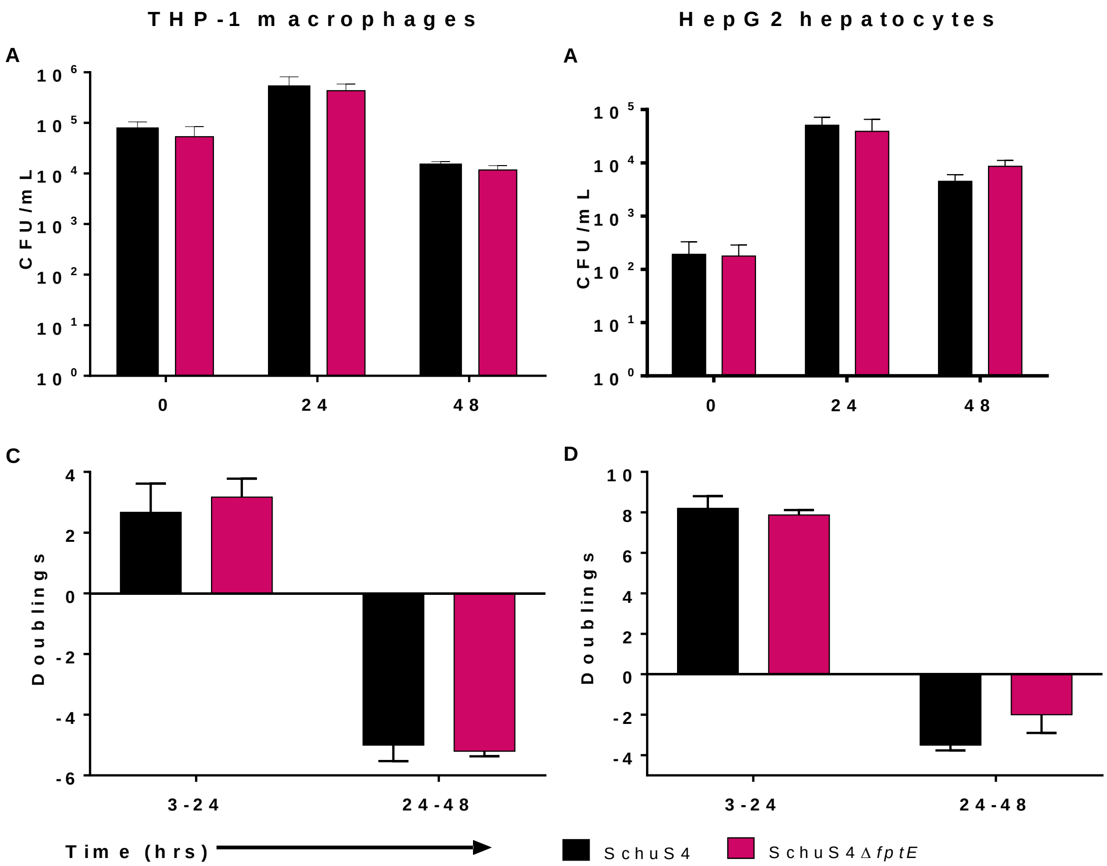

Figure 4.5. Determination of the intracellular replication rate of *F. tularensis* SchuS4Δ*fptE* in THP-1 macrophage-like cells and HepG2 hepatocyte carcinoma cells. THP-1 cells (panels A and C) were infected at an MOI of 100, while HepG2 cells (panels B and D) received an MOI of 300. Intracellular bacteria were enumerated at 3, 24, and 48 hpi and doublings were calculated based on CFU enumerations. A concentration of 50 µg/mL gentamicin was maintained in the media from 3 hpi until the end of the assay. Data are plotted as the arithmetic mean CFU counts ± standard deviations and are representative of two sets of experiments of identical design and outcome. (Average CFU and calculated doublings analyzed by two-way ANOVA).

doublings did not differ significantly from WT *F. tularensis* SchuS4 at any time point measured through to 48 hpi in either THP-1 cells (4.5A, C) or HepG2 cells (4.5B, D), indicating *F. tularensis* Schus4Δ*fptF* replicated at both the same rate as WT and escaped from macrophages at the same rate.

Summary of Chapter 4

Both Type A *F. tularensis* strains SchuS4Δ*fptE* and SchuS4Δ*fptF* exhibited no growth deficiencies in minimal CDM broth, indicating the substrates for these transporters, asparagine for FptE [76], and an unknown substrate for FptF, are not essential for extracellular growth. Furthermore, neither deletion strain replicated or escaped the host cell at a rate different from WT *F. tularensis*, as measured in both THP-1 macrophage-like cells and HepG2 hepatocytes. This finding was not surprising for *F. tularensis* SchuS4Δ*fptF*, as deletion of this gene in the LVS background resulted in no alterations to the intracellular replication cycle (unpublished data). However, the lack of a replication phenotype was not expected for SchuS4Δ*fptE*. Prior findings had demonstrated that deletion of the *fptE* gene from *F. tularensis* LVS and transposon disruption in SchuS4 was growth attenuating for both strains in HepG2 cells [163]. Because transposon mutagenesis was used in the prior study, and because it is unknown as to whether *fptE* is included in an operon, polar effects cannot be ruled out as the explanation for the phenotypes seen by Qin *et al* in HepG2 cells. *F. tularensis* SchuS4Δ*fptE* presented no alterations to its replication cycle in THP-1 or HepG2 cells, signifying either that asparagine transport is accessory to timely replication and cellular escape, or that a second, redundant asparagine transporter exists in the *F. tularensis* genome.

Chapter 5 – Deletion of the MFS transporters *fptG* and *fptB* cause cellular escape delays in Type A *Francisella tularensis*[1]

Abstract

Francisella tularensis is a Gram negative facultative intracellular coccobacillus that can infect a wide variety of hosts. In humans, *F. tularensis* causes the zoonosis tularemia following insect bites, ingestion, inhalation, and the handling of infected animals. That a very small inoculum delivered by the aerosol route can cause severe disease, coupled with the possibility of its use as an aerosolized bioweapon, have led to the classification of *Francisella tularensis* as a Category A select agent and has renewed interest in the formulation of a vaccine. To this end, we engineered Type A strain SchuS4 derivatives containing single deletions of major facilitator superfamily (MFS) transporters, *fptG* and *fptB*. Based on the attenuating capacity of these deletions in the *F. tularensis* LVS background, we hypothesized that deletion of either transporter would alter intracellular replication and cytokine induction by the Type A strain and attenuate virulence in the stringent C57BL/6J mouse model. Here we demonstrate that deletion of either *fpt* transporter significantly alters the intracellular lifecycle of *F. tularensis*, inducing a novel cytosolic escape delay phenotype that was found to be autophagy-dependent for SchuS4Δ*fptG*. Additionally, we observed prominent differences in *in vitro* cytokine profiles in human macrophages for both mutants. Both mutants were attenuated in the C57BL/6J mouse model, and one strain, SchuS4Δ*fptB*, provided partial protection against virulent Type A *F. tularensis* challenge. These results indicate a fundamental necessity

[1] Phillip M. Balzano, Aimee L. Cunningham, Christen Grassel, and Eileen M. Barry
As submitted to Infection & Immunity, October 6, 2017

for these nutrient transporters in the timely progression of *F. tularensis* through its replication cycle and in pathogenesis.

Introduction

Francisella tularensis is a Gram negative facultative intracellular coccobacillus that is the causative agent of the zoonosis tularemia [227, 206]. Two subspecies of *Francisella*, *F. tularensis* subspecies *tularensis* (Type A), and subspecies *holarctica* (Type B), account for virtually all instances of disease in humans, though a third, subspecies *novicida*, is not infectious in man, but is often used as a laboratory model. While there is no documented case of human to human transmission, *F. tularensis* can be transmitted to humans via inhalation of infected aerosols, bite of insect vectors, ingestion of contaminated food or water, and handling of infected animals [16]. Cutaneous exposure, most often via an insect vector, accounts for much of the disease burden and can lead to a protracted, though rarely fatal infection [63, 64]. Conversely, inhalation of as few as 10-15 bacteria of the virulent Type A strain can cause serious illness in humans with a mortality rate approaching 50% if left untreated [91, 200]. Several countries had utilized *Francisella* as a biological weapon during the middle of the 20th century due to its high virulence, low inoculum, and ease of delivery by aersolization [52]. For this reason, the CDC has designated *Francisella tularensis* subspecies *tularensis* as a Tier 1 Category A select agent and a high priority for countermeasure development.

Currently, there is no licensed vaccine against *F. tularensis*, but development efforts continue in light of the potential threat to public safety. Past development efforts have included component and killed whole cell, or "Foshay" vaccines, but these were met with limited success [72, 190, 43, 73]. More recently, it has been demonstrated that cationic vesicles, as carriers for either *F. tularensis* LVS or SchuS4 antigens, could achieve protection rates from intranasal Type A challenge in excess of 60% when used in conjunction with the TLR4 adjuvant monophosphoryl lipid A [174]. These results are promising, and may possibly lead the way forward for a component-based *F. tularensis* vaccine.

To date, the live-attenuated vaccine strategy has shown the most promise. One candidate strain derived from *F. tularensis* subspecies *holarctica* by the Soviet Union through the 1940s and 1950s was transferred to the U.S. in 1956, further passaged, and became known as "live vaccine strain" (LVS) [200]. *F. tularensis* LVS was tested extensively in clinical trials and demonstrated the feasibility of the live vaccine approach in conferring at least partial protection against Type A challenge. Subsequently, multiple attenuated live vaccine candidates have been engineered utilizing the *F. tularensis novicida*, *F. tularensis* LVS, and *F. tularensis* Type A backgrounds [128, 172, 182, 183, 154, 155, 218, 13, 91, 41, 46]. These new vaccine candidates have shown varying degrees of efficacy in animal models and some are being developed further for use in humans. An additional outcome of these studies has been the discovery of novel information about the pathogenic process of *F. tularensis*, including alterations to and impact on the pathogenic lifecycle incurred by targeted deletion of various genes in the attenuation process.

A hallmark of *Francisella* infection is the ability to induce phagocytosis via several routes to gain entry to many cell types, especially macrophages, where it rapidly escapes the phagosome to replicate to high numbers in the cytosol [24, 8, 36, 193, 158]. Because of the distinctive tetraacylated structure of its lipopolysaccharide lipid A component, *Francisella* is largely able to evade TLR4-mediated recognition [86]. Rather, *Francisella* initiates signaling through TLR2, resulting in the production of pro-inflammatory cytokines [40, 102], and, in a manner dependent on guanylate binding proteins (GBPs), STING, and mitochondrial reactive oxygen species, and activates the AIM2 inflammasome [44, 225, 122, 136]. The virulence of *Francisella* stems from its ability to multiply to high numbers in the cytosol of infected cells, especially macrophages [31]. As a result, many attenuation attempts have targeted metabolic or nutrient acquisition genes [128, 182, 183, 177, 76, 77, 154].

We demonstrated previously that deletions in three of eight *Francisella phagosomal transporter* (*fpt*) genes, encoding members of the Major Facilitator Superfamily of secondary transporters, in the *F. tularensis* LVS background, resulted in significant *in vitro* and *in vivo* phenotypes: intracellular replication of these strains in macrophages and hepatocytes was reduced and the mutants were attenuated in BALB/c mice. Furthermore, immunization of mice with strains *F. tularensis* LVSΔ*fptB*, LVSΔ*fptE*, or LVSΔ*fptG* protected against homologous lethal challenge [128]. We hypothesized that engineering deletion mutations in the two most promising of these genes, *fptB*, an isoleucine transporter [77], and *fptG*, a transporter of an as yet unknown substrate, in the *F. tularensis* Type A background, would result in protective vaccine candidate strains. Here, we report that *F. tularensis* strain SchuS4 mutants lacking *fptB* or *fptG* demonstrated altered intracellular replication and cytokine release kinetic profiles in macrophages, and were attenuated in mice, indicating their essential roles in cellular escape and virulence. Additionally, one strain, *F. tularensis* SchuS4Δ*fptB*, demonstrated limited protective capacity against intranasal WT challenge.

Results

Generation of *fpt* deletion Type A *Francisella tularensis* SchuS4 strains

F. tularensis Type A strains with an unmarked deletion of either *fptB* or *fptG* were constructed using allelic exchange technology as described previously [128]. Deletion of the target genes and the generation of mutant strains *F. tularensis* SchuS4Δ*fptB* and SchuS4Δ*fptG* was confirmed by PCR using primers originating in both gene flanks, and intragenically (Fig. 5.1). There is no reported substrate for *fptG* and growth curves performed in CDM demonstrated no growth alterations for *F. tularensis* SchuS4Δ*fptG* compared to WT SchuS4 (Fig. 5.2 A).The substrate for *fptB* has been reported to be isoleucine in both *F. tularensis* subspecies *holarctica* and *novicida* [77]. Given the 99% identity between the Type A and Type B gene sequences, isoleucine was first confirmed as the substrate for *fptB* using Chamberlain's defined medium (CDM); *F. tularensis* SchuS4Δ*fptB* exhibited reduced growth compared to WT, but could be increased to WT levels by the addition of exogenous isoleucine (Fig. 5.2 B).

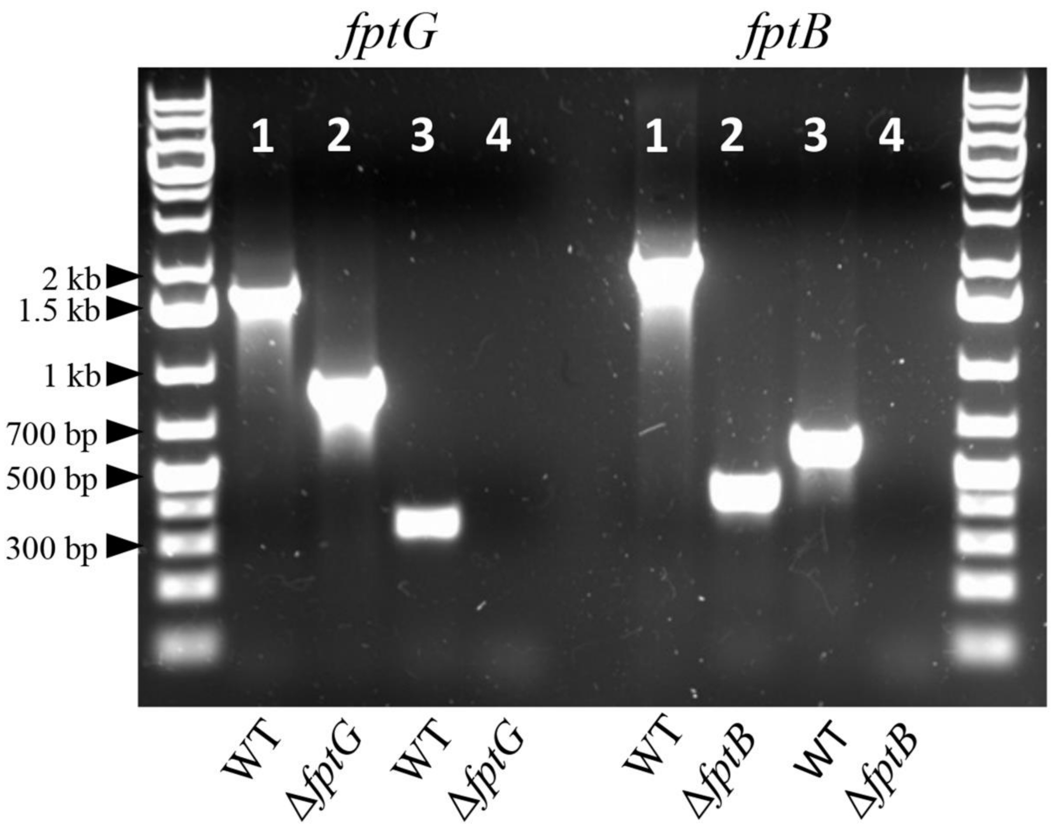

Figure 5.1. Deletion and purification of *F. tularensis* SchuS4 strains lacking either *fptG* or *fptB* genes. DNA was isolated and the presence or absence of the *fpt* genes were ascertained via PCR. Lanes 1 and 2 represent the gene-specific PCR product amplified with primers located in the upstream and downstream flanks in either WT *F. tularensis*, or strains lacking *fptG* or *fptB.* Lanes 3 and 4 represent the PCR product from primers located within the *fpt* gene.

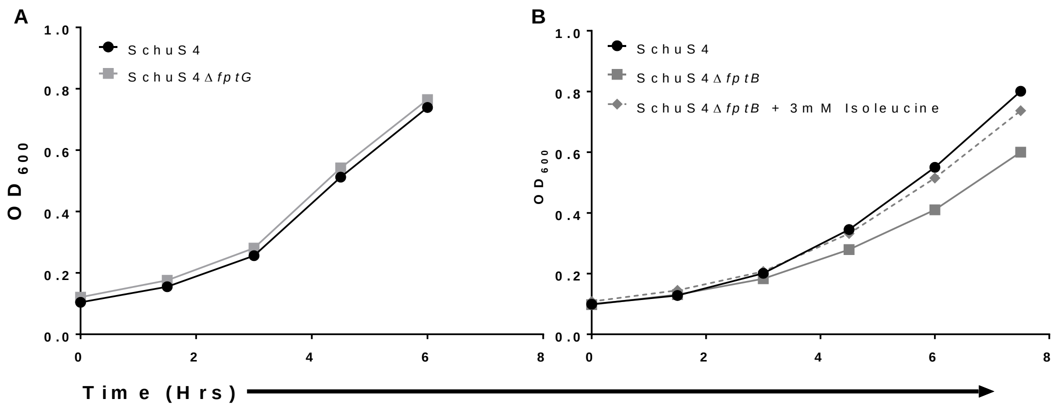

Figure 5.2. Growth of SchuS4Δ*fptG* and SchuS4Δ*fptB* in Chamberlain's Defined Medium. (A) Growth kinetics of WT *F. tularensis* SchuS4 and SchuS4Δ*fptG* were examined in the Chamberlain's defined minimal medium. (B) WT *F. tularensis* SchuS4 and SchuS4Δ*fptB* were examined in CDM without or with supplementation of 3 mM isoleucine. Data are of a single representative experiment (n = 5).

F. tularensis fpt mutant strains are deficient in intracellular replication and cellular escape in multiple cell types

The virulence of *Francisella* is dependent, in part, on its ability to replicate to high numbers intracellularly. The replication kinetics of the *fpt* mutant strains were compared to that of WT *F. tularensis* SchuS4 in THP-1 human macrophage-like cells and HepG2 hepatic carcinoma cells. In order to observe only the initial round of invasion and replication, a bactericidal concentration of gentamicin was maintained in the culture media to prevent cell-to-cell spread. There were significantly higher numbers of both mutant strains in THP-1 macrophages at 24 hours post-infection compared to the WT strain ($p < 0.0001$) (Fig. 5.3 A,B). WT *F. tularensis* doubled 3 to 4.5 times in the first 24 hours, compared to 5.2-6.3 times for *F. tularensis* SchuS4Δ*fptG* and 5-5.4 times for *F. tularensis* SchuS4Δ*fptB*, both significantly more than the WT strain ($p < 0.01$) (Fig. 5.3 E,F).

When cell-to-cell spread was allowed to proceed by removal of gentamicin from the media post-invasion, intracellular bacterial counts and doublings through 24 hpi were equivalent between *F. tularensis* SchuS4Δ*fptG* and WT (Fig. 5.3 C). Both strains doubled ~8-times in the first 24 hours (Fig. 5.3 G). In contrast, *F. tularensis* SchuS4Δ*fptB* exhibited a significant ($p < .0001$) replication defect as evidenced by reduced numbers of intracellular bacteria and significantly fewer doublings ($p < 0.001$) through 24 hours (Fig. 5.3 D, H). Without gentamicin, *F. tularensis* SchuS4Δ*fptB* doubled only 6.8-times compared to 8.7 for WT (Fig. 5.3 H). Together these data suggest that *F. tularensis*

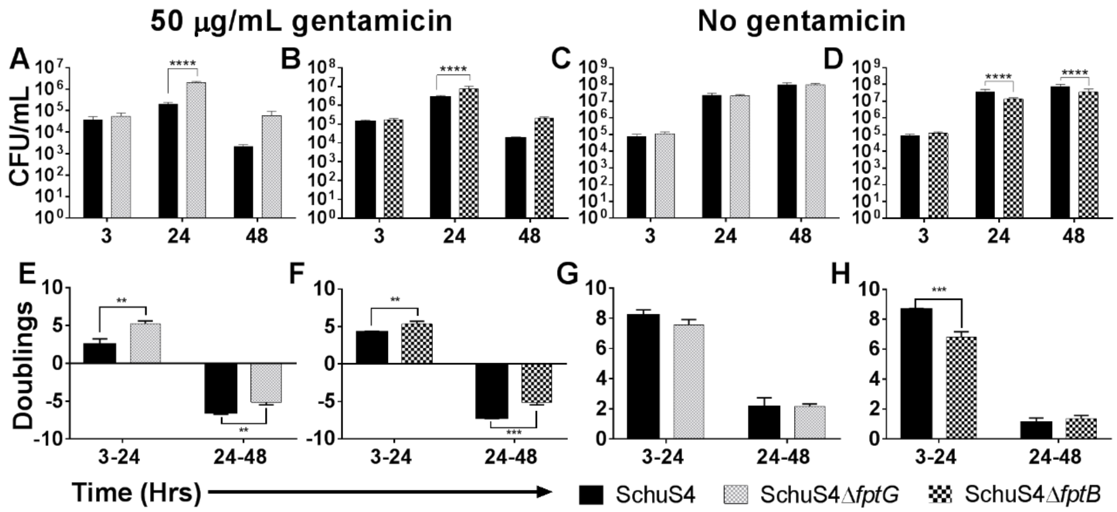

Figure 5.3. SchuS4Δ*fptG* and SchuS4Δ*fptB* exhibit altered intracellular replication kinetics in THP-1 cells. THP-1 cells were infected at an MOI of 100 for 2 hours with SchuS4Δ*fptG* (A, C, E, F) or SchuS4Δ*fptB* (B, D, F, H). Cells were then washed twice with PBS and incubated with 50 µg/mL gentamicin for either 1 hour followed by washing and incubation without antibiotics (C, D, G, H), or for the duration of the experiment (A, B, E, F). Intracellular bacteria were enumerated at 3, 24, and 48 hpi and number of doublings calculated between each interval. Data are plotted as the arithmetic mean CFU counts of three biological replicates performed in quadruplicate ± standard deviations. Data are of a single representative experiment (n = 9). ** $p < 0.01$, *** $p < 0.001$, ****, $p < 0.0001$ (Average CFU and calculated doublings analyzed by two-way ANOVA).

SchuS4Δ*fptG* does not have an increased intracellular replication rate, but rather, is delayed in cellular escape. *F. tularensis* SchuS4Δ*fptB* has a reduced intracellular replication rate compared to WT and is delayed in cellular escape. *Trans*-complementation of both *fpt* genes with an intact plasmid-encoded gene copy restored WT replication kinetics for both mutant strains in THP-1 cells (Fig. 5.4). Furthermore, addition of 3 mM isoleucine, the substrate of *fptB* [77], to the culture media of THP-1 cells infected with *F. tularensis* SchuS4Δ*fptB* was able to rescue the replication defect in a similar fashion to broth assays (Fig. 5.5).

The replication kinetics of the *fpt* mutant strains was also examined in primary mouse and human macrophages. BMDMs were harvested from C57BL/6J mice and used for infection studies, as this model was subsequently used for *in vivo* studies. Fewer intracellular bacteria of both *F. tularensis* SchuS4Δ*fptB* and SchuS4Δ*fptG* strains were enumerated 24 hpi compared to WT (Fig. 5.6 A). The number of doublings for SchuS4Δ*fptG* and SchuS4Δ*fptB* were 4.4 and 1.2, respectively, both significantly lower than the 6.1 for WT ($p < 0.05$, 0.0001) (Fig. 5.6 B). Interestingly, no intracellular replication was detected for WT or mutant strains through 8 hpi. Similar replication kinetics to those seen in BMDMs were observed in human MDMs (Fig. 5.7 A, B). Fewer intracellular bacteria for both *F. tularensis* SchuS4Δ*fptB* and SchuS4Δ*fptG* were observed at 24 hpi compared to WT ($p < 0.001$), though only *F. tularensis* SchuS4Δ*fptB* displayed a significant reduction ($p < 0.05$) by bacterial doublings compared to WT.

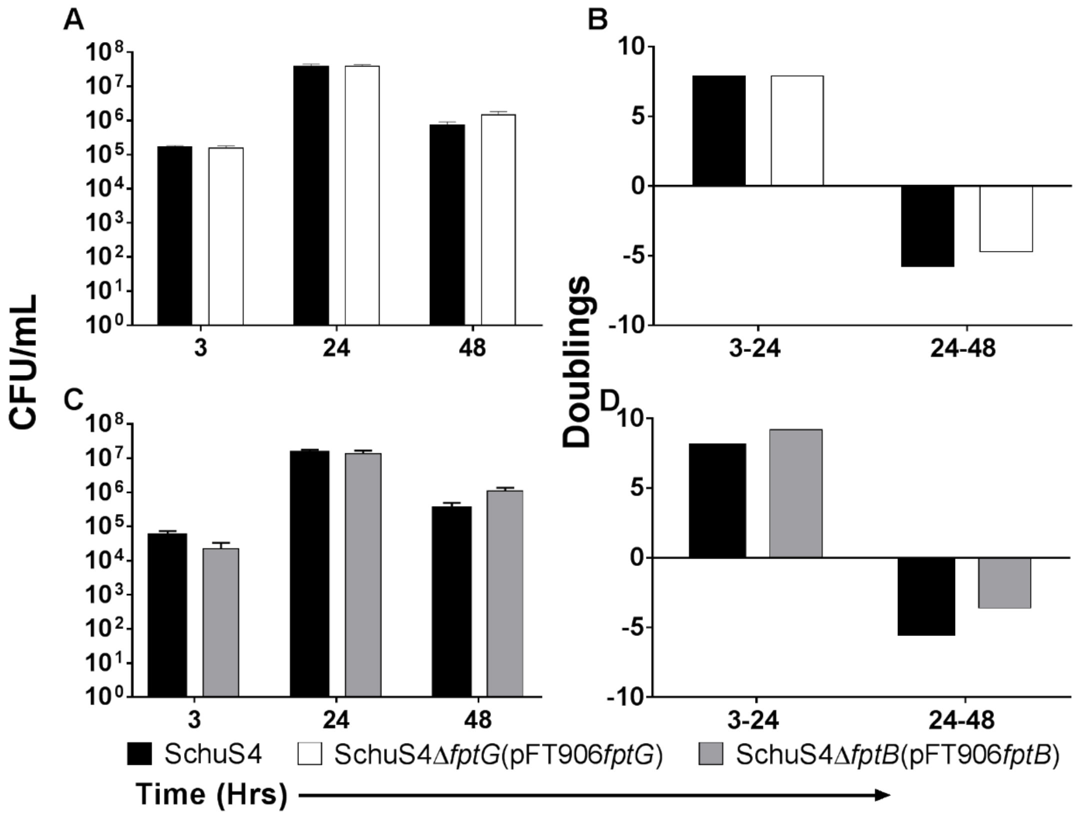

Figure 5.4. Complementation of *fpt* genes restores wildtype growth kinetics in THP-1 cells. THP-1 cells were infected at an MOI of 100 for 2 hours with *F. tularensis* WT, SchuS4Δ*fptG* (A, B), or SchuS4Δ*fptB* (C, D). Cells were then washed twice with PBS and incubated with 50 µg/mL gentamicin for 1 hour before being returned to media lacking gentamicin Intracellular bacteria were enumerated at 3, 24, and 48 hours post-infection. Data are plotted as the arithmetic mean CFU counts of three biological replicates performed in quadruplicate ± standard deviations. Data are of one representative experiment (n = 4). *, $p < 0.05$, **, $p < 0.01$ (Average CFU and calculated doublings analyzed by two-way ANOVA).

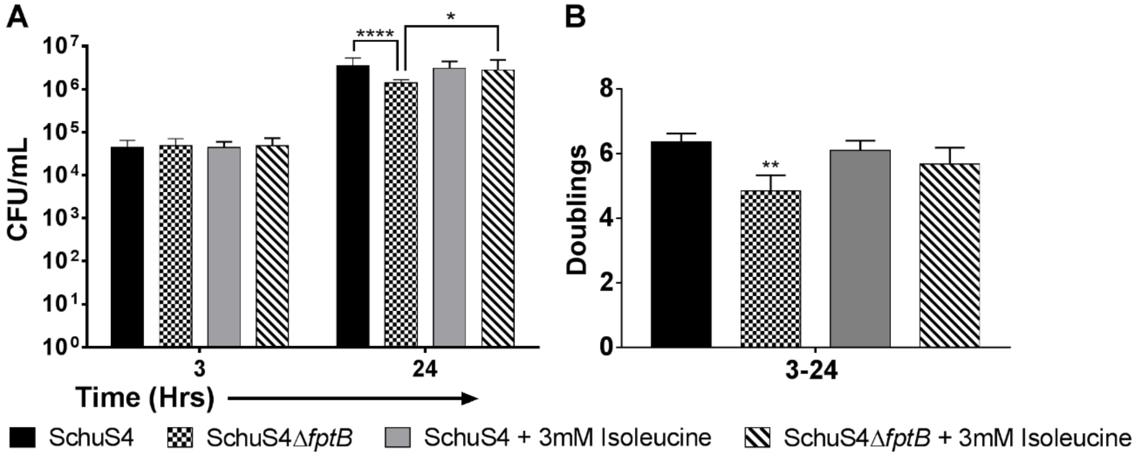

Figure 5.5. Excess isoleucine returns *F. tularensis* SchuS4Δ*fptB* to WT replication kinetics in THP-1 cells. THP-1 cells were infected at an MOI of 100 for 2 hours. Cells were then washed twice with PBS and incubated with 50 µg/mL gentamicin for 1 hour before being returned to media lacking gentamicin. Intracellular bacteria were enumerated at 3, 24, and 48 hours post-infection. Data are plotted as the arithmetic mean CFU counts of three biological replicates performed in quadruplicate ± standard deviations. Data are of a single representative experiment (n = 2). *, $p < 0.05$, **, $p < 0.01$, ****, $p < 0.0001$ (Average CFU and calculated doublings analyzed by two-way ANOVA).

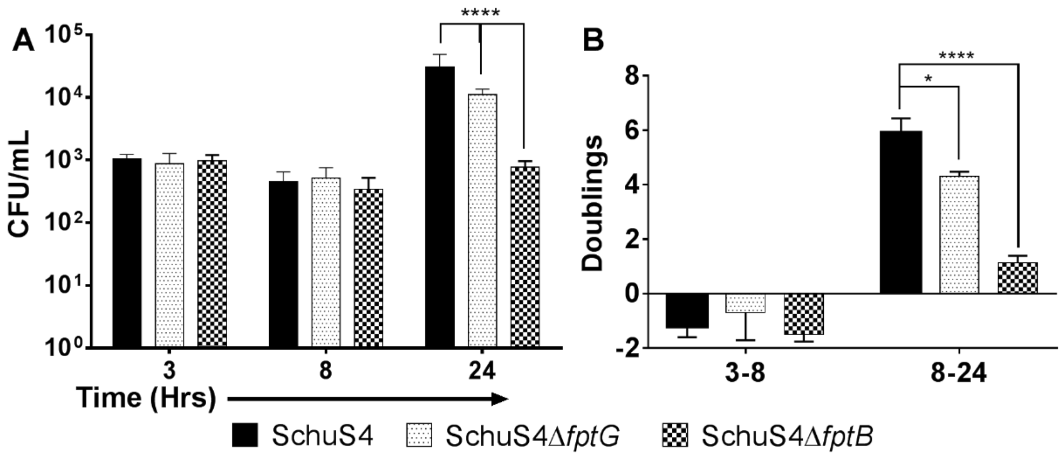

Figure 5.6. *F. tularensis* SchuS4Δ*fptG* and SchuS4Δ*fptB* are replication deficient in C57BL/6J BMDMs. BMDM cells were infected at an MOI of 10 for 2 hours. Cells were then washed twice with PBS and incubated with 50 µg/mL gentamicin for 1 hour before being returned to media lacking gentamicin. Intracellular bacteria were enumerated at 3, 8, and 24 hours post-infection. Data are plotted as the arithmetic mean CFU counts of three biological replicates performed in quadruplicate ± standard deviations. Data are of a single representative experiment (n = 2). *, $p < 0.05$, ****, $p < 0.0001$ (Average CFU and calculated doublings analyzed by two-way ANOVA).

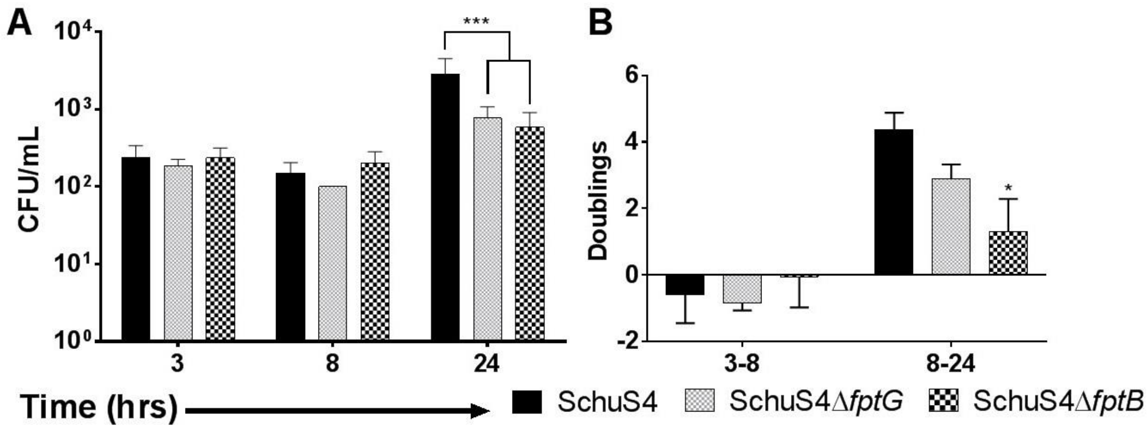

Figure 5.7. *F. tularensis* SchuS4Δ*fptB*, but not SchuS4Δ*fptG*, are replication deficient in human MDMs. MDM cells were infected at an MOI of 10 for 2 hours. Cells were washed twice with PBS and incubated with 50 µg/mL gentamicin for 1 hour before being returned to media lacking gentamicin. Intracellular bacteria were enumerated at 3, 8, and 24 hours post-infection. Data are plotted as the arithmetic mean CFU counts of three biological replicates performed in quadruplicate ± standard deviations. Data are of a single representative experiment (n = 2). *, $p < 0.05$, ***, $p < 0.001$ (Average CFU and calculated doublings analyzed by two-way ANOVA)

F. tularensis is able to invade and replicate in the liver during infection [42]. Invasion assays were performed using HepG2 hepatic carcinoma cells under the conditions described above. *F. tularensis* SchuS4Δ*fptG* exhibited a similar phenotype as that observed in macrophages under conditions that either limited or allowed intercellular spread (Fig. 5.8 A, C). Doublings were higher in the presence of gentamicin, and equivalent when antibiotics were removed (Fig 5.8 C, G), further supporting a delay in escaping the host cytosol. *F. tularensis* SchuS4Δ*fptB* demonstrated WT levels of intracellular replication in HepG2 cells and appeared to escape the host cell at the WT rate (Fig. 5.8 B, F, D, H).

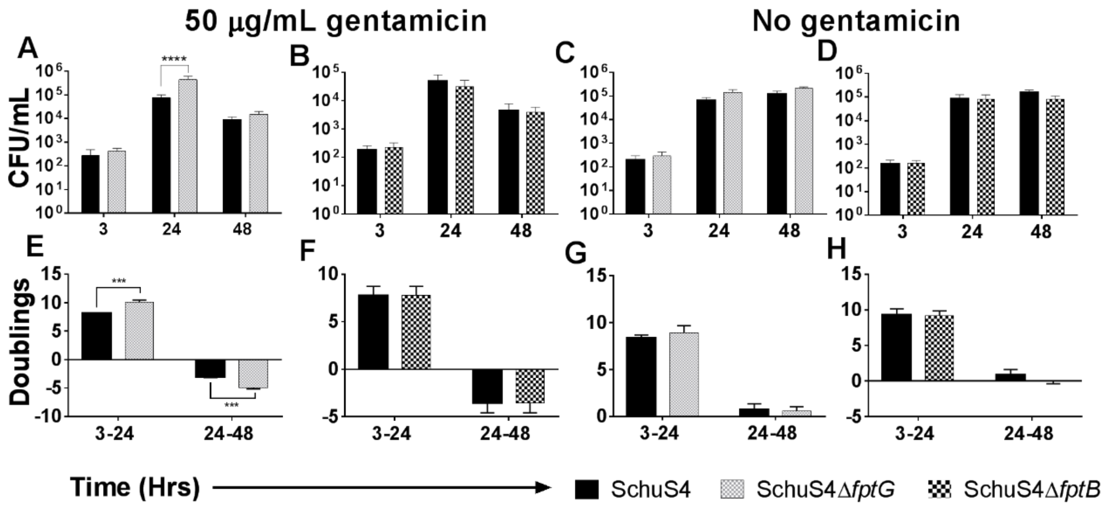

Figure 5.8. SchuS4Δ*fptG*, but not SchuS4Δ*fptB* exhibit altered intracellular replication kinetics in HepG2 cells. HepG2 cells were infected at an MOI of 300 for 2 hours. Cells were then washed twice with PBS and incubated with 50 µg/mL gentamicin for either 1 hour (C, D, G, H), or for the duration of the experiment (A, B, E, F). Intracellular bacteria were enumerated at 3, 24, and 48 hpi and number of doublings calculated between each interval. Data are plotted as the arithmetic mean CFU counts of three biological replicates performed in quadruplicate ± standard deviations. Data are of a single representative experiment (n = 8). *** $p < 0.001$, ****, $p < 0.0001$ (Average CFU and calculated doublings analyzed by two-way ANOVA).

F. tularensis fpt mutants induce altered membrane permeability

To examine more closely the escape delay phenotype displayed by both *fpt* mutants, invasion assays in THP-1 macrophages were carried out under conditions that limit cell spread with time points every 6 hours during 33 hours of infection. Positive doubling rates were interpreted as an indication that replication was outpacing escape, and negative values were interpreted as escape outpacing replication. Supernatants were assayed for the release of lactate dehydrogenase (LDH), an intracellular enzyme whose release is indicative of membrane permeability, possibly due to cell death [151, 108]. Supporting previous findings in THP-1 cells, intracellular numbers of *F. tularensis* SchuS4Δ*fptG* (Fig. 5.9 A) and doubling rates were similar to that of WT through the first 15 hpi (Fig. 5.9 B). *F. tularensis* SchuS4Δ*fptG* continued to replicate, as evidenced by the net-positive doubling rate for an additional 6 hours beyond that of WT. *F. tularensis* SchuS4Δ*fptG* elicited significantly higher CFU counts at 21 and 27 hpi compared to WT. Both *F. tularensis* WT- and SchuS4Δ*fptG*- infected cells released levels of LDH above that of background from 15 hpi to the end of the assay at 33 hpi. LDH release paralleled the decrease in intracellular numbers of *F. tularensis* WT bacteria and the slowing, but still positive, doubling rate of SchuS4Δ*fptG*-infected cells (Fig. 5.9 A, B). This suggests cellular escape was outweighing replication for *F. tularensis* WT, and was beginning, but not outpacing, replication for SchuS4Δ*fptG* (Fig. 5.9 C). Cells infected with *F. tularensis* SchuS4Δ*fptG* released significantly more LDH ($p < .0001$) than those infected with WT from 21-33 hpi (Fig. 5.9 C). This may indicate that cells infected with *F. tularensis* SchuS4Δ*fptG* were struggling to contain the strain that was replicating at a WT rate, but were not escaping. Also in support of our earlier findings in THP-1 macrophages, *F.*

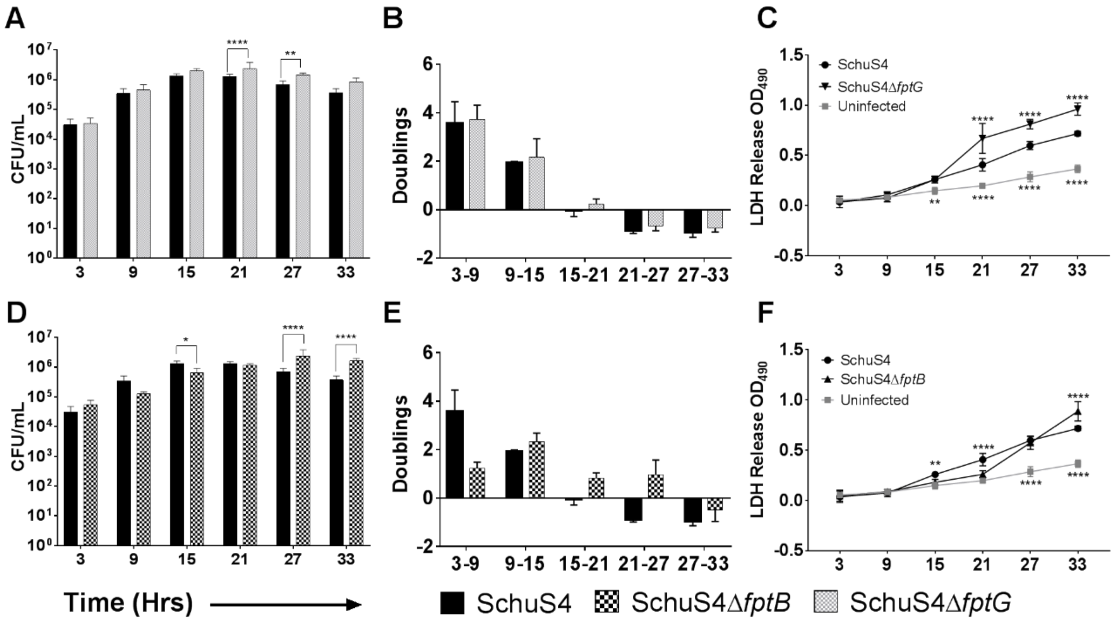

Figure 5.9. Altered cell death accompanies altered replication kinetics of *fpt* mutant strains in THP-1 cells. THP-1 cells were infected at an MOI of 100 for 2 hours with *F. tularensis* WT, SchuS4Δ*fptG* (A, B, C) or SchuS4Δ*fptB* (D, E, F). Cells were then washed twice with PBS and incubated with 50 µg/mL gentamicin for the duration of the experiment. Intracellular bacteria were enumerated at 3, 9, 15, 21, 27 and 33 hpi, doublings calculated between each time interval, and supernatants were analyzed for LDH release. Data are plotted as the arithmetic mean CFU counts of three biological replicates performed in quadruplicate ± standard deviations. Data are of a single representative experiment (n = 5). *, $p < 0.05$, ** $p < 0.01$, ****, $p < 0.0001$ (CFU counts, calculated doublings, and LDH release by two-way ANOVA).

tularensis SchuS4Δ*fptB*, exhibited a significant growth defect that was quantified as reduced intracellular bacterial numbers (Fig. 9 D) and reduced doublings between 3 and 9 hpi (Fig. 5.9 E). *F. tularensis* SchuS4Δ*fptB* continued to double for 12 hours beyond that of WT, exhibiting increasing CFU numbers (Fig. 5.9 D) and positive doubling values (Fig. 5.9 E) through 27 hpi. Similarly, *F. tularensis* SchuS4Δ*fptB* was significantly ($p <$ .0001) delayed in releasing LDH (Fig. 5.9 F). These results support a role for *fptB* and *fptG* in timely escape from the cell, and, in the case of *fptB*, in intracellular replication.

F. tularensis SchuS4Δ*fptG* and SchuS4Δ*fptB* elicit different early pro-inflammatory responses

The production of TLR2-dependent cytokines, and the activation of STING and the AIM2 inflammasome, are necessary for initiation of the host cytokine response to *F. tularensis* infection [51, 38, 102, 169]. The altered intracellular replication kinetics of *F. tularensis* SchuS4Δ*fptG* and SchuS4Δ*fptB* in macrophages suggested that infection with mutant strains would likely result in modified interactions with innate immune components. The levels of secretion of two important early pro-inflammatory cytokines, TNF-α and IL-1β, were measured in supernatants from the THP-1 infection samples from the above assay. *F. tularensis* SchuS4Δ*fptG* and WT infections induced the release of IL-1β at 15 hpi. However, the levels induced by *F. tularensis* SchuS4Δ*fptG* were significantly higher than those induced by WT from 21 – 33 hpi (Fig. 5.10 A). IL-1β release was delayed in *F. tularensis* SchuS4Δ*fptB*-infected cells until 27 hpi. The timing of the IL-1β release for both mutant strains and WT coincided with that of LDH release, demonstrating a correlation between membrane disruption and mature IL-1β release.

F. tularensis SchuS4Δ*fptG*-infected cells secreted TNF-α with similar kinetics to that of WT, while *F. tularensis* SchuS4Δ*fptB* induced significantly less than both other strains at all time points (Fig. 5.10 B). The cytokine secretion patterns induced by both mutant strains mirrored their replication patterns, with *F. tularensis* SchuS4Δ*fptG* being similar to WT, and *F. tularensis* SchuS4Δ*fptB* significantly diminished compared to the other two strains.

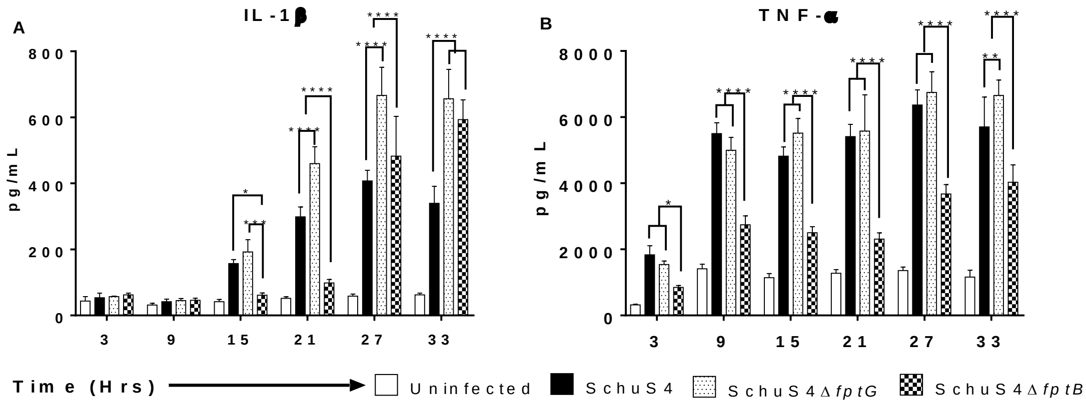

Figure 5.10. *F. tularensis* SchuS4Δ*fptG* and SchuS4Δ*fptB* elicit altered inflammatory responses. THP-1 cells were infected at an MOI of 100 for 2 hours. Cells were then washed twice with PBS and incubated with 50 µg/mL gentamicin for the duration of the experiment. Cell-free supernatants were collected at 3, 9, 15, 21, 27 and 33 hpi and measured for cytokine contents using sandwich ELISAs. Data are plotted as the arithmetic mean of 3 biological replicates performed in duplicate, counts ± standard deviations. Data are of a single representative experiment (n = 5). *, $p < 0.05$, ** $p < 0.01$, *** $p < 0.001$, ****, $p < 0.0001$ (by two-way ANOVA).

The escape delay exhibited by SchuS4Δ*fptG* is autophagy-dependent

It has been demonstrated previously that *F. tularensis* interacts with the cell's autophagy machinery during intracellular replication [26, 204]. Because autophagy can induce transient resistance to pyroptosis [54, 229], we next sought to ascertain if autophagy played a part in the observed escape delay of *F. tularensis* SchuS4Δ*fptG*. Invasion assays utilizing bactericidal concentrations of gentamicin through 24 hours were carried out, with the addition of the autophagy inhibitor bafilomycin A1 at either 3 or 12 hpi for a total treatment time of 21 or 12 hours respectively, to cease vesicular acidification, halting autophagy [129], at either the beginning or midpoint of the infection. No effect was observed on the escape delay with a 12 hour treatment of bafilomycin A1 despite equivalent disruption to autophagy, as visualized as buildup of the 16 kD lipidated form of the autophagosome biogenesis protein, LC3-II [88] (Fig. 5.11); equivalent numbers of intracellular SchuS4Δ*fptG* were quantified in both treated and untreated cells at 24 hpi ($p < 0.0001$) (Fig. 5.12 A, C). However, when autophagy was inhibited for 21 hours, the number of intracellular bacteria and doubling rates of *F. tularensis* SchuS4Δ*fptG* was reduced to WT levels (Fig 5.12 B, D). These data suggest a time-sensitive role for autophagy in the escape stage of the *Francisella* intracellular replication cycle.

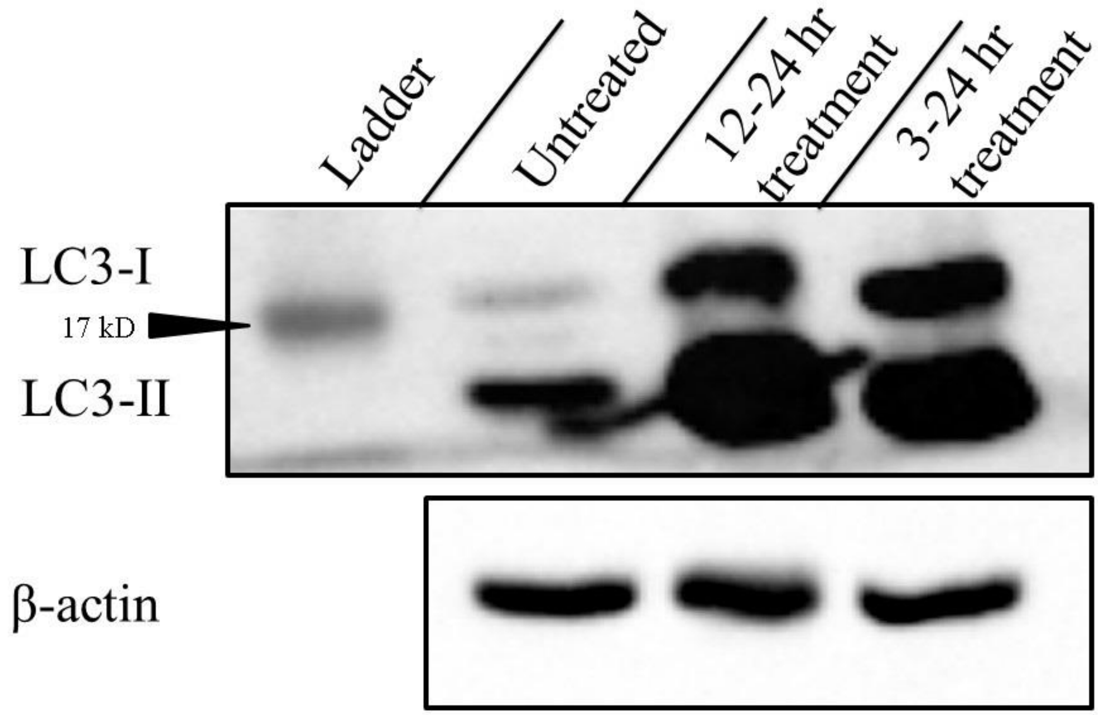

Figure 5.11. Expression of LC3-I and LC3-II in bafilomycin A1 treated THP-1 macrophage-like cells. Whole cell lysates of THP-1 cells untreated (lane 2) or treated with bafilomycin A1 for 12 or 24 hours (lanes 3 and 4) were separated by SDS-PAGE and probed with anti-LC3 (top panel) or anti-β-actin (lower panel).

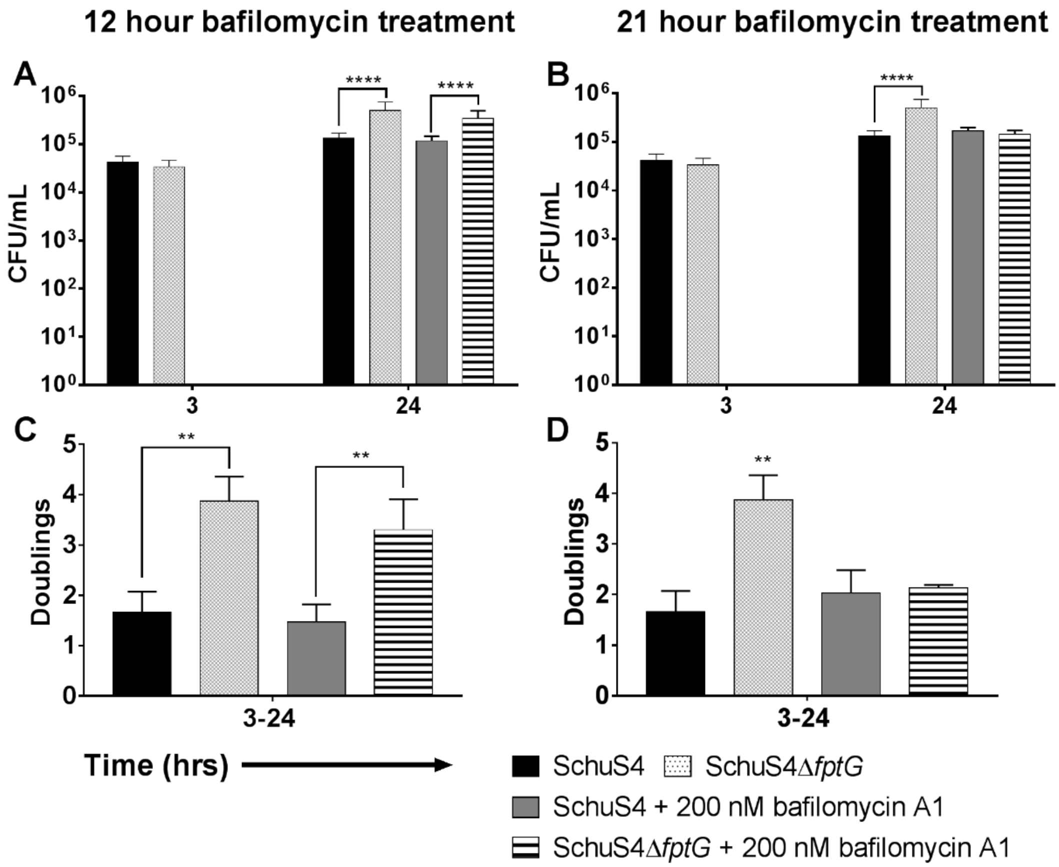

Figure 5.12. *F. tularensis* SchuS4Δ*fptG* is delayed in escape from the host cytosol in an autophagy dependent manner. THP-1 cells were infected at an MOI of 100 for 2 hours. Cells were then washed twice with PBS and incubated with 50 µg/mL gentamicin for the duration of the experiment. Bafilomicin A1 was added to the culture media at either 3 or 12 hpi. Intracellular bacteria were enumerated at 3 and 24 hpi. Data are plotted as the arithmetic mean CFU counts of three biological replicates performed in quadruplicate ± standard deviations. Data are of a single representative experiment (n = 4). ** $p < 0.01$, ****, $p < 0.0001$ (Average CFU and calculated doublings analyzed by two-way ANOVA).

SchuS4Δ*fptB* is highly attenuated in the C57BL/6J mouse model

Altered intracellular replication kinetics and cytokine induction patterns suggested a role for *fptB* and *fptG* in *Francisella* virulence. The C57BL/6J mouse model was used to assess pathogenic defects of these mutant strains as WT Type A *F. tularensis* has an intranasal LD_{50} < 10 CFU in this model [164]. Groups of 4 mice were inoculated intra-nasally with 5×10^1 CFU of WT, or 2×10^1 to over 7×10^6 CFU of the mutant strains. Mice inoculated with WT steadily lost weight over the course of 5 days before succumbing to infection on day 5, exhibiting overt signs of sickness beginning late on day 4 or early on day 5. Half of the mice, one male and one female, inoculated with the lowest dose of *F. tularensis* SchuS4Δ*fptG*, 2×10^1 CFU, succumbed to infection (Table 5.1). These two mice lost weight at the same rate as WT infected mice, but had a 1-2 day delayed time to death compared to WT (data not shown). The two surviving mice from this group never lost weight or showed signs of sickness (data not shown). All higher doses of *F. tularensis* SchuS4Δ*fptG* were lethal at the same rate as WT (Table 5.1). In contrast, no mice inoculated with *F. tularensis* SchuS4Δ*fptB* up to the highest dose succumbed to infection (Table 5.1). No weight loss or overt signs of sickness were evident in any *F. tularensis* SchuS4Δ*fptB* inoculated mice, demonstrating attenuation and an $LD_{50} > 7.6 \times 10^6$ CFU.

Table 5.1: Attenuation of *fpt* mutant strains in C57BL/6J mice.

Strain	Intranasal Dose (CFU)	Survival
SchuS4	1.1×10^1	0/2
SchuS4	1.9×10^1	0/4
SchuS4	4.3×10^1	0/4
SchuS4	5.3×10^1	0/4
SchuS4Δ*fptG*	2.0×10^1	2/4
SchuS4Δ*fptG*	4.8×10^2	0/4
SchuS4Δ*fptG*	1.0×10^3	0/4
SchuS4Δ*fptB*	5.4×10^1	3/3
SchuS4Δ*fptB*	3.1×10^2	4/4
SchuS4Δ*fptB*	5.6×10^2	3/3
SchuS4Δ*fptB*	1.0×10^3	4/4
SchuS4Δ*fptB*	8.7×10^3	4/4
SchuS4Δ*fptB*	9.8×10^4	4/4
SchuS4Δ*fptB*	1.0×10^5	2/2
SchuS4Δ*fptB*	1.0×10^6	4/4
SchuS4Δ*fptB*	7.6×10^6	3/3

<u>*F. tularensis* SchuS4Δ*fptB* vaccination protects against virulent *F. tularensis* SchuS4 challenge</u>

Given the high level of attenuation of SchuS4Δ*fptB*, we assessed the ability of this strain to protect against lethal challenge. Groups of 4 mice in two independent experiments were inoculated with a single dose of ~1×10^6 CFU *F. tularensis* SchuS4Δ*fptB* prior to WT challenge 28 days later with doses ranging from 7 CFU - 360 CFU. Ten of 26 vaccinated mice from two separate experiments survived challenge, as well as one unvaccinated control mouse, resulting in an efficacy value of 28% in vaccinated groups (Table 5.2). An increased delay in time to death was observed in a challenge dose-dependent manner (Table 5.2). The delay to death was accompanied also by differences in weight loss by challenged, vaccinated mice. As shown in Figure 5.13 A, mice receiving the lowest challenge dose of WT *F. tularensis* that succumbed to challenge began losing weight later than mice receiving the middle and high doses (Fig 5.13 B, C). All vaccinated mice that succumbed began losing weight later than unvaccinated control mice. All protected mice showed no overt signs of illness with little to no loss of weight following challenge. These data suggest *F. tularensis* SchuS4Δ*fptB* has limited protective capacity and demonstrates the first example of protection by an MFS transporter targeted vaccine strain from Type A challenge.

Another set of mice were given a prime/boost vaccination regimen to explore the possibility of increased protection, with two doses of ~1×10^6 CFU *F. tularensis* SchuS4Δ*fptB* 14 days apart, before WT challenge 28 days later with doses ranging from 43-840 CFU. Only 2 of 18 mice vaccinated under the prime/boost scheme survived challenge (Table 5.3), resulting in a protection rate of 11.1%. As with the single

Table 5.2: Protection against WT *F. tularensis* SchuS4 challenge after one vaccination with SchuS4Δ*fptB.*

Vaccine Inoculum (CFU)	Challenge Dose (CFU)	Survival	Individual Delay to Death (Days)	Average Delay to Death (Days)
Experiment 1				
7.3×10^5	7	2/5	8, 9, 8, 14<, 14<	4
7.3×10^5	70	1/4	7, 6, 6, 14<	2
7.3×10^5	162/350	2/5	6, 6, 6, 14<	1.67
PBS	162/350	0/3	4, 4, 5	--
Experiment 2				
1.14×10^6	39	2/4	7, 10, 14<, 14<	3.5
1.14×10^6	78	1/4	6, 7, 9, 14<	2.33
1.14×10^6	360	2/4	7, 6, 14<, 14<	1.5
PBS	39	1/4	5, 5, 5, 14<	--

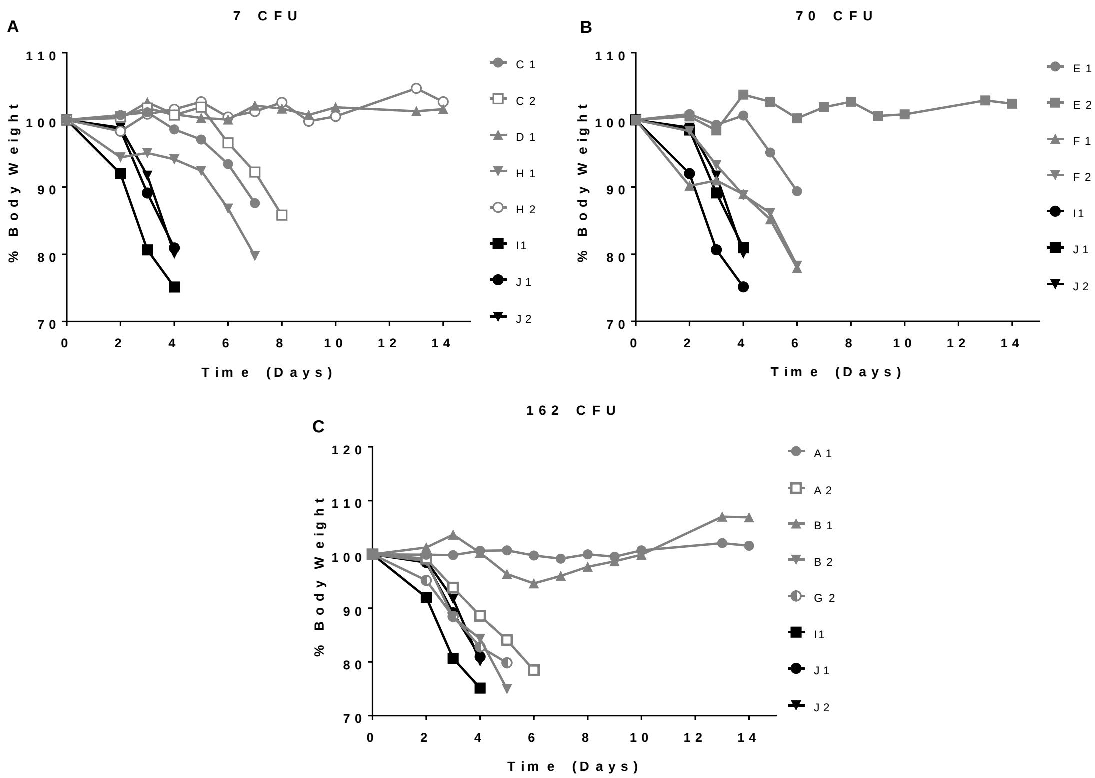

Figure 5.13. Delay in weight loss is challenge dose dependent. Groups of 4 mixed gender C57BL/6J mice were vaccinated with either 7.6×10^5 CFU *F. tularensis* SchuS4Δ*fptB* or PBS before challenging with the concentrations of WT *F. tularensis* as shown above 28 days later. Weights were recorded daily after challenge for 14 days. Graphs show the % bodyweights of individual vaccinated mice (gray) compared to unvaccinated but homologously challenged control mice (black).

Table 5.3: Protection against wildtype challenge after two vaccinations with SchuS4Δ*fptB*.

Vaccine Inocula (CFU)	Challenge Dose SchuS4 (CFU)	Survival	Individual Delay to Death (Days)	Average Delay to Death (Days)
1st - 1.14×10^6 2nd - 1.04×10^6	43	1/4	6, 9, 8, 14<	2.2
1st - 1.14×10^6 2nd - 1.04×10^6	90	1/4	12, 8, 7, 14<	3.5
1st - 1.14×10^6 2nd - 1.04×10^6	540	0/6	7, 5, 8, 6, 8, 5	1
1st - 1.14×10^6 2nd - 1.04×10^6	840	0/4	6, 6, 7, 9	1.5
1st - PBS 2nd - PBS	43	0/6	6, 5, 6, 6, 5, 5	--

dose vaccination system, a delay to death was challenge dose-dependent manner (Table 5.3). These data suggest that while *F. tularensis* SchuS4Δ*fptB* can provide limited protection, it is unable to improve efficacy when administered a second dose through the intranasal route.

Discussion

The formulation of a licensed, efficacious live attenuated vaccine against *Francisella tularensis* has remained an elusive goal, despite increased efforts since the anthrax bioterror attacks of 2001. Prior studies in humans with *F. tularensis* LVS in the 1960's demonstrated the proof of concept for the protective capacity of the live attenuated vaccine strategy, and has pointed the way forward for the engineering of live attenuated strains harboring targeted deletions [91, 218, 128, 172, 104]. Here, we investigated the potential of two MFS transporters, FptG and FptB, as attenuating targets in the virulent Type A strain, and the effects of their loss on the intracellular lifecycle of Type A *F. tularensis*. Our prior studies demonstrated the importance of both genes in the *F. tularensis* LVS background, for both *in vitro* replication kinetics and *in vivo* virulence [128]. Both *F. tularensis* LVSΔ*fptB* and LVSΔ*fptG* exhibited severe replication defects in multiple cell types and were both attenuated and protective in the BALB/c model [128]. We hypothesized that, given the high protein identity between the *F. tularensis* LVS and Type A strains for these proteins (99% for FptB and 100% for FptG), similar phenotypes would be observed in the clinically relevant Type A background.

In contrast to our prior results in *F. tularensis* LVS, SchuS4Δ*fptG* did not display a replication defect in broth or in any cell line tested, highlighting a difference between the LVS and Type A strains, though a replication deficiency was noted in mouse BMDMs. *F. tularensis* SchuS4Δ*fptB* displayed a significant growth defect in macrophages, similar to observations with the *F. tularensis* LVS-derived mutant [128, 77]. The restriction of intracellular growth defects to macrophages and not hepatic cells may stem from the fact that the substrate of FptB, isoleucine, is regulated in macrophages. Isoleucine is one of nine amino acids to be depleted by activated macrophages [146]. This, coupled with the fact that excess isoleucine in culture rescues growth of *F. tularensis* SchuS4Δ*fptB*, implies that isoleucine is a rate-limiting nutrient for intracellular replication of *Francisella tularensis*, and that there likely exists another, previously hypothesized [77], lower affinity transporter that contributes to transport of isoleucine in the absence of FptB. It may be that FptB functions as a high affinity transporter to scavenge isoleucine intracellularly, even at depleted levels.

The delay in cytosolic escape observed with both *fptB* and *fptG* mutant strains has not been reported previously in *Francisella*. Extensive work by multiple laboratories has revealed the process by which *Francisella* escapes the phagosome early in the replication cycle, what host and bacterial genes are key to this process, and the consequences of delays at this stage [80, 35, 186, 37, 32]. However, escape from the host cell at the final stage of the intracellular cycle remains an aspect of the *Francisella* lifecycle that is poorly understood. Current models of escape involve *Francisella* replicating to high numbers before triggering pyroptotic cell death mediated through AIM2 and caspase 8 [159], during which the bacteria are presumed to be released from the necrotic cell [14, 2, 31]. While the escape process appears tied to the cell death machinery, the control of timing of cell death and subsequent escape includes both host and bacterial factors. *F. tularensis* SchuS4Δ*fptG* replicates at the same rate as WT, but is delayed in its escape, implying that the processes of replication and cellular escape are dissociable. The mechanism by which *Francisella* controls escape timing may be regulated by the cell's autophagic machinery. It has been demonstrated that *Francisella* triggers autophagy by depleting cellular glutathione, and then associates with the autophagic machinery to harvest this microenvironment for nutrients, especially amino acids [26, 204, 4, 184]. Autophagy has been shown, especially in the context of other intracellular bacterial infections including *Shigella* and *Legionella*, to transiently delay the induction of pyroptosis by the host [54, 229]. The sharply increased secretion of IL-1β, an inflammasome-dependent process, in *F. tularensis* SchuS4Δ*fptG* infected cells, coupled with the necessity for autophagy to delay cytosolic escape for SchuS4Δ*fptG*, suggests that the release of cytokines often associated with pyroptosis and the process of cell death itself may be separate. Interestingly, the escape delay, with its dependence on both autophagy and certain nutrient transporters, implies a necessity to interact with this microenvironment, perhaps as part of a "checklist" for escape. When the cell was prevented from undergoing autophagy, following the addition of bafilomycin A1, *F. tularensis* SchuS4Δ*fptG* appeared to forgo the autophagy interaction step and escape at the WT rate. Though the escape delay phenotype of *F. tularensis* SchuS4Δ*fptG* is bafilomycin A1-sensitive, alternative approaches will be necessary to definitively tie autophagy to delay of the cell death machinery in the context of *F. tularensis* infection.

A fundamental key to the virulence of *Francisella* is its ability to invade and replicate intracellularly in many cell types, especially macrophages, where host responses have been extensively studied, revealing the induction of a potent, yet atypical inflammatory response, that can ultimately lead to sepsis and hypercytokinemia [123, 196]. The avoidance of TLR4, yet stimulation of TLR2/6, AIM2, and STING may produce an immune response that is less than effective for host survival [102, 40, 86], and highlights the extreme virulence of this bacterium. Both *fpt* mutant strains elicited altered inflammatory cytokine secretion; infection with *F. tularensis* SchuS4Δ*fptB* resulted in a delayed IL-1β and reduced TNF-α response, while SchuS4Δ*fptG* stimulated increased levels of IL-1β compared to WT, and comparable levels of TNF-α. Both strains were attenuated in the C57BL/6J mouse model with LD_{50} 2-10 times and >700,000 times of that of WT for SchuS4Δ*fptG* and SchuS4Δ*fptB*, respectively. The level of attenuation exhibited by *F. tularensis* SchuS4Δ*fptB* places it among the most attenuated Type A-derived vaccine strains [127], and confirms the importance of intracellular replication and host cell interactions early in infection. Though we have not yet reached the lethal dose for this strain, challenge results suggest that *F. tularensis* SchuS4Δ*fptB* may be over-attenuated. Historically, the prime difficulty of live attenuated vaccine development has been achieving the optimal balance of safety/attenuation and immunogenicity/protection. The reduced inflammatory response elicited by *F. tularensis* SchuS4Δ*fptB* in the early stages of macrophage infection compared to WT may indicate that an altered host cell interaction at the time of initial macrophage infection does not guarantee the onset of a long-term protective response.

These data represent the first utilization of MFS transporters, and in the case of *fptB*, an amino acid transporter specifically, as potential attenuating targets in the virulent *F. tularensis* Type A background. Prior efforts have centered upon biosynthetic [183, 155, 94], capsule [117, 218, 168], and virulence genes [166], but transporters represent a largely untapped source of potentially attenuating targets. Importantly, nutrient transporters, including those defined to be within the MFS, may be of increased importance to intracellular pathogens. It is appreciated that bacteria residing in the intracellular space undergo genome reductions, resulting in the shedding of genes involved in transport and metabolism at a rate that is much higher than that of genes involved in replication and defense [135]. This implies that any remaining transporter and metabolite genes are necessary for the survival, and possibly, virulence of the organism. The Type A strain of *Francisella tularensis* is predicted to have 35 MFS transporters, and 182 transporters in total [107], representing close to 12% of the SchuS4 protein coding sequences. This represents a very large pool of potential novel targets for not just vaccines, but for antibiotic therapies as well. Intriguingly, similar gene proportions exist in many clinically relevant pathogenic organisms.

F. tularensis SchuS4Δ*fptB* is the first MFS-based live attenuated strain in the Type A background to demonstrate protection against WT Type A *Francisella* challenge. While the efficacy was modest following vaccination with this strain, these data support the idea of targeting nutrient transporters as part of an attenuation strategy. These strains represent insightful tools allowing more intimate study the intracellular lifecycle of *F. tularensis*, especially the understudied molecular steps leading to cellular escape.

Acknowledgements

This work was supported by NIH NIAID 1R01AI102966, R01AI123129, and 5T32AI095190-04.

The authors wish to acknowledge Dr. William Jackson for technical assistance with the autophagy assays, and Dr. Stefanie Vogel for critical review of the manuscript.

Chapter 6 – Investigation of the identity of the FptG substrate

Supplementation of CDM to identify the substrate of FptG

Previous experiments examining mutation in *fptG* both the *F. tularensis* LVS and SchuS4 backgrounds have demonstrated significant effects on bacterial virulence and host cell interactions [128]. Despite phenotypic characterization of strains lacking this important transporter, the identity of the substrate of FptG remains elusive. Growth and nutrient supplementation in (CDM) has revealed the substrates of two *fpt* transporters: FptE was found to transport the amino acid asparagine, and FptB was found to transport isoleucine [76, 77]. The substrates for both transporters were defined in the non-virulent *F. tularensis* LVS or subspecies *novicida* backgrounds. There is 99% - 100% amino acid sequence identity between the less virulent strains and the virulent Type A strain at the *fptB* and *fptE* loci, as defined by BLAST-P analysis. We confirmed that isoleucine was the substrate for *fptB* in the Type A strain SchuS4 (Figure 5.5).

Given the 99% amino acid sequence identity between FptG proteins from LVS and Type A SchuS4, we undertook a similar approach to identify the substrate of FptG. We utilized LVS as the strain background since a greater range of studies could be performed in the BSL-2 laboratory. A significant growth delay for *F. tularensis* LVSΔ*fptG* compared to parental LVS was identified in an initial 6 hour growth course in CDM broth, implying the substrate of FptG was likely contained in the CDM mixture (Figure 6.1 A). While the mutant growth rate lagged compared to WT, as seen in Figure 6.1 A, *F. tularensis* LVSΔ*fptG* eventually reached an OD_{600} close to that attained by parental LVS. Attempts to identify the substrate began with supplementation of standard

CDM with 0.5% casamino acids. Casamino acids are a general mix of amino acids created through the acid hydrolysis of

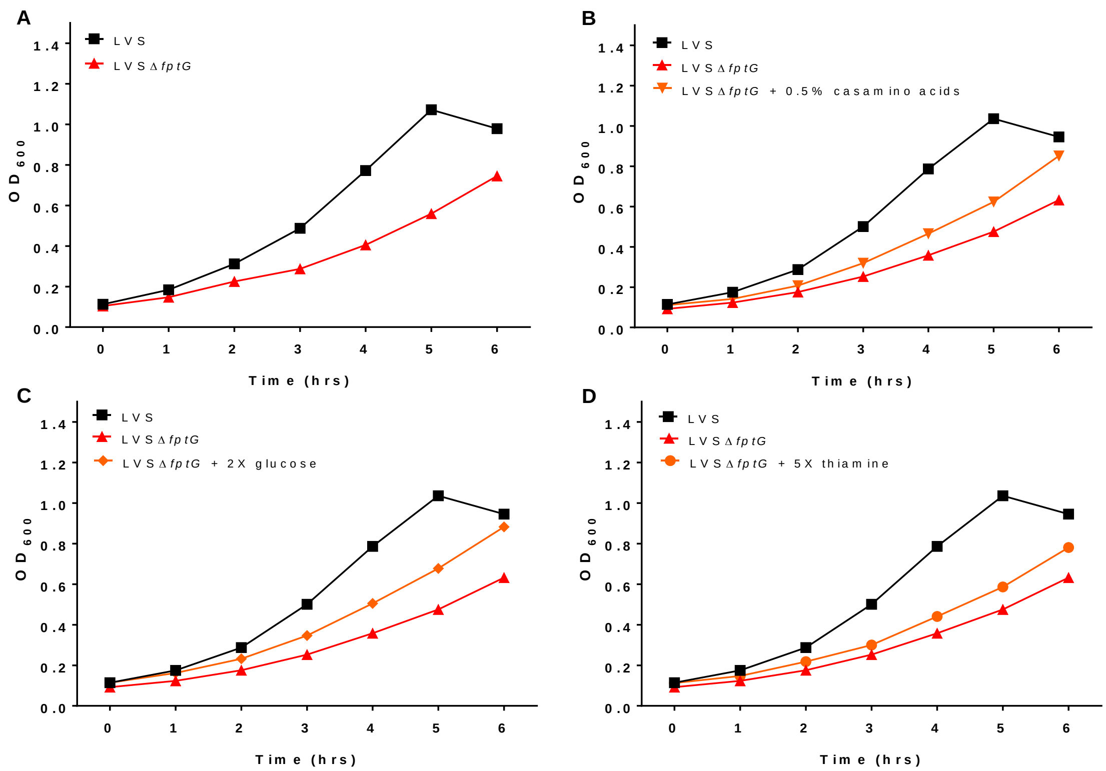

Figure 6.1. Growth of *F. tularensis* LVSΔ*fptG* compared to parental LVS in standard or supplemented CDM. CDM was supplemented with 0.5% casamino acids (B), 5X thiamine (C), or 2X glucose (D). Bacterial cultures were normalized to an OD_{600} of approximately 0.1 and were grown, shaking at 250 RPM in 37° C, 5% CO_2. Measurements were taken every hour for 6 hours. Data are representative of two independent experiments.

the protein casein and allows for the supplementation of all amino acids, except tryptophan. Amino acid enrichment did not restore *F. tularensis* LVSΔ*fptG* to the growth rate of parental LVS (Figure 6.1B). Similarly, supplementation of standard CDM with twice the concentration of glucose (Figure 6.1C), or 5 times the concentration of thiamine (vitamin B1) (Figure 6.1D) did not fully restore the growth rate of *F. tularensis* LVSΔ*fptG* to that of parental LVS, though some improvement was observed. The two remaining carbon sources in the CDM mix were subsequently investigated. Supplementation with spermine, a compound required for *F. tularensis*'s virulence [177], did not restore *F. tularensis* LVSΔ*fptG* to parental LVS replication rates (Figure 6.2A). Similarly, pantothenic acid (vitamin B5) supplementation did not restore the replication rate (Figure 6.2B). Investigation next turned away from the *F. tularensis* LVS background to investigate what effect the loss of the FptG transporter had on the Type A strain. As shown in Figure 6.3, unlike its LVS counterpart, SchuS4Δ*fptG* exhibited no growth defect in standard CDM.

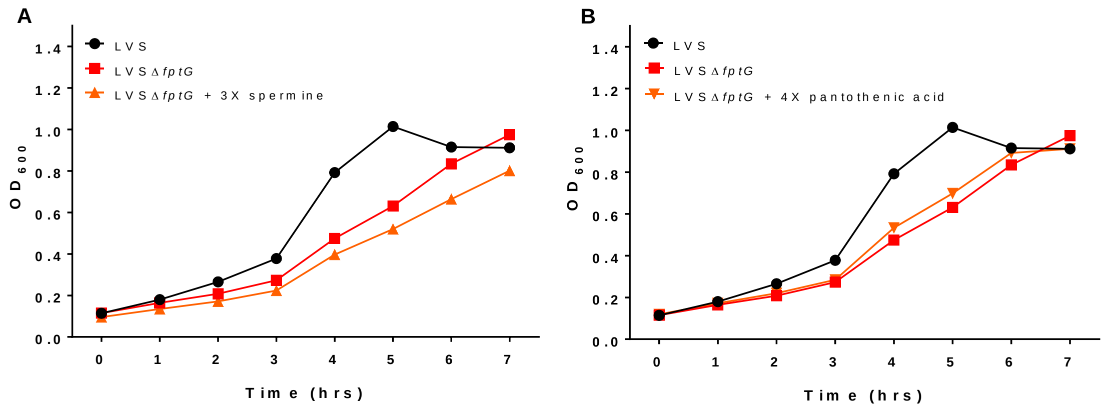

Figure 6.2. Growth of *F. tularensis* LVSΔ*fptG* compared to parental LVS in standard or supplemented CDM. CDM was supplemented with 3X spermine (A) or 4X pantothenic acid (B). Bacterial cultures were normalized to an OD_{600} of approximately 0.1 and were grown, shaking at 250 RPM in 37° C, 5% CO_2. Measurements were taken every hour for 6 hours. Data are representative of two independent experiments.

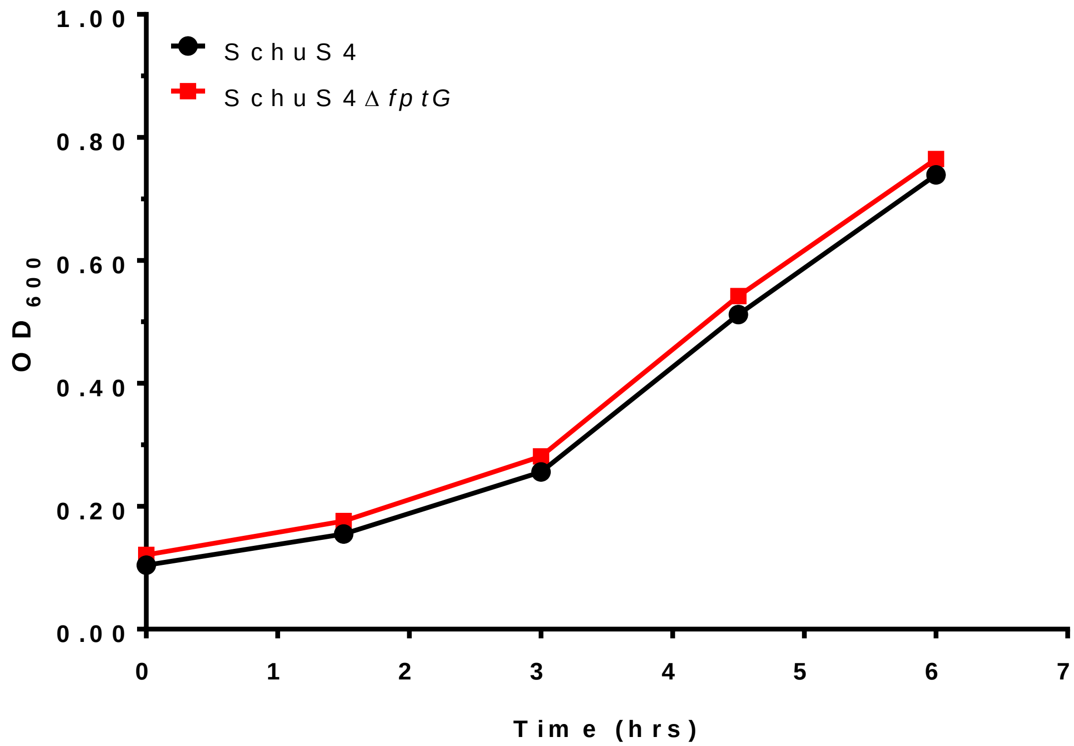

Figure 6.3. Growth of *F. tularensis* SchuS4Δ*fptG* compared to WT SchuS4 in CDM. Bacterial cultures were normalized to an OD_{600} of approximately 0.1 and were grown, shaking at 250 RPM in 37° C, 5% CO_2. Measurements were taken every hour for 6 hours. Data are representative of two independent experiments.

Supplementation of cells during *in vitro* infection

Studies were undertaken to test the ability of supplementation with casamino acids to restore WT cellular escape kinetics to SchuS4Δ*fptG* in THP-1 cells. Previous data from this study established the necessity for the FptG transporter in timely escape from the host cell, but discounted its involvement in replication (Fig. 5.3). Following the addition of 0.5% casamino acids, a concentration used in previous studies [76, 77], to cell culture media, an unexpected phenotype was observed. The addition of the extra amino acids induced an escape delay in the WT strain; the number of intracellular WT bacteria was significantly higher in cells with supplemented amino acids compared to numbers in cells in normal media at 24 hpi (Figure 6.4). Furthermore, the escape delay for SchuS4Δ*fptG* was similarly increased in the presence of casamino acids compared to normal media.

To investigate whether supplementation with a single amino acid was sufficient to retain WT *F. tularensis* similarly to the addition of casamino acids, supplementation experiments with 3 mM isoleucine in culture were carried out. It was observed that the addition of isoleucine alone was sufficient to cause an escape delay of WT *F. tularensis* similar to that observed when 0.5% casamino acids were used for supplementation (Figure 6.5). Observed CFU and calculated doublings between 3 mM isoleucine-supplemented WT *F. tularensis* and WT without supplementation were significantly different ($p < 0.01$), demonstrating that the addition of a single amino acid was sufficient to arrest the WT bacteria in THP-1 cytosols.

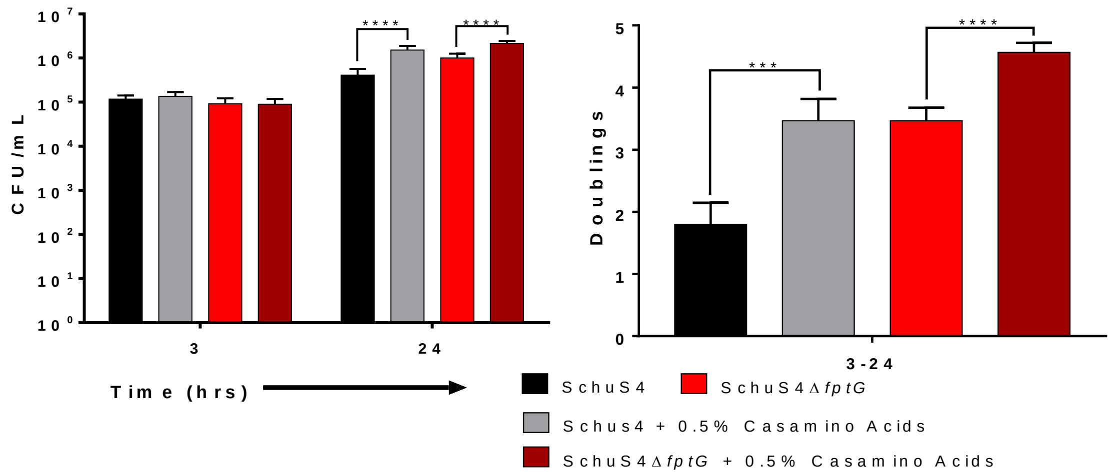

Figure 6.4. Addition of 0.5% casamino acids does not return *F. tularensis* SchuS4Δ*fptG* to WT escape kinetics in THP-1 cells. THP-1 cells were infected at an MOI of 100 for 2 hours. Cells were then washed twice with PBS and incubated with 50 µg/mL gentamicin from 2 hpi through the end of the assay. Intracellular bacteria were enumerated at 3 and 24 hpi. Data are plotted as the arithmetic mean CFU counts of three biological replicates performed in quadruplicate ± standard deviations. Data are of a single representative experiment (n = 1). ***, $p < 0.001$, ****, $p < 0.0001$ (Average CFU and calculated doublings analyzed by two-way ANOVA).

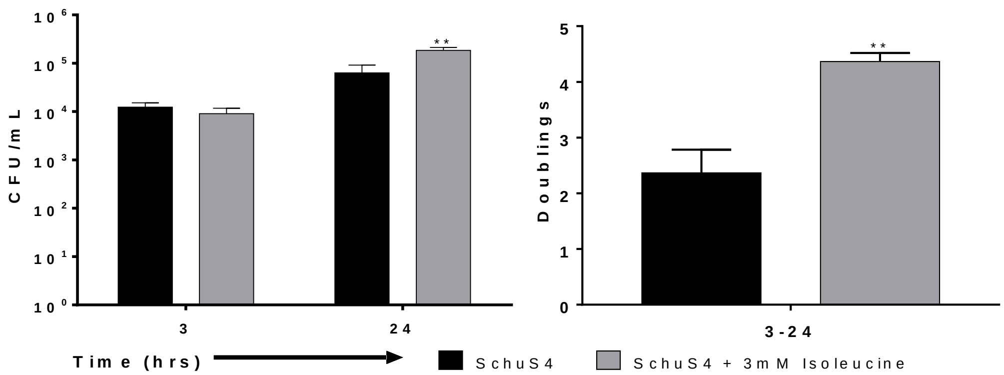

6.5. Addition of 3 mM isoleucine is sufficient to arrest WT *F. tularensis* in the cytosol of THP-1 cells. THP-1 cells were infected at an MOI of 100 for 2 hours. Cells were then washed twice with PBS and incubated with 50 µg/mL gentamicin from 2 hpi through the end of the assay. Intracellular bacteria were enumerated at 3 and 24 hpi. Data are plotted as the arithmetic mean CFU counts of three biological replicates performed in quadruplicate ± standard deviations. Data are of a single representative experiment (n = 2). **, $p < 0.01$, ****, $p < 0.0001$ (Average CFU and calculated doublings analyzed by two-way ANOVA).

Summary of Chapter 6

Despite 99% amino acid sequence identity between the *F. tularensis* LVS and SchuS4 FptG sequences, the LVSΔ*fptG* strain could not be utilized as a BSL-2 model to find the FptG substrate, as had been done previously with FptB [77] and FptE [76]. The *F. tularensis* LVS genome contains 37 mutations that affect protein sequences, and of those, 15 are predicted to have major impairment or entirely lost function [176]. Several of these genes are biosynthetic enzymes, meaning that the LVS metabolism is likely altered in an unpredictable fashion compared to that of WT Type A *F. tularensis*. For example, it is possible that *F. tularensis* LVS may have different biosynthetic pathways active in a given condition compared to the Type A strain under similar conditions. Because the loss of the *fptG* gene in the Type A strain has no effect to growth in broth, any effect seen in the *F. tularensis* LVS background is likely due to complications stemming from the many mutations inherent to the LVS genome. The loss of FptG has altered the replication kinetics of *F. tularensis* LVS in a complex manner such that supplementation of one carbon source, or even 19 amino acids, is insufficient to overcome the consequences of many mutations in the LVS genome.

Another possibility for the inability of supplementation to rescue replication of *F. tularensis* LVSΔ*fptG* may be that there is no redundant transporter for the substrate of FptG. During the identification of the substrates of both FptE [76] and FptB [77], supplementation with asparagine and isoleucine, respectively, was possible due to the likely existence of another, previously hypothesized [76, 77], lower affinity transporter. Increasing the media concentration of the substrate was able to restore mutant growth to WT replication mechanics. It is possible that the *F. tularensis* genome encodes no other transporter for the substrate of FptG, in which case, supplementation screening experiments using rescue of growth as a readout are unlikely to be effective. A less targeted method to identity the FptG substrate may be to screen the mutant, compared to the parental strain, using a defined panel of radiolabeled metabolite substrates. The mutant, in either the *F. tularensis* Type A or LVS backgrounds, would not be able to take up the metabolite at levels similar to that of as the parental strain, and a measurable difference in radioactivity would be evident between normalized pellets of each strain. While a similar method was used to confirm the identities of the FptE and FptB transporters, this method was not used for initial screening. Additionally, this method would require a considerable array of unique radiolabeled common metabolite substrates to effectively screen common candidates like amino acids, nucleotides, and sugars.

The surprising results gathered from the casamino acid and isoleucine supplementation experiments suggest that *F. tularensis* utilizes a host mechanism to produce the escape delay phenotype. That the deletion of a nutrient transporter, or the disruption of normal amino acid level can induce the same phenotype, with even the WT bacterium, highlights the complexity of the interplay between the bacterium and the host cell's metabolic state. It is interesting to note how excess amino acids are dealt with metabolically by the cell. Excess amino acids are oxidized via the arginase pathway, creating urea [181] which is processed further by several pathways. One pathway in particular, the ornithine amino transferase pathway, is a pro-survival pathway [47], and may account for cells remaining alive longer, and harboring the bacteria intracellularly longer, which is reflected in the cell escape delay. Further investigation into the role of cellular metabolism and nutrient homeostasis pathways in the context of *F. tularensis* infection may uncover direct interplay between the host and the bacteria.

Chapter 7 – Discussion

Despite years of research, and a surge in interest after the bioterror attacks of 2001, no licensed vaccine exists to prevent disease due to *Francisella tularensis*. Human clinical studies dating back to the 1950s-1960s demonstrating partial protection conferred by LVS vaccination against Type A challenge support the promise of the live attenuated vaccine strategy [91]. Given that the ultimate target for a tularemia vaccine is the highly virulent Type A strain,   we reasoned that the use of a live attenuated derivative based on the Type A background would provide a greater level of protection. Current molecular biology techniques allow the engineering of specifically targeted deletions in rationally selected genes in in the Type A strain. Targets have included biosynthetic genes, such as those involved in capsule, nucleotide, or O-antigen biogenesis [182, 183, 154, 155, 170, 104, 202], defense genes, such as catalase and superoxide dismutase [7, 117], or virulence factors, such as those in the *Francisella* pathogenicity island [11, 19, 21, 120, 188]. Candidate strains harboring these mutations have exhibited varying degrees of attenuation and protection in several mammalian models.

Absent from the list of commonly targeted genes are those encoding transporters. Bacteria employ a multitude of transporters to move a large number of biologically important substrates, and transporters of the MFS, represent the largest group of secondary transporters on Earth [171, 222]. The Type A strain of *Francisella tularensis* is predicted to have 35 MFS transporters, and 182 transporters in total [107], representing close to 12% of the SchuS4 protein coding sequences. This represents a very large pool of potential novel targets, not just for vaccines, but also, for antibiotic therapies as well. The blockage of an important transporter with a chemical compound may induce a similar attenuating effect on pathogenic bacteria mid-infection. Furthermore, it has been found that bacteria residing in the intracellular space, like *F. tularensis*, undergo genome reductions, resulting in the shedding of genes involved in transport and metabolism at a rate that is much higher than that of genes involved in replication and defense [135]. This implies that any remaining transporter and metabolite genes are especially necessary for the survival, and possibly, virulence of the organism.

A subset of 9 MFS genes identified in *F. tularensis*, based on their homology to the attenuating *phtA* threonine transporter of *Legionella pneumophila*, were named the *Francisella* phagosomal transporters (*fpt*) [191]. The introduction of mutations into 3 of the 9 *fpt* genes in the LVS background resulted in significantly attenuated phenotypes *in vitro* and/or *in vivo*. Studies by our lab, as well as others, demonstrated that deletion of the isoleucine transporter, FptB, the asparagine transporter, FptE, or FptG, a transporter with an unknown substrate, significantly altered the intracellular replication rate of *F. tularensis* LVS *in vitro*, and rendered LVS highly attenuated and protective in the BALB/c mouse model [128, 76, 77]. These data prompted us to choose the transporters FptB, FptE, FptG, and another, less attenuating transporter, FptF (unpublished data), with which to move forward for the construction and evaluation of a *F. tularensis* Type A-based vaccine candidate.

The resultant strains were evaluated in the minimal broth CDM for growth deficiencies. Three strains, SchuS4Δ*fptF*, SchuS4Δ*fptE*, and SchuS4Δ*fptG* exhibited no alterations in replication rates compared to WT *F. tularensis*, suggesting the substrates of these three transporters are dispensable for growth in broth. On the other hand, SchuS4Δ*fptB*, the strain lacking the high affinity isoleucine transporter, consistently exhibited a replication deficiency in CDM. Growth of SchuS4Δ*fptB* could be rescued to WT levels by the addition of 3 mM isoleucine to the media. These data demonstrate the importance of isoleucine transport to *F. tularensis*, as neither Type A nor Type B strains are able to synthesize isoleucine *de novo* from threonine [99-101]. These data also support the notion that there likely exists another, previously hypothesized [77], lower affinity transporter for isoleucine in the *F. tularensis* proteome.

Intracellular survival assays in macrophages and hepatocytes were initially performed with all four *fpt* deletion strains in two cell line types, THP-1 human macrophage-like cells, and HepG2 human hepatocyte carcinoma cells. Invasion and replication in macrophages is key to *F. tularensis* virulence, and systemic spread of the bacterium eventually leads to infection of the liver [31]. Two *fpt* mutants, *F. tularensis* SchuS4Δ*fptF* and SchuS4Δ*fptE*, exhibited no alterations to their intracellular replication kinetics compared to WT in either cell type. These findings suggest that the as yet unknown substrate of FptF, and asparagine, the substrate of FptE, are either not essential for intracellular replication or are compensated for by either *de novo* biosynthesis or other transporters.

In contrast, SchuS4Δ*fptG* and SchuS4Δ*fptB* exhibited significant intracellular alterations. Intracellular replication assays were performed using two antibiotic conditions: one condition removes all gentamicin from the media after 3 hpi, allowing cell-to-cell spread, and enumeration of the total replication rate of the strains. A second condition includes 50 µg/mL of gentamicin, a bactericidal concentration, in the culture media throughout the experiment, effectively eliminating intercellular spread. This condition allows for the enumeration of only the first round of invasion, replication, and escape, as bacteria that have escaped the initially infected cells are killed by the extracellular gentamicin. *F. tularensis* SchuS4Δ*fptG* replicated at the same rate as WT in both THP-1 macrophages and HepG2 hepatocytes when cell-to-cell spread was allowed. But under conditions where cell spread was limited, a significant escape delay was evident; escape of SchuS4Δ*fptG* was delayed by ~6 hours compared to WT, despite replicating at the same rate. Importantly, complementation *in trans* with an intact *fptG* gene restored *F. tularensis* SchuS4Δ*fptG* to WT growth kinetics.

Similarly, *F. tularensis* SchuS4Δ*fptB* exhibited a significant escape delay compared to WT under cell spread-limiting conditions in macrophages. When cell spread was allowed by removal of the antibiotics, a significant growth defect compared to the WT strain, similar to the one observed in CDM, was evident in THP-1 macrophages. Similar to studies in broth culture, supplementation of THP-1 cells with 3 mM isoleucine at the time of invasion restored the replication rate of *F. tularensis* SchuS4Δ*fptB* to that of WT SchuS4. Furthermore, complementation *in trans* with the *fptB* gene restored *F. tularensis* SchuS4Δ*fptB* to the level of WT replication kinetics. No replication defect or escape delay was observed with *F. tularensis* SchuS4Δ*fptB* in HepG2 cells. Restriction of the escape delay and replication defect of *F. tularensis* SchuS4Δ*fptB* to macrophages is not surprising as it has been found that isoleucine is among 9 amino acids that are downregulated by macrophages upon activation [146]. It has not been shown that hepatocytes have the ability modulate their amino acid levels in such a fashion, and the data presented here with *F. tularensis* SchuS4Δ*fptB* would suggest that hepatocytes cannot appreciably alter isoleucine levels during infection. These data, coupled with the fact that excess isoleucine rescues growth of *F. tularensis* SchuS4Δ*fptB* in broth, implies that isoleucine is a rate-limiting nutrient for replication of *Francisella tularensis,* and further supports the hypothesis of the existence of another, lower affinity transporter that contributes to transport of isoleucine in the absence of FptB. It may be that FptB functions as a high affinity transporter to scavenge isoleucine intracellularly, even at depleted levels. The fact that SchuS4Δ*fptB* starts replicating intracellularly at the same time as WT suggests that the mutant has escaped the phagosome, as the literature demonstrates phagosomal escape is required for intracellular growth [116, 119, 187]. Direct evidence for timely phagosomal escape by SchuS4Δ*fptB* would require further experiments utilizing confocal microscopy in the first 1-2 hpi to investigate this matter further.

The delay in cytosolic escape observed with both *fptB* and *fptG* mutant strains has not been reported previously in *Francisella*, and thus warranted deeper examination. Both mutant strains were compared to WT *F. tularensis* through the first 33 hours of infection. Experimentally, a positive doubling rate and increasing CFU numbers were interpreted as intracellular replication outpacing escape, and decreasing CFU numbers as escape outpacing new replication. WT *F. tularensis* exhibited positive doublings and increasing intracellular CFU values through 15 hpi; escape begins 15-21 hpi. Release of LDH from infected cells correlated with the timing of cell escape [108, 151]. In this experimental system, *F. tularensis* SchuS4Δ*fptG* replicated at the same rate as WT, but continued doubling at a positive rate for an additional 6 hours beyond that of WT. Interestingly, *F. tularensis* SchuS4Δ*fptG* induced LDH release at the same time as WT, and at significantly higher levels. It can be hypothesized that the increased LDH release elicited by *F. tularensis* SchuS4Δ*fptG* results from THP-1 cells that are struggling to contain high intracellular numbers of this mutant strain that is doubling at the WT rate, but not escaping in a timely fashion, and thus exhibit greater membrane permeability leading to transient release of LDH. Further experiments, possibly utilizing fluorescent microscopy, could potentially support or disprove this hypothesis.

In contrast, in THP-1 cells, *F. tularensis* SchuS4Δ*fptB* doubled at a slower rate than WT SchuS4 through 15-21 hpi, yielding significantly fewer bacteria. Furthermore, *F. tularensis* SchuS4Δ*fptB* continued to replicate for 12 hours beyond that of WT with increasing numbers of intracellular CFU, exhibiting a substantial escape delay, at between 27-33 hpi. Doubling values are never significantly different, statistically, from that of WT *F. tularensis*, but that may stem from the relatively short 6 hour time periods utilized in this assay. Statistical significance is reached only with larger values stemming from a 24 hour experimental period, but trends still remain, primarily that *F. tularensis* SchuS4Δ*fptB* doubles 12 hours beyond that of WT. Also of significance is the fact that *F. tularensis* SchuS4Δ*fptB* reached a significantly higher peak of intracellular CFU than WT. Approximately twice as many *F. tularensis* SchuS4Δ*fptB* were present at 27 hpi, the strain's peak, than WT at 15 hpi, suggesting bacterial number alone is not a trigger for cellular escape.

Further analysis of *F. tularensis* SchuS4Δ*fptB* and SchuS4Δ*fptG* was carried out in BMDMs harvested from C57BL/6J mice and human MDMs harvested from blood, in order to bridge *in vitro* and *in vivo* studies. The C57BL/6J mouse strain is widely used in *F. tularensis* studies where WT SchuS4 has an intranasal LD_{50} < 10 CFU [164]. Infection assays that allowed cell-to-cell spread were carried out. Both *F. tularensis* SchuS4Δ*fptB* and SchuS4Δ*fptG* harbored significant defects in their intracellular replication rates in both types of macrophages. As had been previously shown, mouse macrophages can deplete isoleucine levels, and this may partially explain the poor replication rate of *F. tularensis* SchuS4Δ*fptB*. Curiously, the replication defect observed for *F. tularensis* SchuS4Δ*fptG* suggests the possibility that the substrate for the FptG transporter may be depleted in primary macrophages, but not in human cell line macrophages, possibly offering insights into the identity of this substance.

Both *F. tularensis* SchuS4Δ*fptG* and SchuS4Δ*fptB* were assessed for attenuation in the C57BL/6J mouse model. Intranasal inoculation with WT *F. tularensis* was lethal in both male and female mice which succumbed to inocula of 10-53 CFU by day 5 post inoculation. The LD_{50} of *F. tularensis* SchuS4Δ*fptG* was calculated as 2.0×10^1 CFU, with one male and one female mouse each surviving this inoculation dose. The two mice that died did so 1 and 2 days beyond that of the mice inoculated with WT *F. tularensis*, suggesting a delay to death. All higher inoculation doses of *F. tularensis* SchuS4Δ*fptG* were lethal at the same rate as WT *F. tularensis*, demonstrating the limited attenuating capacity deletion of the FptG transporter.

F. tularensis SchuS4Δ*fptB* was significantly more attenuated than SchuS4Δ*fptG*. In doses ranging from 5.4×10^1 to 7.6×10^6 CFU, no mouse receiving *F. tularensis* SchuS4Δ*fptB* displayed any clinical signs of illness or died, exhibiting a high level of attenuation, >7.60×10^6 CFU. These data further underscore the importance of isoleucine to the pathogenesis of *Francisella*. Type A *F. tularensis* does not have the ability to synthesize isoleucine *de novo* from threonine, and depriving the bacterium of its high affinity isoleucine transporter induced virtual avirulence. One hypothesis that can explain the high levels of attenuation of *F. tularensis* SchuS4Δ*fptB* is, due to low replicative ability, as demonstrated in BMDMs, the bacteria may be rapidly cleared, precluding the efficient systemic spread characteristic of a fatal WT *F. tularensis* infection [63]. This could be tested by quantifying organ burdens at regular intervals post-inoculation. A second hypothesis to explain the attenuation of *F. tularensis* SchuS4Δ*fptB* may stem more directly from the lack of isoleucine transport caused by deletion of *fptB*. A role for nutritional status has been demonstrated for the virulence of *F. tularensis* [133, 184]. For example, it has been demonstrated that uptake of biotin affects the timing of phagosomal escape in BMDMs [145]. It may be that sufficient isoleucine uptake is required to trigger the virulence program of the bacterium. To test this, sequencing of RNA of both *F. tularensis* WT and SchuS4Δ*fptB* during intracellular invasion would identify changes in the transcriptomes associated with virulence. Furthermore, any changes found may then be tested for reversion back to WT with the addition of exogenous isoleucine.

Due to the high levels of attenuation exhibited by *F. tularensis* SchuS4Δ*fptB*, this strain was assessed in the C57BL/6J mouse model for its protective capacity. Vaccination with either one or two doses of ~1 $\times 10^6$ *F. tularensis* SchuS4Δ*fptB* was followed by WT challenge. Interestingly, survival of mice that received vaccination was independent of the challenge dose. However, mice that succumbed to challenge exhibited a delay to death that was challenge dose-dependent. This suggests that *F. tularensis* SchuS4Δ*fptB* was unable to consistently induce a suitable memory response under the dose schemes used. Further vaccinations, or alternate routes of vaccination may be needed to boost efficacy.

The relatively modest vaccine efficacy induced by *F. tularensis* SchuS4Δ*fptB* prompted us to test a prime/boost vaccination schedule to boost efficacy. Surprisingly, there was no increase in vaccine efficacy conferred by a second vaccine dose. This suggests again that *F. tularensis* SchuS4Δ*fptB* is not consistently inducing a fully protective response. The high levels of attenuation and modest vaccine efficacy may be an indication that *F. tularensis* SchuS4Δ*fptB* is over-attenuated. If the very low levels of intracellular replication found in BMDM assays are indicative of *in vivo* growth, *F. tularensis* SchuS4Δ*fptB* may be cleared too quickly to induce a robust response. Further investigation of this would require study of dissemination rates from the lungs to other organs and organ burdens in comparison to WT.

While the suboptimal immune response engendered by *F. tularensis* SchuS4Δ*fptB* may render the strain a less than ideal vaccine candidate, this strain remains a valuable tool for study of the immune response. The correlates of protection against *Francisella* are as yet unknown [50], but *F. tularensis* SchuS4Δ*fptB* offers a unique opportunity for study of the immune response. When vaccinated, some mice achieve full protection, while others are merely delayed to death, implying the induction of an incomplete immune response. In-depth examination and characterization of the responses of a cohort of mice vaccinated with *F. tularensis* SchuS4Δ*fptB* and later challenged with the WT strain may highlight molecular differences between a protected mouse and one with a delay to death. To test this, blood samples taken from all mice on a time course during the first week post-vaccination and during challenge, can be tested for cytokine and antibody composition and quantities once the experiment has separated mice that survive from those that die. Furthermore, because a successful immune response to *F. tularensis* relies heavily upon a robust cell-mediated response [6], assays to test T cell activity, such as a splenocyte co-culture assay, would be necessary to examine this arm of the immune response. Such an experiment would compare the ability of vaccinated and unvaccinated splenocytes to control bacterial replication of infected BMDMs and differences in cytokine and effector proteins secreted.

Both *F. tularensis* SchuS4Δ*fptG* and SchuS4Δ*fptB* induce early cytokine secretion profiles that are significantly altered from that of WT *F. tularensis*. Fundamental to the virulence of the WT bacterium is its ability to enter many cell types and induce a potent, if atypical, inflammatory response that can ultimately lead to uncontrolled hypercytokinemia and sepsis [123, 196]. Modifications to the standard *F. tularensis*-induced cytokine profile offer a chance to ascertain what components are important early in infection. *F. tularensis* SchuS4Δ*fptG* induced similar levels of TNF-α as WT across all time points measured, while SchuS4Δ*fptB* elicited significantly less than both strains across all time points measured. Interestingly, these data mirrored the observed replication kinetics of the strains. This suggests then that translation and secretion levels may be modulated continuously through the early phase of macrophage infection. Transcription of TNF-α has been demonstrated to peak between 14-16 hpi [39], leaving time for the magnitude of the response to be modified. Whether modulation of TNF-α secretion is actively controlled by the bacteria or is the result of the host cell response to aspects of the bacteria remains to be determined.

Both *fpt* deletion strains elicited an altered IL-1β secretion profile compared to that of WT *F. tularensis*. The mutant *F. tularensis* SchuS4Δ*fptG* induced the secretion of significantly more IL-1β than WT from 21 hpi through to the end of the assay. These data may be further indirect evidence that *F. tularensis* SchuS4Δ*fptG* infected cells are surviving longer due to the mutant's escape delay than corresponding cells infected with

WT, allowing them to produce and secrete significantly more IL-1β. Alternatively, evidence exists that NLRP3 may be activated during the course of Type A *F. tularensis* infection [157]; activation of a second inflammasome may also account for the increase in IL-1β processing. Further examination of *F. tularensis* strain SchuS4Δ*fptG* may reveal whether or not the bacterial escape delay is hyper-stimulating IL-1β translation, allowing for the AIM2 inflammasome to process significantly more mature IL-1β in response to the mutant compared to WT. Conversely, *F. tularensis* SchuS4Δ*fptB* was delayed in the secretion of IL-1β by approximately 12 hours, again mirroring LDH release kinetics, supporting both the escape delay and replication deficiencies inherent to this strain. The reduced inflammatory cytokine profile induced by *F. tularensis* SchuS4Δ*fptB* may be part of the explanation for why this strain is highly attenuated *in vivo*. An insufficient inflammatory response engendered by this strain may not initiate a long-lived memory response against the bacterium. Further *in vivo* experiments analyzing the cytokine profile of animals inoculated with *F. tularensis* SchuS4Δ*fptB* may support or dismiss this hypothesis for the lack of protective capacity for this strain.

The mutant strain *F. tularensis* SchuS4Δ*fptE*, unexpectedly, did not produce any *in vitro* phenotype, in replication or escape. A transposon mutant with insertion in the SchuS4 *fptE* gene had been shown previously to have a replication defect in HepG2 hepatocytes [163], though polar effects cannot be ruled out due to the method of strain construction. Furthermore, *F. tularensis* LVSΔ*fptE* similarly exhibited a replication deficiency in HepG2 cells, signifying asparagine transport to be important for LVS during invasion of these cells [128, 76]. While we cannot explain our different results in HepG2 cells the use of the THP-1 cell line presents different conditions for the SchuS4-

derived mutant than those of the mouse macrophages used with the LVS mutant. The *F. tularensis* LVS mutant was highly attenuated in BALB/c mice and protective against lethal LVS challenge. It remains to be determined if SchuS4Δ*fptE* is attenuated in the mouse model.

While the *F. tularensis* SchuS4Δ*fptG* and SchuS4Δ*fptB*, and their LVS-derived counterparts, demonstrate the usefulness of targeting nutrient transporters in an intracellular pathogen as an attenuating measure, there appears to be a need for rationality in the choice of the transporter. The lack of additive attenuation observed in the double mutant strains LVSΔ*fptC*Δ*fptB* and LVSΔ*fptF*Δ*fptA* demonstrates that simply compounding transporter deletions is not a viable means to further attenuate *F. tularensis*. In retrospect, this makes sense, but a rationally targeted combination, likely transporters that affect multiple metabolic pathways, may prove efficacious. Transporters, much like the biosynthetic enzymes or virulence factors targeted for attenuation, should be chosen logically, based on the importance of the substrate transported and thus, the predicted need for the transporter to the bacterium. For example, isoleucine, the substrate of FptB, is an amino acid whose levels are down-modulated by host cells during infection, underscoring the necessity for a high-affinity scavenging transporter. This suggests a high level of importance for FptB, and may explain why deletion of *fptB*, but not *fptF*, *fptC*, *fptA*, or *fptE* was attenuating. Therefore, the targeting of transporters for use in the creation of live attenuated strains should be paired with knowledge of the auxotrophies and metabolic deficiencies inherent to the bacteria in question and the cellular environment encountered by the bacteria during infection.

Because *F. tularensis* LVSΔ*fptG* exhibited a profound growth defect in minimal CDM, it implied that the substrate for the FptG transporter was present in the media and simply could not be transported into the cells. By utilizing the supplementation method successfully employed to identify substrate identities for two other Fpt transporters [76, 77], the rationale was that the key substrate could be taken up into the bacteria via a putative lower affinity transporter, restoring growth to WT levels. None of the carbon sources found in CDM, when supplemented in excess, restored the growth rate of *F. tularensis* LVSΔ*fptG* to parental LVS levels. Furthermore, *F. tularensis* SchuS4Δ*fptG*, the Type A derived strain, exhibited no growth deficiencies in CDM, suggesting that the phenotypes seen with the LVS-derived strain are an artifact of a bacterium that harbors multiple other mutations. The LVS genome has been sequenced to reveal 40 major mutations in protein coding sequences, of which, 15 are predicted to impair or abrogate function [176]. It is likely that the baseline metabolic profile of *F. tularensis* LVS is significantly different from that of WT *F. tularensis* subspecies *holarctica*, and especially subspecies *tularensis*. Therefore, metabolic screenings with this organism are prone to unpredictable variation, and any results found in the LVS background may not be applicable to the virulent Type A strain. Though deletion of *fptG* does not hinder replication of Type A *F. tularensis in vitro*, and is only minimally attenuating *in vivo*, discovering the identity of this transporter would reveal a substrate whose role appears to center upon host escape.

Supplementation of THP-1 macrophages with amino acids before invasion led to the unexpected phenotype of escape delay, not just for *fpt* mutant strains, but also WT *F. tularensis*. These results support the idea that *F. tularensis* is employing host cell machinery, possibly autophagy, during the cytosolic replication phase of its lifecycle. Evidence exists that supplementation of cells with branched-chain amino acids, such as isoleucine and valine, is a strong pro-survival stimulus [106]. The exogenous supplementation of amino acids, especially branched-chain amino acids, may be mimicking the metabolic stress *F. tularensis* induces during cytosolic replication. Further investigation into the interplay between the metabolic switches of the cell, like mTOR and ULK1, and *Francisella tularensis* would further elucidate the interplay between bacterial replication and host nutrient levels.

In a similar vein, these data support further investigation focusing on *F. tularensis* during cytosolic replication. Supplementation with all amino acids in the form of casamino acids, or isoleucine alone, induced the same escape delay phenotype for WT *F. tularensis*. It is possible that any amino acid supplemented above cell concentrations is enough to trigger an escape delay, or it could be a select few, of which isoleucine is one. Further experiments with selective amino acid supplementation could identify which amino acids are critical to the timely escape of *F. tularensis*. While other common carbon sources can also be investigated, such as glucose or galactose, it has been demonstrated that amino acids are the primary carbon source of *F. tularensis* for protein synthesis and respiration during intracellular replication [184], and thus represent important compounds for the bacteria.

The work presented here was the first to link transporters of the MFS to virulence and pathogenesis in Type A *F. tularensis*. There is a surprising lack of study of the role of transporters in bacterial pathogenesis, with several studies utilizing *Legionella pneumophila* being the most prominent [27, 67, 191]. Over the course of this study, analysis focused on only two MFS transporters, FptG and FptB. Loss of either induced significant changes to the intracellular replication cycle of *F. tularensis*, and the virulence of the bacteria *in vivo*. But data from this studies suggests there is much value in targeting transporters, not necessarily just of the MFS, for vaccine or small molecular inhibitor research, and for in depth research into intracellular pathogenesis. The targeting of transporters offers a novel approach that may yield a fresh perspective on the lifecycle of *Francisella tularensis*, as well as yield a viable, efficacious live-attenuated vaccine.

References

[1] Abd H, Johansson T, Golovliov I, Sandström G, Forsman M. Survival and Growth of Francisella tularensis in Acanthamoeba castellanii. Applied and Environmental Microbiology 2003;69:600-6.

[2] Abu Kwaik Y, Asare R. Exploitation of Host Cell Biology and Evasion of Immunity by Francisella Tularensis. Frontiers in Microbiology 2011;1.

[3] Alibek K, Handelman S. Biohazard: the chilling true story of the largest covert biological weapons program in the world. New York, NY: Random House, 1999.

[4] Alkhuder K, Meibom KL, Dubail I, Dupuis M, Charbit A. Glutathione Provides a Source of Cysteine Essential for Intracellular Multiplication of Francisella tularensis. PLoS Pathogens 2009;5:e1000284.

[5] Andersen JL, He G-X, Kakarla P, Kc R, Kumar S, Lakra WS, et al. Multidrug Efflux Pumps from Enterobacteriaceae, Vibrio cholerae and Staphylococcus aureus Bacterial Food Pathogens. International Journal of Environmental Research and Public Health 2015;12:1487-547.

[6] Anthony LSD, Ghadirian E, Nestel FP, Kongshavn PAL. The requirement for gamma Interferon in resistance of mice to experimental tularemia. Microbial Pathogenesis 1989;7:421-8.

[7] Bakshi CS, Malik M, Regan K, Melendez JA, Metzger DW, Pavlov VM, et al. Superoxide Dismutase B Gene (sodB)-Deficient Mutants of Francisella tularensis Demonstrate Hypersensitivity to Oxidative Stress and Attenuated Virulence. Journal of Bacteriology 2006;188:6443-8.

[8] Balagopal A, MacFarlane AS, Mohapatra N, Soni S, Gunn JS, Schlesinger LS. Characterization of the Receptor-Ligand Pathways Important for Entry and Survival of Francisella tularensis in Human Macrophages. Infection and Immunity 2006;74:5114-25.

[9] Barel M, Hovanessian AG, Meibom K, Briand J-P, Dupuis M, Charbit A. A novel receptor – ligand pathway for entry of Francisella tularensis in monocyte-like THP-1 cells: interaction between surface nucleolin and bacterial elongation factor Tu. BMC Microbiology 2008;8:145-.

[10] Barker JH, McCaffrey RL, Baman NK, Allen L-AH, Weiss JP, Nauseef WM. The role of complement opsonization in interactions between F. tularensis subsp. novicida and human neutrophils. Microbes and Infection / Institut Pasteur 2009;11:762-9.

[11] Barker JR, Chong A, Wehrly TD, Yu J-J, Rodriguez SA, Liu J, et al. The Francisella tularensis Pathogenicity Island Encodes a Secretion System that is required for Phagosome Escape and Virulence. Molecular Microbiology 2009;74:1459-70.

[12] Baron SD, Singh R, Metzger DW. Inactivated Francisella tularensis Live Vaccine Strain Protects against Respiratory Tularemia by Intranasal Vaccination in an Immunoglobulin A-Dependent Fashion. Infection and Immunity 2007;75:2152-62.

[13] Barry EM, Cole LE, Santiago AE. Vaccines against tularemia. Human vaccines 2009;5:832-8.

[14] Belhocine K, Monack DM. Francisella infection triggers activation of the AIM2 inflammasome in murine dendritic cells. Cellular Microbiology 2012;14:71-80.

[15] Bjørn Peter Berdal RMHHMLRGJBCMHM. Field Detection of Francisella tularensis. Scandinavian Journal of Infectious Diseases 2000;32:287-91.

[16] Bosio CM. The Subversion of the Immune System by Francisella Tularensis. Frontiers in Microbiology 2011;2:9.

[17] Bosio CM, Bielefeldt-Ohmann H, Belisle JT. Active suppression of the pulmonary immune response by Francisella tularensis Schu4. The Journal of Immunology 2007;178:4538-47.

[18] Bosio CM, Dow SW. Francisella tularensis induces aberrant activation of pulmonary dendritic cells. The Journal of Immunology 2005;175:6792-801.

[19] Bröms JE, Meyer L, Lavander M, Larsson P, Sjöstedt A. DotU and VgrG, Core Components of Type VI Secretion Systems, Are Essential for Francisella LVS Pathogenicity. PLoS ONE 2012;7:e34639.

[20] Brotcke A, Monack DM. Identification of fevR, a Novel Regulator of Virulence Gene Expression in Francisella novicida. Infection and Immunity 2008;76:3473-80.

[21] Brotcke A, Weiss DS, Kim CC, Chain P, Malfatti S, Garcia E, et al. Identification of MglA-Regulated Genes Reveals Novel Virulence Factors in Francisella tularensis. Infection and Immunity 2006;74:6642-55.

[22] Buchan BW, McCaffrey RL, Lindemann SR, Allen L-AH, Jones BD. Identification of migR, a Regulatory Element of the Francisella tularensis Live Vaccine Strain iglABCD Virulence Operon Required for Normal Replication and Trafficking in Macrophages. Infection and Immunity 2009;77:2517-29.

[23] Burke DS. Immunization against tularemia: analysis of the effectiveness of live Francisella tularensis vaccine in prevention of laboratory-acquired tularemia. Journal of Infectious Diseases 1977;135:55-60.

[24] Celli J, Zahrt TC. Mechanisms of Francisella tularensis Intracellular Pathogenesis. Cold Spring Harbor Perspectives in Medicine 2013;3:a010314.

[25] Chamberlain RE. Evaluation of Live Tularemia Vaccine Prepared in a Chemically Defined Medium. Applied Microbiology 1965;13:232-5.

[26] Checroun C, Wehrly TD, Fischer ER, Hayes SF, Celli J. Autophagy-mediated reentry of Francisella tularensis into the endocytic compartment after cytoplasmic replication. Proceedings of the National Academy of Sciences 2006;103:14578-83.

[27] Chen DE, Podell S, Sauer J-D, Swanson MS, Saier MH. The phagosomal nutrient transporter (Pht) family. Microbiology 2008;154:42-53.

[28] Chen S, Wang H, Katzianer DS, Zhong Z, Zhu J. LysR family activator-regulated major facilitator superfamily transporters are involved in Vibrio cholerae antimicrobial compound resistance and intestinal colonisation. International Journal of Antimicrobial Agents 2013;41:188-92.

[29] Chen W, Shen H, Webb A, KuoLee R, Conlan JW. Tularemia in BALB/c and C57BL/6 mice vaccinated with Francisella tularensis LVS and challenged intradermally, or by aerosol with virulent isolates of the pathogen: protection varies depending on pathogen virulence, route of exposure, and host genetic background. Vaccine 2003;21:3690-700.

[30] Chiavolini D, Alroy J, King CA, Jorth P, Weir S, Madico G, et al. Identification of Immunologic and Pathologic Parameters of Death versus Survival in Respiratory Tularemia. Infection and Immunity 2008;76:486-96.

[31] Chong A, Celli J. The Francisella intracellular life cycle: towards molecular mechanisms of intracellular survival and proliferation. Frontiers in Microbiology 2010;1.

[32] Chong A, Wehrly TD, Nair V, Fischer ER, Barker JR, Klose KE, et al. The Early Phagosomal Stage of Francisella tularensis Determines Optimal Phagosomal Escape and Francisella Pathogenicity Island Protein Expression. Infection and Immunity 2008;76:5488-99.

[33] Chow T, Whiteley J, Li M, Rogers IM. The transfer of host MHC class I protein protects donor cells from NK cell and macrophage-mediated rejection during hematopoietic stem cell transplantation and engraftment in mice. STEM CELLS 2013;31:2242-52.

[34] Chu P, Cunningham AL, Yu J-J, Nguyen JQ, Barker JR, Lyons CR, et al. Live Attenuated Francisella novicida Vaccine Protects against Francisella tularensis Pulmonary Challenge in Rats and Non-human Primates. PLoS Pathogens 2014;10:e1004439.

[35] Clemens DL, Lee B-Y, Horwitz MA. Virulent and Avirulent Strains of Francisella tularensis Prevent Acidification and Maturation of Their Phagosomes and Escape into the Cytoplasm in Human Macrophages. Infection and Immunity 2004;72:3204-17.

[36] Clemens DL, Lee B-Y, Horwitz MA. Francisella tularensis Enters Macrophages via a Novel Process Involving Pseudopod Loops. Infection and Immunity 2005;73:5892-902.

[37] Clemens DL, Lee B-Y, Horwitz MA. Francisella tularensis Phagosomal Escape Does Not Require Acidification of the Phagosome. Infection and Immunity 2009;77:1757-73.

[38] Cole LE, Santiago A, Barry E, Kang TJ, Shirey KA, Roberts ZJ, et al. Macrophage Proinflammatory Response to Francisella tularensis Live Vaccine Strain Requires

Coordination of Multiple Signaling Pathways. The Journal of Immunology 2008;180:6885-91.

[39] Cole LE, Shirey KA, Barry E, Santiago A, Rallabhandi P, Elkins KL, et al. Toll-like receptor 2-mediated signaling requirements for Francisella tularensis live vaccine strain infection of murine macrophages. Infect Immun 2007;75.

[40] Cole LE, Shirey KA, Barry E, Santiago A, Rallabhandi P, Elkins KL, et al. Toll-Like Receptor 2-Mediated Signaling Requirements for Francisella tularensis Live Vaccine Strain Infection of Murine Macrophages. Infection and Immunity 2007;75:4127-37.

[41] Cong Y, Yu J-J, Guentzel MN, Berton MT, Seshu J, Klose KE, et al. Vaccination with a Defined Francisella tularensis subsp. novicida Pathogenicity Island Mutant (ΔiglB) Induces Protective Immunity Against Homotypic and Heterotypic Challenge. Vaccine 2009;27:5554-61.

[42] Conlan JW, Chen W, Shen H, Webb A, KuoLee R. Experimental tularemia in mice challenged by aerosol or intradermally with virulent strains of Francisella tularensis: bacteriologic and histopathologic studies. Microbial Pathogenesis 2003;34:239-48.

[43] Conlan JW, Shen H, Webb A, Perry MB. Mice vaccinated with the O-antigen of Francisella tularensis LVS lipopolysaccharide conjugated to bovine serum albumin develop varying degrees of protective immunity against systemic or aerosol challenge with virulent type A and type B strains of the pathogen. Vaccine 2002;20:3465-71.

[44] Crane DD, Bauler TJ, Wehrly TD, Bosio CM. Mitochondrial ROS potentiates indirect activation of the AIM2 inflammasome. Frontiers in Microbiology 2014;5:438.

[45] Cremer TJ, Amer A, Tridandapani S, Butchar JP. Francisella tularensis regulates autophagy-related host cell signaling pathways. Autophagy 2009;5:125-8.

[46] Cunningham AL, Dang KM, Yu J-J, Guentzel MN, Heidner H, Klose KE, et al. Enhancement of Vaccine Efficacy by Expression of a TLR5 Ligand in the Defined Live Attenuated Francisella tularensis subsp. novicida Strain U112▲iglB::fljB. Vaccine 2014;32:5234-40.

[47] Das P, Lahiri A, Lahiri A, Chakravortty D. Modulation of the Arginase Pathway in the Context of Microbial Pathogenesis: A Metabolic Enzyme Moonlighting as an Immune Modulator. PLoS Pathogens 2010;6:e1000899.

[48] Davies J, Davies D. Origins and Evolution of Antibiotic Resistance. Microbiology and Molecular Biology Reviews : MMBR 2010;74:417-33.

[49] de Bruin OM, Duplantis BN, Ludu JS, Hare RF, Nix EB, Schmerk CL, et al. The biochemical properties of the Francisella pathogenicity island (FPI)-encoded proteins IglA, IglB, IglC, PdpB and DotU suggest roles in type VI secretion. Microbiology 2011;157:3483-91.

[50] De Pascalis R, Chou AY, Bosio CM, Huang C-Y, Follmann DA, Elkins KL. Development of Functional and Molecular Correlates of Vaccine-Induced Protection for a Model Intracellular Pathogen, F. tularensis LVS. PLoS Pathogens 2012;8:e1002494.

[51] del Barrio L, Sahoo M, Lantier L, Reynolds JM, Ceballos-Olvera I, Re F. Production of Anti-LPS IgM by B1a B Cells Depends on IL-1β and Is Protective against Lung Infection with Francisella tularensis LVS. PLoS Pathogens 2015;11:e1004706.

[52] Dennis DT, Inglesby TV, Henderson DA, et al. Tularemia as a biological weapon: Medical and public health management. JAMA 2001;285:2763-73.

[53] Dettman JR, Rodrigue N, Aaron SD, Kassen R. Evolutionary genomics of epidemic and nonepidemic strains of Pseudomonas aeruginosa. Proceedings of the National Academy of Sciences of the United States of America 2013;110:21065-70.

[54] Diacovich L, Gorvel J-P. Bacterial manipulation of innate immunity to promote infection. Nat Rev Micro 2010;8:117-28.

[55] Dienst Jr F. Tularemia: a perusal of three hundred thirty-nine cases. The Journal of the Louisiana State Medical Society: official organ of the Louisiana State Medical Society 1963;115:114-27.

[56] E. F. Tularemia. Journal of the American Medical Association 1925;84:1243-50.

[57] Edgar R, Bibi E. MdfA, an Escherichia coli multidrug resistance protein with an extraordinarily broad spectrum of drug recognition. Journal of Bacteriology 1997;179:2274-80.

[58] Eigelsbach HT, Downs CM. Prophylactic effectiveness of live and killed tularemia vaccines. The Journal of Immunology 1961;87:415-25.

[59] El-Etr SH, Margolis JJ, Monack D, Robison RA, Cohen M, Moore E, et al. Francisella tularensis Type A Strains Cause the Rapid Encystment of Acanthamoeba castellanii and Survive in Amoebal Cysts for Three Weeks Postinfection. Applied and Environmental Microbiology 2009;75:7488-500.

[60] El Sahly H, Atmar R, Patel S, Wells J, Cate T, Ho M, et al. Safety, reactogenicity and immunogenicity of Francisella tularensis live vaccine strain in humans. Vaccine 2009;27:4905-11.

[61] Elkins KL, Cowley Siobhán C, Bosio Catharine M. Innate and adaptive immune responses to an intracellular bacterium, Francisella tularensis live vaccine strain. Microbes and Infection 2003;5:135-42.

[62] Elkins KL, Rhinehart-Jones T, Nacy CA, Winegar RK, Fortier AH. T-cell-independent resistance to infection and generation of immunity to Francisella tularensis. Infection and Immunity 1993;61:823-9.

[63] Ellis J, Oyston PCF, Green M, Titball RW. Tularemia. Clinical Microbiology Reviews 2002;15:631-46.

[64] Evans ME GD, Schaffner W, McGee ZA. Tularemia: a 30-year experience with 88 cases., Medicine (Baltimore), 1985, pp. 251-69.

[65] Evans ME, Gregory DW, Schaffner W, Mcgee ZA. Tularemia: a 30-year experience with 88 cases. Medicine 1985;64:251-69.

[66] Fernandes-Alnemri T, Yu J-W, Juliana C, Solorzano L, Kang S, Wu J, et al. The AIM2 inflammasome is critical for innate immunity against Francisella tularensis. Nature immunology 2010;11:385-93.

[67] Fonseca MV, Sauer J-D, Crepin S, Byrne B, Swanson MS. The phtC-phtD Locus Equips Legionella pneumophila for Thymidine Salvage and Replication in Macrophages. Infection and Immunity 2014;82:720-30.

[68] Food, Drug Administration H. New drug and biological drug products; evidence needed to demonstrate effectiveness of new drugs when human efficacy studies are not ethical or feasible. Final rule. Federal register 2002;67:37988.

[69] Fortier AH, Leiby DA, Narayanan R, Asafoadjei E, Crawford RM, Nacy CA, et al. Growth of Francisella tularensis LVS in macrophages: the acidic intracellular

compartment provides essential iron required for growth. Infection and Immunity 1995;63:1478-83.

[70] Fortier AH, Polsinelli T, Green SJ, Nacy CA. Activation of macrophages for destruction of Francisella tularensis: identification of cytokines, effector cells, and effector molecules. Infection and Immunity 1992;60:817-25.

[71] Fortier AH, Slayter MV, Ziemba R, Meltzer MS, Nacy CA. Live vaccine strain of Francisella tularensis: infection and immunity in mice. Infection and Immunity 1991;59:2922-8.

[72] Foshay L. Tularemia. Annual review of microbiology 1950;4:313-30.

[73] Fulop M, Manchee R, Titball R. Role of lipopolysaccharide and a major outer membrane protein from Francisella tularensis in the induction of immunity against tularemia. Vaccine 1995;13:1220-5.

[74] Fulop M, Mastroeni P, Green M, Titball RW. Role of antibody to lipopolysaccharide in protection against low- and high-virulence strains of Francisella tularensis. Vaccine 2001;19:4465-72.

[75] Geier H, Celli J. Phagocytic Receptors Dictate Phagosomal Escape and Intracellular Proliferation of Francisella tularensis. Infection and Immunity 2011;79:2204-14.

[76] Gesbert G, Ramond E, Rigard M, Frapy E, Dupuis M, Dubail I, et al. Asparagine assimilation is critical for intracellular replication and dissemination of Francisella. Cellular Microbiology 2014;16:434-49.

[77] Gesbert G, Ramond E, Tros F, Dairou J, Frapy E, Barel M, et al. Importance of Branched-Chain Amino Acid Utilization in Francisella Intracellular Adaptation. Infection and Immunity 2015;83:173-83.

[78] Gill V, Cunha BA. Tularemia pneumonia. Seminars in respiratory infections, 1997, pp. 61-7.

[79] Gillette DD, Curry HM, Cremer T, Ravneberg D, Fatehchand K, Shah PA, et al. Virulent Type A Francisella tularensis actively suppresses cytokine responses in human monocytes. Frontiers in Cellular and Infection Microbiology 2014;4:45.

[80] Golovliov I, Baranov V, Krocova Z, Kovarova H, Sjöstedt A. An Attenuated Strain of the Facultative Intracellular Bacterium Francisella tularensis Can Escape the Phagosome of Monocytic Cells. Infection and Immunity 2003;71:5940-50.

[81] Golovliov I, Ericsson M, Åkerblom L, Sandström G, Tärnvik A, Sjöstedt A. Adjuvanticity of ISCOMs incorporating a T cell-reactive lipoprotein of the facultative intracellular pathogen Francisella tularensis. Vaccine 1995;13:261-7.

[82] Golovliov I, Twine SM, Shen H, Sjostedt A, Conlan W. A ΔclpB Mutant of Francisella tularensis Subspecies holarctica Strain, FSC200, Is a More Effective Live Vaccine than F. tularensis LVS in a Mouse Respiratory Challenge Model of Tularemia. PLoS ONE 2013;8:e78671.

[83] Griffin AJ, Crane DD, Wehrly TD, Scott DP, Bosio CM. Alternative Activation of Macrophages and Induction of Arginase Are Not Components of Pathogenesis Mediated by Francisella Species. PLoS ONE 2013;8:e82096.

[84] Guan L, Kaback HR. Lessons from Lactose Permease. Annual review of biophysics and biomolecular structure 2006;35:67-91.

[85] Guryčová D. First isolation of Francisella tularensis subsp. tularensis in Europe. European Journal of Epidemiology 1998;14:797-802.

[86] Hajjar AM, Harvey MD, Shaffer SA, Goodlett DR, Sjöstedt A, Edebro H, et al. Lack of In Vitro and In Vivo Recognition of Francisella tularensis Subspecies Lipopolysaccharide by Toll-Like Receptors. Infection and Immunity 2006;74:6730-8.

[87] Hall JD, Craven RR, Fuller JR, Pickles RJ, Kawula TH. Francisella tularensis Replicates within Alveolar Type II Epithelial Cells In Vitro and In Vivo following Inhalation. Infection and Immunity 2007;75:1034-9.

[88] Hansen TE, Johansen T. Following autophagy step by step. BMC Biology 2011;9:39.

[89] Harris R, Paxman J. A higher form of killing: the secret history of chemical and biological warfare. Random House, 2007.

[90] Harris S. Japanese biological warfare research on humans: a case study of microbiology and ethics. Annals of the New York Academy of Sciences 1992;666:21-52.

[91] Hornick RB, Eigelsbach HT. Aerogenic immunization of man with live Tularemia vaccine. Bacteriological Reviews 1966;30:532-8.

[92] Horzempa J, O'Dee DM, Stolz DB, Franks JM, Clay D, Nau GJ. Invasion of Erythrocytes by Francisella tularensis. The Journal of Infectious Diseases 2011;204:51-9.

[93] Hvorup RN, Saier MH. Sequence similarity between the channel-forming domains of voltage-gated ion channel proteins and the C-terminal domains of secondary carriers of the major facilitator superfamily. Microbiology 2002;148:3760-2.

[94] Ireland PM, LeButt H, Thomas RM, Oyston PCF. A Francisella tularensis SCHU S4 mutant deficient in γ-glutamyltransferase activity induces protective immunity: characterization of an attenuated vaccine candidate. Microbiology 2011;157:3172-9.

[95] Jayakar HR, Parvathareddy J, Fitzpatrick EA, Bina XR, Bina JE, Re F, et al. A galU mutant of francisella tularensisis attenuated for virulence in a murine pulmonary model of tularemia. BMC Microbiology 2011;11:179.

[96] Jia Q, Lee B-Y, Bowen R, Dillon BJ, Som SM, Horwitz MA. A Francisella tularensis Live Vaccine Strain (LVS) Mutant with a Deletion in capB, Encoding a Putative Capsular Biosynthesis Protein, Is Significantly More Attenuated than LVS yet Induces Potent Protective Immunity in Mice against F. tularensis Challenge. Infection and Immunity 2010;78:4341-55.

[97] Jones CL, Sampson TR, Nakaya HI, Pulendran B, Weiss DS. Repression of Bacterial Lipoprotein Production by F. novicida Facilitates Evasion of Innate Immune Recognition. Cellular Microbiology 2012;14:1531-43.

[98] Jones JW, Broz P, Monack DM. Innate Immune Recognition of Francisella Tularensis: Activation of Type-I Interferons and the Inflammasome. Frontiers in Microbiology 2011;2:16.

[99] Kanehisa M, Furumichi M, Tanabe M, Sato Y, Morishima K. KEGG: new perspectives on genomes, pathways, diseases and drugs. Nucleic Acids Research 2017;45:D353-D61.

[100] Kanehisa M, Goto S. KEGG: Kyoto Encyclopedia of Genes and Genomes. Nucleic Acids Research 2000;28:27-30.

[101] Kanehisa M, Sato Y, Kawashima M, Furumichi M, Tanabe M. KEGG as a reference resource for gene and protein annotation. Nucleic Acids Research 2016;44:D457-D62.

[102] Katz J, Zhang P, Martin M, Vogel SN, Michalek SM. Toll-Like Receptor 2 Is Required for Inflammatory Responses to Francisella tularensis LVS. Infection and Immunity 2006;74:2809-16.

[103] Keim P, Johansson A, Wagner DM. Molecular Epidemiology, Evolution, and Ecology of Francisella. Annals of the New York Academy of Sciences 2007;1105:30-66.

[104] Kim T-H, Pinkham JT, Heninger SJ, Chalabaev S, Kasper DL. Genetic Modification of the O-Polysaccharide of Francisella tularensis Results in an Avirulent Live Attenuated Vaccine. The Journal of Infectious Diseases 2012;205:1056-65.

[105] Kingry LC, Petersen JM. Comparative review of Francisella tularensis and Francisella novicida. Frontiers in Cellular and Infection Microbiology 2014;4:35.

[106] Koike H, Zhang R-R, Ueno Y, Sekine K, Zheng Y-W, Takebe T, et al. Nutritional modulation of mouse and human liver bud growth through a branched-chain amino acid metabolism. Development 2017;144:1018-24.

[107] L.D.H. Elbourne ST, K. Hassan and I. T. Paulsen. TransportDB 2.0: a database for exploring membrane transporters in sequenced genomes from all domains of life. Nucleic Acids Research 2017.

[108] Lai X-H, Golovliov I, Sjöstedt A. Francisella tularensis Induces Cytopathogenicity and Apoptosis in Murine Macrophages via a Mechanism That Requires Intracellular Bacterial Multiplication. Infection and Immunity 2001;69:4691-4.

[109] Larsson P, Oyston PCF, Chain P, Chu MC, Duffield M, Fuxelius H-H, et al. The complete genome sequence of Francisella tularensis, the causative agent of tularemia. Nat Genet 2005;37:153-9.

[110] Lavine CL, Clinton SR, Angelova-Fischer I, Marion TN, Bina XR, Bina JE, et al. Immunization with heat-killed Francisella tularensis LVS elicits protective antibody-mediated immunity. European Journal of Immunology 2007;37:3007-20.

[111] Law CJ, Maloney PC, Wang D-N. Ins and Outs of Major Facilitator Superfamily Antiporters. Annual review of microbiology 2008;62:289-305.

[112] Lewinson O, Padan E, Bibi E. Alkalitolerance: A biological function for a multidrug transporter in pH homeostasis. Proceedings of the National Academy of Sciences of the United States of America 2004;101:14073-8.

[113] Li H, Nookala S, Bina XR, Bina JE, Re F. Innate immune response to Francisella tularensis is mediated by TLR2 and caspase-1 activation. Journal of Leukocyte Biology 2006;80:766-73.

[114] Li J, Ryder C, Mandal M, Ahmed F, Azadi P, Snyder DS, et al. Attenuation and protective efficacy of an O-antigen-deficient mutant of Francisella tularensis LVS. Microbiology 2007;153:3141-53.

[115] Li L, Kim S, Herndon JM, Goedegebuure P, Belt BA, Satpathy AT, et al. Cross-dressed CD8α(+)/CD103(+) dendritic cells prime CD8(+) T cells following vaccination. Proceedings of the National Academy of Sciences of the United States of America 2012;109:12716-21.

[116] Lindgren H, Golovliov I, Baranov V, Ernst RK, Telepnev M, Sjöstedt A. Factors affecting the escape of Francisella tularensis from the phagolysosome. Journal of Medical Microbiology 2004;53:953-8.

[117] Lindgren H, Shen H, Zingmark C, Golovliov I, Conlan W, Sjöstedt A. Resistance of Francisella tularensis Strains against Reactive Nitrogen and Oxygen Species with Special Reference to the Role of KatG. Infection and Immunity 2007;75:1303-9.
[118] Lindgren H, Stenman L, Tärnvik A, Sjöstedt A. The contribution of reactive nitrogen and oxygen species to the killing of Francisella tularensis LVS by murine macrophages. Microbes and Infection 2005;7:467-75.
[119] Lindgren M, Tancred L, Golovliov I, Conlan W, Twine SM, Sjöstedt A. Identification of Mechanisms for Attenuation of the FSC043 Mutant of Francisella tularensis SCHU S4. Infection and Immunity 2014;82:3622-35.
[120] Long ME, Lindemann SR, Rasmussen JA, Jones BD, Allen L-AH. Disruption of Francisella tularensis Schu S4 iglI, iglJ, and pdpC Genes Results in Attenuation for Growth in Human Macrophages and In Vivo Virulence in Mice and Reveals a Unique Phenotype for pdpC. Infection and Immunity 2013;81:850-61.
[121] Malik M, Bakshi CS, Sahay B, Shah A, Lotz SA, Sellati TJ. Toll-Like Receptor 2 Is Required for Control of Pulmonary Infection with Francisella tularensis. Infection and Immunity 2006;74:3657-62.
[122] Man SM, Karki R, Malireddi RKS, Neale G, Vogel P, Yamamoto M, et al. The transcription factor IRF1 and guanylate-binding proteins target activation of the AIM2 inflammasome by Francisella infection. Nat Immunol 2015;advance online publication.
[123] Mares CA, Ojeda SS, Morris EG, Li Q, Teale JM. Initial Delay in the Immune Response to Francisella tularensis Is Followed by Hypercytokinemia Characteristic of Severe Sepsis and Correlating with Upregulation and Release of Damage-Associated Molecular Patterns. Infection and Immunity 2008;76:3001-10.

[124] Mares CA, Sharma J, Li Q, Rangel EL, Morris EG, Enriquez MI, et al. Defect in efferocytosis leads to alternative activation of macrophages in Francisella infections. Immunol Cell Biol 2011;89:167-72.

[125] Marger MD, Saier Jr MH. A major superfamily of transmembrane facilitators that catalyse uniport, symport and antiport. Trends in Biochemical Sciences 1993;18:13-20.

[126] Mariathasan S, Weiss DS, Dixit VM, Monack DM. Innate immunity against Francisella tularensis is dependent on the ASC/caspase-1 axis. The Journal of Experimental Medicine 2005;202:1043-9.

[127] Marohn ME, Barry EM. Live Attenuated Tularemia Vaccines: Recent Developments and Future Goals. Vaccine 2013;31:3485-91.

[128] Marohn ME, Santiago AE, Shirey KA, Lipsky M, Vogel SN, Barry EM. Members of the Francisella tularensis Phagosomal Transporter Subfamily of Major Facilitator Superfamily Transporters Are Critical for Pathogenesis. Infection and Immunity 2012;80:2390-401.

[129] Mauvezin C, Neufeld TP. Bafilomycin A1 disrupts autophagic flux by inhibiting both V-ATPase-dependent acidification and Ca-P60A/SERCA-dependent autophagosome-lysosome fusion. Autophagy 2015;11:1437-8.

[130] McCaffrey RL, Allen L-AH. Pivotal Advance: Francisella tularensis LVS evades killing by human neutrophils via inhibition of the respiratory burst and phagosome escape. Journal of Leukocyte Biology 2006;80:1224-30.

[131] McCrumb Jr FR. Aerosol infection of man with Pasteurella tularensis. Bacteriological Reviews 1961;25:262.

[132] McLendon MK, Apicella MA, Allen L-AH. Francisella tularensis: Taxonomy, Genetics, and Immunopathogenesis of a Potential Agent of Biowarfare. Annual review of microbiology 2006;60:167-85.

[133] Meibom KL, Charbit A. Francisella Tularensis Metabolism and its Relation to Virulence. Frontiers in Microbiology 2010;1:140.

[134] Melillo AA, Foreman O, Bosio CM, Elkins KL. T-bet Regulates Immunity to Francisella tularensis Live Vaccine Strain Infection, Particularly in Lungs. Infection and Immunity 2014;82:1477-90.

[135] Merhej V, Royer-Carenzi M, Pontarotti P, Raoult D. Massive comparative genomic analysis reveals convergent evolution of specialized bacteria. Biology Direct 2009;4:13-.

[136] Meunier E, Wallet P, Dreier RF, Costanzo S, Anton L, Ruhl S, et al. Guanylate-binding proteins promote activation of the AIM2 inflammasome during infection with Francisella novicida. Nat Immunol 2015;advance online publication.

[137] Meyer L, Bröms JE, Liu X, Rottenberg ME, Sjöstedt A. Microinjection of Francisella tularensis and Listeria monocytogenes Reveals the Importance of Bacterial and Host Factors for Successful Replication. Infection and Immunity 2015;83:3233-42.

[138] Michell SL, Dean RE, Eyles JE, Hartley MG, Waters E, Prior JL, et al. Deletion of the Bacillus anthracis capB homologue in Francisella tularensis subspecies tularensis generates an attenuated strain that protects mice against virulent tularaemia. Journal of Medical Microbiology 2010;59:1275-84.

[139] Milton H. Saier J, Beatty JT, Goffeau A, Harley KT, Heijne WHM, Huang S-C, et al. The Major Facilitator Superfamily. Journal of Molecular Microbiology Biotechnology and Biotechnology 1999;1:257-79.

[140] Mohapatra NP, Balagopal A, Soni S, Schlesinger LS, Gunn JS. AcpA Is a Francisella Acid Phosphatase That Affects Intramacrophage Survival and Virulence. Infection and Immunity 2007;75:390-6.

[141] Mohapatra NP, Soni S, Bell BL, Warren R, Ernst RK, Muszynski A, et al. Identification of an Orphan Response Regulator Required for the Virulence of Francisella spp. and Transcription of Pathogenicity Island Genes. Infection and Immunity 2007;75:3305-14.

[142] Mörner T. The ecology of tularaemia. Rev Sci Tech 1992;11:1123-30.

[143] Mulligan MJ, Stapleton JT, Keitel WA, Frey SE, Chen WH, Rouphael N, et al. Tularemia vaccine: Safety, reactogenicity, “Take” skin reactions, and antibody responses following vaccination with a new lot of the Francisella tularensis live vaccine strain – A phase 2 randomized clinical Trial. Vaccine 2017;35:4730-7.

[144] Nano FE, Zhang N, Cowley SC, Klose KE, Cheung KKM, Roberts MJ, et al. A Francisella tularensis Pathogenicity Island Required for Intramacrophage Growth. Journal of Bacteriology 2004;186:6430-6.

[145] Napier BA, Meyer L, Bina JE, Miller MA, Sjöstedt A, Weiss DS. Link between intraphagosomal biotin and rapid phagosomal escape in Francisella. Proceedings of the National Academy of Sciences of the United States of America 2012;109:18084-9.

[146] NISHIYAMA A, YOKOTE Y, SAKAGAMI H. Changes in Amino Acid Metabolism During Activation of Mouse Macrophage-like Cell Lines. In Vivo 2010;24:857-60.

[147] O'Riordan M, Portnoy DA. The host cytosol: front-line or home front? Trends in Microbiology 2002;10:361-4.

[148] Ohara Y, Sato T, Fujita H, Ueno T, Homma M. Clinical manifestations of tularemia in Japan — Analysis of 1,355 cases observed between 1924 and 1987. Infection 1991;19:14-7.

[149] Okan NA, Kasper DL. The atypical lipopolysaccharide of Francisella. Carbohydrate research 2013;378:79-83.

[150] Oyston PCF, Sjostedt A, Titball RW. Tularaemia: bioterrorism defence renews interest in Francisella tularensis. Nat Rev Micro 2004;2:967-78.

[151] Ozanic M, Marecic V, Lindgren M, Sjöstedt A, Santic M. Phenotypic characterization of the Francisella tularensis ΔpdpC and ΔiglG mutants. Microbes and Infection 2016;18:768-76.

[152] Parsa KVL, Butchar JP, Rajaram MVS, Cremer TJ, Tridandapani S. The tyrosine kinase Syk promotes phagocytosis of Francisella through the activation of Erk. Molecular immunology 2008;45:3012-21.

[153] Pasetti MF, Cuberos L, Horn TL, Shearer JD, Matthews SJ, House RV, et al. An improved Francisella tularensis live vaccine strain (LVS) is well tolerated and highly immunogenic when administered to rabbits in escalating doses using various immunization routes. Vaccine 2008;26:1773-85.

[154] Pechous R, Celli J, Penoske R, Hayes SF, Frank DW, Zahrt TC. Construction and Characterization of an Attenuated Purine Auxotroph in a Francisella tularensis Live Vaccine Strain. Infection and Immunity 2006;74:4452-61.

[155] Pechous RD, McCarthy TR, Mohapatra NP, Soni S, Penoske RM, Salzman NH, et al. A Francisella tularensis Schu S4 Purine Auxotroph Is Highly Attenuated in Mice but

Offers Limited Protection against Homologous Intranasal Challenge. PLoS ONE 2008;3:e2487.

[156] Peng K, Broz P, Jones J, Joubert L-M, Monack D. Elevated AIM2-mediated pyroptosis triggered by hypercytotoxic Francisella mutant strains is attributed to increased intracellular bacteriolysis. Cellular Microbiology 2011;13:1586-600.

[157] Periasamy S, Le HT, Duffy EB, Chin H, Harton JA. Inflammasome-Independent NLRP3 Restriction of a Protective Early Neutrophil Response to Pulmonary Tularemia. PLoS Pathogens 2016;12:e1006059.

[158] Pierini LM. Uptake of serum-opsonized Francisella tularensis by macrophages can be mediated by class A scavenger receptors. Cellular Microbiology 2006;8:1361-70.

[159] Pierini R, Juruj C, Perret M, Jones CL, Mangeot P, Weiss DS, et al. AIM2/ASC triggers caspase-8-dependent apoptosis in Francisella-infected caspase-1-deficient macrophages. Cell Death and Differentiation 2012;19:1709-21.

[160] Polsinelli T, Meltzer MS, Fortier AH. Nitric oxide-independent killing of Francisella tularensis by IFN-gamma-stimulated murine alveolar macrophages. The Journal of Immunology 1994;153:1238-45.

[161] Price CTD, Richards AM, Von Dwingelo JE, Samara HA, Kwaik YA. Amoeba host-Legionella synchronization of amino acid auxotrophy and its role in bacterial adaptation and pathogenic evolution. Environmental Microbiology 2014;16:350-8.

[162] Putzova D, Senitkova I, Stulik J. Tularemia vaccines. Folia Microbiol 2016;61:495-504.

[163] Qin A, Mann BJ. Identification of transposon insertion mutants of Francisella tularensis tularensis strain Schu S4 deficient in intracellular replication in the hepatic cell line HepG2. BMC Microbiology 2006;6:69-.

[164] Qin A, Scott DW, Mann BJ. Francisella tularensis subsp. tularensis Schu S4 Disulfide Bond Formation Protein B, but Not an RND-Type Efflux Pump, Is Required for Virulence. Infection and Immunity 2008;76:3086-92.

[165] Qin A, Scott DW, Thompson JA, Mann BJ. Identification of an Essential Francisella tularensis subsp. tularensis Virulence Factor. Infection and Immunity 2009;77:152-61.

[166] Qin A, Zhang Y, Clark ME, Rabideau MM, Millan Barea LR, Mann BJ. FipB, an Essential Virulence Factor of Francisella tularensis subsp. tularensis, Has Dual Roles in Disulfide Bond Formation. Journal of Bacteriology 2014;196:3571-81.

[167] Ramakrishnan G, Sen B, Johnson R. Paralogous Outer Membrane Proteins Mediate Uptake of Different Forms of Iron and Synergistically Govern Virulence in Francisella tularensis tularensis. The Journal of Biological Chemistry 2012;287:25191-202.

[168] Rasmussen JA, Fletcher JR, Long ME, Allen L-AH, Jones BD. Characterization of Francisella tularensis Schu S4 mutants identified from a transposon library screened for O-antigen and capsule deficiencies. Frontiers in Microbiology 2015;6:338.

[169] Rathinam VAK, Jiang Z, Waggoner SN, Sharma S, Cole LE, Waggoner L, et al. The AIM2 inflammasome is essential for host-defense against cytosolic bacteria and DNA viruses. Nature immunology 2010;11:395-402.

[170] Raynaud C, Meibom KL, Lety M-A, Dubail I, Candela T, Frapy E, et al. Role of the wbt Locus of Francisella tularensis in Lipopolysaccharide O-Antigen Biogenesis and Pathogenicity. Infection and Immunity 2007;75:536-41.

[171] Reddy VS, Shlykov MA, Castillo R, Sun EI, Saier MH. The Major Facilitator Superfamily (MFS) Revisited. The FEBS journal 2012;279:2022-35.

[172] Reed DS, Smith LKP, Cole KS, Santiago AE, Mann BJ, Barry EM. Live Attenuated Mutants of Francisella tularensis Protect Rabbits against Aerosol Challenge with a Virulent Type A Strain. Infection and Immunity 2014;82:2098-105.

[173] Rhinehart-Jones TR, Fortier AH, Elkins KL. Transfer of immunity against lethal murine Francisella infection by specific antibody depends on host gamma interferon and T cells. Infection and Immunity 1994;62:3129-37.

[174] Richard K, Mann BJ, Stocker L, Barry EM, Qin A, Cole LE, et al. Novel Catanionic Surfactant Vesicle Vaccines Protect against Francisella tularensis LVS and Confer Significant Partial Protection against F. tularensis Schu S4 Strain. Clinical and Vaccine Immunology : CVI 2014;21:212-26.

[175] Rockx-Brouwer D, Chong A, Wehrly TD, Child R, Crane DD, Celli J, et al. Low Dose Vaccination with Attenuated Francisella tularensis Strain SchuS4 Mutants Protects against Tularemia Independent of the Route of Vaccination. PLoS ONE 2012;7:e37752.

[176] Rohmer L, Brittnacher M, Svensson K, Buckley D, Haugen E, Zhou Y, et al. Potential Source of Francisella tularensis Live Vaccine Strain Attenuation Determined by Genome Comparison. Infection and Immunity 2006;74:6895-906.

[177] Russo BC, Horzempa J, O'Dee DM, Schmitt DM, Brown MJ, Carlson PE, et al. A Francisella tularensis Locus Required for Spermine Responsiveness Is Necessary for Virulence. Infection and Immunity 2011;79:3665-76.

[178] Saier MH. Families of transmembrane sugar transport proteins. Molecular Microbiology 2000;35:699-710.

[179] Saier MH, Paulsen IT, Sliwinski MK, Pao SS, Skurray RA, Nikaido H. Evolutionary origins of multidrug and drug-specific efflux pumps in bacteria. The FASEB Journal 1998;12:265-74.

[180] Salomonsson E, Kuoppa K, Forslund A-L, Zingmark C, Golovliov I, Sjöstedt A, et al. Reintroduction of Two Deleted Virulence Loci Restores Full Virulence to the Live Vaccine Strain of Francisella tularensis. Infection and Immunity 2009;77:3424-31.

[181] Sancak Y, Peterson TR, Shaul YD, Lindquist RA, Thoreen CC, Bar-Peled L, et al. The Rag GTPases bind raptor and mediate amino acid signaling to mTORC1. Science (New York, N.Y.) 2008;320:1496-501.

[182] Santiago AE, Cole LE, Franco A, Vogel SN, Levine MM, Barry EM. Characterization of rationally attenuated Francisella tularensis vaccine strains that harbor deletions in the guaA and guaB genes. Vaccine 2009;27:2426-36.

[183] Santiago AE, Mann BJ, Qin A, Cunningham AL, Cole LE, Grassel C, et al. Characterization of Francisella tularensis Schu S4 defined mutants as live-attenuated vaccine candidates. Pathogens and Disease 2015;73:ftv036.

[184] Santic M, Abu Kwaik Y. Nutritional virulence of Francisella tularensis. Frontiers in Cellular and Infection Microbiology 2013;3:112.

[185] Santic M, Asare R, Skrobonja I, Jones S, Abu Kwaik Y. Acquisition of the Vacuolar ATPase Proton Pump and Phagosome Acidification Are Essential for Escape of Francisella tularensis into the Macrophage Cytosol. Infection and Immunity 2008;76:2671-7.

[186] Santic M, Molmeret M, Abu Kwaik Y. Modulation of biogenesis of the Francisella tularensis subsp. novicida-containing phagosome in quiescent human macrophages and its maturation into a phagolysosome upon activation by IFN-γ. Cellular Microbiology 2005;7:957-67.

[187] Santic M, Molmeret M, Klose KE, Jones S, Kwaik YA. The Francisella tularensis pathogenicity island protein IglC and its regulator MglA are essential for modulating phagosome biogenesis and subsequent bacterial escape into the cytoplasm. Cellular Microbiology 2005;7:969-79.

[188] Santic M, Molmeret M, Klose KE, Jones S, Kwaik YA. The Francisella tularensis pathogenicity island protein IglC and its regulator MglA are essential for modulating phagosome biogenesis and subsequent bacterial escape into the cytoplasm. Cell Microbiol 2005;7.

[189] Sarathy JP, Dartois V, Lee EJD. The Role of Transport Mechanisms in Mycobacterium Tuberculosis Drug Resistance and Tolerance. Pharmaceuticals 2012;5:1210-35.

[190] Saslaw S, Eigelsbach HT, Prior JA, Wilson HE, Carhart S. Tularemia vaccine study: Ii. respiratory challenge. Archives of Internal Medicine 1961;107:702-14.

[191] Sauer J-D, Bachman MA, Swanson MS. The phagosomal transporter A couples threonine acquisition to differentiation and replication of Legionella pneumophila in

macrophages. Proceedings of the National Academy of Sciences of the United States of America 2005;102:9924-9.

[192] Schmerk CL, Duplantis BN, Howard PL, Nano FE. A Francisella novicida pdpA mutant exhibits limited intracellular replication and remains associated with the lysosomal marker LAMP-1. Microbiology 2009;155:1498-504.

[193] Schulert GS, Allen L-AH. Differential infection of mononuclear phagocytes by Francisella tularensis: role of the macrophage mannose receptor. Journal of Leukocyte Biology 2006;80:563-71.

[194] Schulert GS, McCaffrey RL, Buchan BW, Lindemann SR, Hollenback C, Jones BD, et al. Francisella tularensis Genes Required for Inhibition of the Neutrophil Respiratory Burst and Intramacrophage Growth Identified by Random Transposon Mutagenesis of Strain LVS. Infection and Immunity 2009;77:1324-36.

[195] Sen B, Meeker A, Ramakrishnan G. The fslE Homolog, FTL_0439 (fupA/B), Mediates Siderophore-Dependent Iron Uptake in Francisella tularensis LVS. Infection and Immunity 2010;78:4276-85.

[196] Sharma J, Mares CA, Li Q, Morris EG, Teale JM. Features of sepsis caused by pulmonary infection with Francisella tularensis Type A strain. Microbial Pathogenesis 2011;51:39-47.

[197] Shirey KA, Cole LE, Keegan AD, Vogel SN. Francisella tularensis Live Vaccine Strain Induces Macrophage Alternative Activation as a Survival Mechanism. The Journal of Immunology 2008;181:4159-67.

[198] Sigal N, Cohen-Karni D, Siemion S, Bibi E. MdfA from <i>Escherichia coli</i>, a Model Protein for Studying Secondary Multidrug Transport. Journal of Molecular Microbiology and Biotechnology 2006;11:308-17.

[199] Sigal N, Molshanski-Mor S, Bibi E. No Single Irreplaceable Acidic Residues in the Escherichia coli Secondary Multidrug Transporter MdfA. Journal of Bacteriology 2006;188:5635-9.

[200] SjÖstedt A. Tularemia: History, Epidemiology, Pathogen Physiology, and Clinical Manifestations. Annals of the New York Academy of Sciences 2007;1105:1-29.

[201] Sjöstedt A, North RJ, Conlan JW. The requirement of tumour necrosis factor-α and interferon-γ for the expression of protective immunity to secondary murine tularaemia depends on the size of the challenge inoculum. Microbiology 1996;142:1369-74.

[202] SL M, RE D, JE E, MG H, E W, JL P, et al. Deletion of the Bacillus anthracis capB homologue in Francisella tularensis subspecies tularensis generates an attenuated strain that protects mice against virulent tularaemia. Journal of Medical Microbiology 2010;59:1278-84.

[203] Somerville GA, Proctor RA. At the Crossroads of Bacterial Metabolism and Virulence Factor Synthesis in Staphylococci. Microbiology and Molecular Biology Reviews : MMBR 2009;73:233-48.

[204] Steele S, Brunton J, Ziehr B, Taft-Benz S, Moorman N, Kawula T. Francisella tularensis Harvests Nutrients Derived via ATG5-Independent Autophagy to Support Intracellular Growth. PLoS Pathogens 2013;9:e1003562.

[205] Steele S, Radlinski L, Taft-Benz S, Brunton J, Kawula TH. Trogocytosis-associated cell to cell spread of intracellular bacterial pathogens. eLife 2016;5:e10625.

[206] Steiner DJ, Furuya Y, Metzger DW. Host–pathogen interactions and immune evasion strategies in Francisella tularensis pathogenicity. Infection and Drug Resistance 2014;7:239-51.

[207] Storek KM, Gertsvolf NA, Ohlson MB, Monack DM. cGAS and Ifi204 cooperate to produce type I interferon in response to Francisella infection. Journal of immunology (Baltimore, Md. : 1950) 2015;194:3236-45.

[208] Straskova A, Cerveny L, Spidlova P, Dankova V, Belcic D, Santic M, et al. Deletion of IglH in virulent Francisella tularensis subsp. holarctica FSC200 strain results in attenuation and provides protection against the challenge with the parental strain. Microbes and Infection 2012;14:177-87.

[209] Su J, Yang J, Zhao D, Kawula TH, Banas JA, Zhang J-R. Genome-Wide Identification of Francisella tularensis Virulence Determinants. Infection and Immunity 2007;75:3089-101.

[210] Sunagar R, Kumar S, Franz BJ, Gosselin EJ. Vaccination evokes gender-dependent protection against tularemia infection in C57BL/6Tac mice. Vaccine 2016;34:3396-404.

[211] Tamilselvam B, Daefler S. Francisella targets cholesterol-rich host cell membrane domains for entry into macrophages. The Journal of Immunology 2008;180:8262-71.

[212] Tärnvik A. Nature of protective immunity to Francisella tularensis. Reviews of infectious diseases 1989;11:440-51.

[213] Tärnvik A, Sandström G, Sjöstedt A. Epidemiological analysis of tularemia in Sweden 1931–1993. FEMS immunology and medical microbiology 1996;13:201-4.

[214] Telepnev M, Golovliov I, Grundström T, Tärnvik A, Sjöstedt A. Francisella tularensis inhibits Toll-like receptor-mediated activation of intracellular signalling and

secretion of TNF-α and IL-1 from murine macrophages. Cellular Microbiology 2003;5:41-51.

[215] Tesh MJ, Miller RD. Amino acid requirements for Legionella pneumophila growth. Journal of Clinical Microbiology 1981;13:865-9.

[216] Titball RW, Sjöstedt A. *Francisella tularensis*: an overview. ASM News 2003;69:558.

[217] Twine S, Byström M, Chen W, Forsman M, Golovliov I, Johansson A, et al. A Mutant of Francisella tularensis Strain SCHU S4 Lacking the Ability To Express a 58-Kilodalton Protein Is Attenuated for Virulence and Is an Effective Live Vaccine. Infection and Immunity 2005;73:8345-52.

[218] Twine S, Shen H, Harris G, Chen W, Sjostedt A, Ryden P, et al. BALB/c mice, but not C57BL/6 mice immunized with a ΔclpB mutant of Francisella tularensis subspecies tularensis are protected against respiratory challenge with wild-type bacteria: Association of protection with post-vaccination and post-challenge immune responses. Vaccine 2012;30:3634-45.

[219] Van Metre TE, Kadull PJ. Laboratory-acquired tularemia in vaccinated individuals: a report of 62 cases. Annals of internal medicine 1959;50:621-32.

[220] W. MG, C. CC. Studies of plague, a plague-like disease and tuberculosis among rodents in California. Journal of Infectious Diseases 1912;VI:170-80.

[221] Wang D, Hu E, Chen J, Tao X, Gutierrez K, Qi Y. Characterization of novel ybjG and dacC variants in Escherichia coli. Journal of Medical Microbiology 2013;62:1728-34.

[222] Wang R, Zhang Z, Xie L, Xie J. Implications of *Mycobacterium* Major Facilitator Superfamily for Novel Measures against Tuberculosis. 2015;25:315-21.

[223] Wayne Conlan J, Oyston PCF. Vaccines Against Francisella Tularensis. Annals of the New York Academy of Sciences 2007;1105:325-50.

[224] Wehrly TD, Chong A, Virtaneva K, Sturdevant DE, Child R, Edwards JA, et al. Intracellular biology and virulence determinants of Francisella tularensis revealed by transcriptional profiling inside macrophages. Cellular Microbiology 2009;11:1128-50.

[225] Weiss DS, Henry T, Monack DM. Francisella Tularensis: Activation of the Inflammasome. Annals of the New York Academy of Sciences 2007;1105:219-37.

[226] West TE, Pelletier MR, Majure MC, Lembo A, Hajjar AM, Skerrett SJ. Inhalation of Francisella novicida ΔmglA causes replicative infection that elicits innate and adaptive responses but is not protective against invasive pneumonic tularemia. Microbes and infection / Institut Pasteur 2008;10:773-80.

[227] Wherry WB, Lamb BH. Infection of Man with Bacterium Tularense. Journal of Infectious Diseases 2004;189:1321-31.

[228] Wickstrum JR, Bokhari SM, Fischer JL, Pinson DM, Yeh H-W, Horvat RT, et al. Francisella tularensis Induces Extensive Caspase-3 Activation and Apoptotic Cell Death in the Tissues of Infected Mice. Infection and Immunity 2009;77:4827-36.

[229] Yonekawa T, Thorburn A. Autophagy and Cell Death. Essays in biochemistry 2013;55:105-17.

[230] Zhang A, He X, Meng Y, Guo L, Long M, Yu H, et al. Antibiotic and Disinfectant Resistance of Escherichia coli Isolated from Retail Meats in Sichuan, China. Microbial Drug Resistance 2015.

[231] Zhang Q-J, Li X-L, Wang D, Huang X-C, Mathis JM, Duan W-M, et al. Trogocytosis of MHC-I/Peptide Complexes Derived from Tumors and Infected Cells Enhances Dendritic Cell Cross-Priming and Promotes Adaptive T Cell Responses. PLoS ONE 2008;3:e3097.